AN INVESTIGATION INTO THE OPTIMISATION OF THE USE OF DIAMOND ABRASIVE TOOLS FOR HARD ROCK CUTTING

A thesis
submitted to the University of London
(Imperial College of Science, Technology and Medicine)

by

Cunguo DONG

In fulfilment of the requirements
for the degree of
Doctor of Philosophy

May 1993

BTL. LONDN. UNIV.

ABSTRACT

Because it has become customary to regard sawability of stone solely as a property of the rock material - a custom that has led to a variety of descriptive machinability definitions in rock cutting - there urgently arises a need to define the sawability correctly, theoretically and methodically. Rock cutting tests can be traced from at least as far back as 1962, however, traditional rock cutting tests do not attempt to determine the optimum production cost at a given cutting condition as these tests can not express tool wear quantitatively as a function of operating parameters.

In this thesis, sawability was viewed as an interaction rather than a property. Sawing tests were clearly subdivided into three basic categories: determining the absolute sawability, comparing the relative sawability and assessing the defined sawability. A standard sawability test was therefore recommended.

Based on a large scale laboratory test on diamond circular sawing, the wear mechanism of diamond abrasive cutting and the balanced wear region were clearly defined. The long time accepted opinion on optimum sawing speed was modified. Tool life equations have been established and a new concept called the R-C characteristic curve was developed. The R-C curve provides a rigorous approach for determining the absolute sawability and also in assessing the relative sawability. The most economic conditions can be found along the R-C characteristic curve. A user friendly computer program has been developed, which provides the most convenient approach to the optimization of sawing operations. It was further noted that the cutting forces are directly affected by the worn diamond particle types of microfracturing and flat wear and is not related to the diamond relative wear. Cutting forces can be kept in a quasi-stable state conditionally, as sawing rate increases.

For the purpose of predicting the defined sawability according to the properties of rock material, the author believes that the use of a predictive equation for assessing sawability is not a rigorous method. However, Shore hardness and quartz content can be lined together as the indicator in assessing the defined sawability.

To put the proposed kerf and rip mining method in practice, a diamond wire saw was successfully used for cutting kerfs in hard rock at a high cutting rate in a test mine. Theoretical studies and the site trials led to the development of the tension equations for the diamond wire sawing.

ACKNOWLEDGEMENT

The author is very much indebted to Prof. C.T. Shaw, the Dean of the Royal School of Mines and professor of Mining Engineering, for his kind offer of the opportunity to undertake this research.

He wishes to express his appreciation to his supervisors Prof. C.T. Shaw and Dr. S. Durucan, Head of the Mine Environment and Computer Aided Mine Design Research Group, for their constant aid, guidance and encouragement during his studies.

The author is very grateful to Mr. B. Thoreau, Chef de Service of Diamant Boart, for his kind support and well arrangement of the sawing trails. Meanwhile, many thanks are given to the following people in Diamant Boart for their generous help to conduct the tests: Mr. X. Heine, Mr. G. Wannyn, Mr. T. Seghers, Mr. A. Dessy, Mr. C. Messina and Mr. J. Marcoli.

Thanks are due to Mr. E.H. Fraser-Smith, Mine Manager, Laporte Minerals, for his well arrangement and kind support for the in-situ test.

The author also wishes to thank following people for their help and encouragement:

Mr. R. Marsden and Mr. J. Dennis in the Rock Mechanics Laboratories of Imperial College; Dr. L Gunduz, a former Ph.D student in the Department; All colleagues and all the members of staff in the Department.

Finally, the author owes a debt of gratitude to his wife Ping and son Jihao for their love and encouragement, as well as to his parents for their patience to endure the time while the author spent so long time studying abroad instead of taking care of them.

TABLE OF CONTENTS

ACKNOWLEDGEMENT i
TABLE OF CONTENTS ii
LIST OF FIGURES vi
LIST OF TABLES x
NOMENCLATURE xi

CHAPTER 1: INTRODUCTION
1.1 RESEARCH BACKGROUND 1
1.2 RESEARCH OBJECTIVES 4
1.3 THESIS STRUCTURE 5

CHAPTER 2: GENERAL STUDIES ON ROCK CUTTING
2.1 INTRODUCTION 7
2.2 MECHANISMS OF ROCK CUTTING 8
2.2.1 Pure cutting models 8
2.2.2 Numerical models 12
2.2.3 Cutting and friction models 13
2.3 CORRELATIONS BETWEEN ROCK PROPERTIES AND MACHINING PERFORMANCES 18
2.4 SOME RELATIVE THEORIES ON METAL CUTTING 20
2.5 SUMMARY 23

CHAPTER 3: DIAMOND ABRASIVE CUTTING AND THE CUTTING TOOL
3.1 DIAMOND ABRASIVE TOOLS 25
3.1.1 Diamond type 25
3.1.2 Diamond size and concentration 26
3.1.3 Properties of bond and diamond segment 27
3.1.4 Selection of diamond tools 28
3.2 CUTTING PROCESS AND SPECIFIC FEATURES 30
3.3 DIAMOND RELATIVE WEAR AND PARTICLE WEAR 34

3.4 REVIEW OF THE MECHANISMS OF DIAMOND ABRASIVE CUTTING 38
3.5 PREVIOUS RESULTS ON DIAMOND ABRASIVE CUTTING 41
3.5.1 Sawability predictions 41
3.5.2 Diamond relative wear 45
3.5.3 Optimum sawing speed 47
3.5.4 Sawing forces 49
3.6 SUMMARY 49

CHAPTER 4: STATE OF THE ART IN DIAMOND SAWS
4.1 INTRODUCTION 51
4.2 DIAMOND CIRCULAR SAW 52
4.3 DIAMOND WIRE SAW 54
4.3.1 Cutting techniques employed using diamond wire saws 57
4.3.2 Technical considerations for cutting hard rock 63
4.3.3 Wire performance evolution 68
4.4 CHAIN SAW 71
4.5 BANDSAW 73
4.6 FRAME SAW 74
4.7 SUMMARY 75

CHAPTER 5: DEVELOPMENT OF THE THEORIES OF DIAMOND ABRASIVE CUTTING
5.1 INTRODUCTION 76
5.2 CUTTING PARAMETERS AND CHIP CROSS-SECTION 77
5.3 EXPERIMENTAL PROCEDURES 81
5.3.1 Equipment and testing materials 81
5.3.2 Sawing test arrangements 82
5.3.3 Sawing force, relative wear and particle wear examinations 84
5.4 BALANCED WEAR REGION, TOOL LIFE EQUATION AND R-C CHARACTERISTIC CURVE 86
5.4.1 Wear mechanism of diamond cutting 88
5.4.2 The concept of balanced wear region 91
5.4.3 The minimum tool wear and optimum sawing speed 97
5.4.4 Relative wear curve and tool life equations 101
5.4.5 R-C characteristic curve 110

5.5 CUTTING MECHANISMS AND SAWING FORCES 116
5.5.1 Resolution of forces in circular sawing 116
5.5.2 Mode of sawing 117
5.5.3 The hypothesis of diamond abrasive cutting mechanism 120
5.5.4 Force ratio of diamond abrasive cutting 121
5.5.5 The effects of engineering parameters on cutting forces 124
5.5.6 A possible force pattern for diamond abrasive cutting 131
5.6 THE RELATIONSHIP BETWEEN ε - s 133

CHAPTER 6: THEORIES OF DIAMOND WIRE SAWING AND UNDERGROUND TRIALS
6.1 INTRODUCTION 136
6.2 DEVELOPMENT OF THE THEORIES OF DIAMOND WIRE SAWING 137
6.2.1 The principle of drives utilizing friction force 137
6.2.2 The proposed wire tension equation 142
6.3 UNDERGROUND DIAMOND WIRE SAWING TRIALS 146
6.3.1 Test site and test procedures 146
6.3.2 Discussions of the test results 153

CHAPTER 7: DETERMINING, COMPARING AND ASSESSING THE SAWABILITY OF STONE
7.1 INTRODUCTION 160
7.2 DEFINITION OF SAWABILITY 161
7.3 PROPOSED METHODOLOGY FOR SAWABILITY TEST 163
7.3.1 Objectives 163
7.3.2 R-C curves for determining sawability 164
7.3.3 Sawability index for comparing the relative sawability 165
7.3.4 R-C curves for comparing the relative sawability 167
7.3.5 The recommended standard sawability test 170
7.4 ASSESSING THE DEFINED SAWABILITY 173
7.4.1 Introduction 173
7.4.2 Test procedure of assessing the defined sawability 174
7.4.3 Rock tests for determining the properties 176
7.4.4 Test results in assessing the defined sawability 182

7.4.5 Discussions 184

CHAPTER 8: CONCLUSIONS AND RECOMMENDATIONS FOR FURTHER RESEARCH

8.1 GENERAL CONCLUSIONS 189

8.2 RECOMMENDATIONS FOR FURTHER RESEARCH 193

REFERENCES 195

APPENDIX 205

LIST OF FIGURES

Figure 1.1: The proposed Kerf and Rip Mining method (After shaw *et al*, 1991)
Figure 2.1: Tensile breakage theory by Evans (1965)
Figure 2.2: An illustration of the failure process of rock cutting by Nishimatsu (1972)
Figure 2.3: Stress and cutting forces for orthogonal cutting (After Nishimatsu, 1972)
Figure 2.4: Sharp wedge bit penetration (After Wang *et al*,1976)
Figure 2.5: Final deflected shape and crack trajectory (After Ingraffea,1987)
Figure 2.6: Forces acting on a sharp cutter (After Detournay *et al*, 1992)
Figure 2.7: Forces acting on a blunt cutter (After Detournay *et al*, 1992)
Figure 2.8: ε - s diagram (After Detournay *et al*, 1992)
Figure 3.1: Wear patterns of the sandwich (left) and conventional (right) diamond impregnated segments (After Konstanty, 1991)
Figure 3.2: Typical cutting conditions under a saw blade segment (After Bridwell *et al*, 1974)
Figure 3.3: Height of penetration of diamond particles versus cumulative area sawn (After Wright,1988)
Figure 3.4: Diamond particle protrusion (After Jennings, 1988)
Figure 3.5: Wear patterns on diamond particles (After Miller *et al*, 1990)
Figure 3.6: Diagram illustrating the effect of material removal rate on the principle mechanism of diamond particle wear (After Ertingshausen, 1985)
Figure 3.7: Blade wear in sawing hard rock depending on the sawing rate (After Buttner, 1972)
Figure 3.8: Blade wear relative to sawing rate when sawing concrete (After Busch *et al*, 1973)
Figure 3.9: The graphical relationship between tool life and production rate (After Jennings, 1988)
Figure 3.10: Effect of blade speed when sawing Impala (After Bailey *et al*, 1979)
Figure 3.11: Blade wear relative to blade peripheral speed in sawing concretes (After Busch *et al*, 1973)
Figure 4.1: Diamond circular saw used for mining purpose (After Bracken, 1988)

Figure 4.2: TDV 55 Diamond wire machine and diamond wires
Figure 4.3: Diamond wire sawing method with descending pulleys (After Cai *et al*, 1988)
Figure 4.4: Multi-diamond wire block slabbing machine (After Cai *et al*, 1988)
Figure 4.5: Vertical bench sawing (After Pinzari, 1983)
Figure 4.6: Vertical bench sawing with a sunk pulley (After Pinzari, 1983)
Figure 4.7: Horizontal bench sawing (After Decroly, 1981)
Figure 4.8: Horizontal sawing at different level (After Herbert, 1989)
Figure 4.9: Traditional method of opening cut (After Pinzari, 1983)
Figure 4.10: Combination extraction method of opening cut (After Decroly, 1981)
Figure 4.11: How to reduce stress σ_y on the wire (After Cai *et al*, 1988)
Figure 4.12: Dimensions of round and square Syndrill as used on chain saw (After Daniel, 1986)
Figure 4.13: Chain link with diamond segment (After Meier, 1983)
Figure 5.1: Undeformed chip thickness in diamond circular sawing
Figure 5.2: Bridge saw for the tests
Figure 5.3: Segment surface was examined under a binocular microscope
Figure 5.4: Production rate in relation to costs (After Buttner, 1974)
Figure 5.5: The variable behavior of the diamond sawblade for sawing Rose De La Clarte (v=47m/s)
Figure 5.6: Relative wear versus feed and depth of cut at constant sawing rate at low peripheral speed (v= 20 m/sec, A_s = 300 cm^2/min)
Figure 5.7: Relative wear versus feed and depth of cut at constant sawing rate at medium peripheral speed (v= 31 m/sec, A_s = 300 cm^2/min)
Figure 5.8: Relative wear versus feed and depth of cut at constant sawing rate at high peripheral speed (v= 47 m/sec, A_s = 300 cm^2/min)
Figure 5.9: Abrasive wear relative to feed and depth of cut within the balanced wear region
Figure 5.10: Fracture wear relative to feed and depth of cut within the balanced wear region
Figure 5.11: Diagram of feed and depth of cut on the balanced relative wear under both modes of control
Figure 5.12: The affect of sawing speed on the balanced relative wear
Figure 5.13: Diagram of the dependence of relative wear G_{min} during self-dressing on time of cutting by particles until torn out of bond t_G

Figure 5.14: Optimum sawing speed for Rose De La Clarte (a_p = 30 mm, v_f = 100 cm/min)
Figure 5.15: Effect of sawing speed on relative wear when sawing Rose De La Clarte (v_f = 600 cm/min, a_p = 5 mm)
Figure 5.16: Effect of sawing speed on relative wear when sawing Rose De La Clarte (a_p = 60 mm, v_f = 50 cm/min)
Figure 5.17: Development of the relative wear with feed speed
Figure 5.18: The worn segment surfaces at different conditions
Figure 5.19: The relationship between tool life and feed speed
Figure 5.20: The development of the relative wear with sawing rate for Marlin
Figure 5.21: Development of the relative wear with sawing rate for five granites
Figure 5.22: The relationships between tool life and sawing rate
Figure 5.23: R-C characteristic curve for sawing 50 m^2 of Celtic [where, c_m=10 (Pounds/hour); c_t=430 (Pounds); t_o=3 (hours)]
Figure 5.24: R-C curve for sawing Marlin
Figure 5.25: R-C curve for sawing Rose De La Clarte
Figure 5.26: R-C curve for sawing Lanhelin
Figure 5.27: R-C curve for sawing Balmoral
Figure 5.28: Diagram of sawing forces on a sawblade in both down- and up-cutting modes
Figure 5.29: Cutting forces verses down- and up- cutting for sawing Rose De La Clarte (v_f = 300 cm/min, a_p = 10 mm)
Figure 5.30: Diagram illustrating the abrasive cutting mechanism
Figure 5.31(a): Effect of rock types on the force ratio (v_f = 400 cm/min, a_p = 10 mm)
Figure 5.31(b): Effect of rock types on the force ratio (v_f = 222 cm/min, a_p = 18 mm)
Figure 5.32: Effect of operating parameters on the force ratio
Figure 5.33: Sawing forces relative to feed speed when sawing Balmoral (a_p=10 mm)
Figure 5.34: Sawing forces relative to feed speed when sawing Celtic (a_p=10 mm)
Figure 5.35: Microfracture and flat wear relative to feed speed (for Balmoral)
Figure 5.36: Microfracture and flat wear relative to feed speed (for Celtic)
Figure 5.37: Force curves relative to feed in both uniform and rapid wear region
Figure 5.38: Microfracture relative to feed in both uniform and rapid wear region
Figure 5.39: Sawing forces relative to depth cut and feed speed at constant sawing rate when sawing Rose De La Clarte

Figure 5.40: Microfracture and flat wear relative to depth cut when sawing Rose De La Clarte
Figure 5.41: Cutting forces relative to sawing speed (v_f=300cm/min, a_p=10mm)
Figure 5.42: Microfracture and flat wear relative to sawing speed for sawing Rose De La Clarte
Figure 5.43: Sawing forces versus sawing rate when sawing Marlin [166x12; 200x15; 223x18; 243x18.5 (cm/min x mm)]
Figure 5.44: Microfracture versus sawing rate when sawing Marlin [166x12; 200x15; 223x18;243x18.5 (cm/min x mm)]
Figure 5.45: ε - s diagram for abrasive diamond cutting with different depths cut
Figure 6.1: Diagram of diamond wire cutting
Figure 6.2: Wire rope rests on the V-shaped drive pulley
Figure 6.3: Forces and tensions on a diamond wire
Figure 6.4: Diagram of the friction force of the diamond wire cutting
Figure 6.5: Site preparation for kerf cutting (drilling)
Figure 6.6: Copper joints used for wire connection
Figure 6.7: The arrangement of the guide pulleys and the drive pulley
Figure 6.8: Underground test of diamond wire sawing at Milldam Mine
Figure 6.9: Mine plan showing the Raise 12 from C Drive to B Drive to A Drive
Figure 6.10: Diamond wire sawing layout for parallel cuts
Figure 6.11: Diamond wire sawing layout for back slot cutting
Figure 6.12: The electroplated diamond bead after 125 m^2 of cut of limestone
Figure 6.13: Finished raise made by use of the diamond wire saw
Figure 6.14: The change of the direction of the drive pulley
Figure 6.15: Relationship between sawing rate and wire speed at a constant power
Figure 7.1: Computer screen from the program used for determining sawability of rock utilizing the R-C curve concept
Figure 7.2: Optimum sawing conditions for sawing Rose De La Clarte
Figure 7.3: Slops expressing the relationship between tool life and sawing rate
Figure 7.4: R-C curve used for in comparing the relative sawability
Figure 7.5: Test data and envelopes for Balmoral granite
Figure 7.6(a): Diamond relative wear and sawing forces for different rocks (v_f = 400 cm/min, a_p = 10 mm)
Figure 7.6(b): Diamond relative wear and sawing forces for different rocks (v_f = 222 cm/min, a_p = 18 mm)

LIST OF TABLES

Table 3.1: Selection of diamond type
Table 4.1: Impregnated diamond wire life and performance (After Herbert, 1985)
Table 5.1: Sawing parameters for test Step 1 (v=20m/s, Rose De La Clarte)
Table 5.2: Sawing parameters for test Step 1 (v=31m/s, Rose De La Clarte)
Table 5.3: Sawing parameters for test Step 1 (v=47m/s, Rose De La Clarte)
Table 5.4: Sawing parameters for test Step 2 (v=30m/s, Rose De La Clarte)
Table 5.5: Sawing parameters for test Step 2 (v=30m/s, Balmoral and Celtic)
Table 5.6: Sawing parameters for test Step 3 (v=30m/s, Marlin)
Table 5.7: Sawing parameters for test Step 3 (v=30m/s, Lanhelin)
Table 5.8: Sawing parameters for test Step 3 (v=30m/s, Limestone)
Table 5.9: Analysis of diamond particles after sawing Rose De La Claret
Table 5.10: Regression analyses of log tool life and log sawing rate
Table 5.11: The variable extent of tool life of DTA blade for sawing different rocks
Table 5.12: Parameters for studying the relationship ε - s
Table 6.1: Underground wire sawing test results obtained in Laporte Minerals
Table 7.1: Comparison of the sawability index
Table 7.2: Comparison of the relative sawability using the R-C concept
Table 7.3: The potential profit when sawing five granites
Table 7.4: Test results in assessing the defined sawability
Table 7.5: Correlation coefficients between T_{300} and various parameters
Table 7.6: Re-analyzing the data of D.N.Wright's results
Table 7.7: Re-analyzing the data of D.Birle's results
Table 7.8: Analyzing the data of authors results

NOMENCLATURE

A'	diamond wire cross section area
A_o	cross sectional area of the cut
A_m	machined surface area
A_s	sawing rate
a_p	depth of cut of the sawblade
B_w	width of sawblade segment
C_s	cutting constant of tool life equation
C_T	total cost of a machining operation
c_t	purchase price of the sawblade
c_m	machine and operator (including overheads) cost per unit time
Coh	cohesion of rock
D	diameter of the sawblade
d_t	diameter of the diamond wire beads
e	base of Napierian logarithms
E_w	modulus of elasticity of the wire material
F_f	resistance to diamond wire rotation due to friction
F_q	undeformed chip cross-section which an individual diamond particle has to remove when using a sawblade
F_t	tangential component or peripheral component of cutting force
F_v	thrust component or radial component of cutting force
F'_v	thrust force produced by one diamond bead
F_w	dead weight of diamond wire
F_x	axial component of cutting force
F_y	vertical component or supporting component of cutting force
F_z	horizontal component or transverse component of cutting force
FA	internal friction angle of rock
FT	fracture toughness of rock
f_r	advance distance of diamond wire machine
Δf	advance per round of cutting locus of the wire in the feed direction
G	relative volumetric wear of the diamond tool
G_A	relative superficial wear of the diamond tool
G_B	relative linear wear of the diamond tool

G_{min}	minimum relative wear
h_{min}	minimum diamond cutting tool penetration depth
I	electrical current
K_M	machine time costs for a machining operation
K_T	tool costs for n machining operation.
L_t	linear loss of the cutting tool
Δl	length of the diamond wire beads
M_R	resistance of diamond wire machine due to move along the rials
N'_d	number of diamond particles per unit length of segment along its girth
N_d	number of diamond particles per unit area of segment surface (proportional to diamond concentration)
n	number of diamond beads in cutting locus simultaneously
n'	number of wires in one layer of the wire
P_n	normal force acting on the driven pulley's groove
P_w	power transmitted by the drive pulley of diamond wire machine
QC	quartz content of rock
R	mean radius of the cutting locus of diamond wire
r	radius of the drive pulley of diamond wire machine
SH	schmidt hardness of rock
SI	relative sawability index
SSH	shore scleroscope hardness of rock
SV	sound velocity of rock
S_s	slack side tension of diamond wire
S_t	tight side tension of diamond wire
T	total useful tool life
T_i	tool life produced at a specified sawing rate
T_o	optimum tool life which minimize the production cost
TS	tensile strength of rock
t_m	machining time
t_o	down time (loading and unloading, transport, inspection)
UCS	uniaxial compressive strength of rock
V	electrical voltage
V_m	volumetric loss of the rock material
V_t	volumetric loss of the cutting tool
v	cutting speed (blade peripheral speed)

v_f	feed speed (blade traverse speed)
v_i	mean diamond wire cutting speed
W_t	useful work transmitted by driven pulley
W_y	characteristic index of the share of thrust force and tangent force
x	tool life exponent of tool life equation
α	wire lay angle
β_o	contact angle between wire and the groove surface of the driven pulley
ε	specific cutting energy (F_z/A_o)
S	specific friction energy (F_y/A_o)
η	efficiency of electrical motor
μ	adhesive factor between the diamond wire and the packed groove surface of the driven pulley
μ_c	friction coefficient between the cutting tool and the rock
μ_o	friction coefficient between the diamond wire and the groove material of the driven pulley
θ	angle of wrap of the diamond wire around the driven pulley (radians)
ρ	actual radius of wire bending on the rock
σ_s	sawing strength of the rock
σ_x	stress produced by tensile loads acting in the wire
σ_y	stress due to the run of the wire onto the driven pulley
σ_z	stress produced by curving the wire onto the cut rock surface
$\cos\xi$	power factor of electrical motor

CHAPTER 1

INTRODUCTION

1.1 RESEARCH BACKGROUND

The use of diamond tools in stone cutting is accepted as essential today. For cutting small blocks of stone to size, the diamond circular saw has virtually taken over from all competitors. For large block stone cutting and extraction of stones, the diamond wire saw has introduced a cost-effective system and with a lot of advantages, compared with the traditional stone extraction techniques, such as blasting, thermic cutting and helicoidal wire.

Sawability, a specific topic of the machinability of stone, has been concentrated on by various researchers for a rather long time. Like other topics such as drillability and cuttability, these researchers have tried to correlate the rock properties with the actual performance of cutting and the published papers have gradually increased in volume. Although it is almost always possible to find some parameters that give a reasonable mathematical correlation with machining performance, the lack of fundamental theory and a standard test have led to the situation that there appear to be little or no correlation between the different tests being suggested. Actually, the commonly used term of machinability is still not clearly defined in the field of rock cutting and therefore, there arises an urgent need to correctly define the machinability theoretically and methodically.

The economic advantage of making the right choice of operating parameters, cutting tools and machining conditions has been well recognized. When the cutting rate is increased while the other conditions are held constant, the actual machining time will be reduced, and the tool wear rate will increase. A low cutting rate will result in low tool wear, but the machining time will be increased. Therefore, production costs can be significantly reduced by making the appropriate choice, especially in operations where the costs of cutting tools are a significant proportion of the total machining costs. Because, in modern high production rock cutting processes, diamond tool costs are a significant factor in the total production costs, there is a great potential for deriving substantial economic benefits.

Rock cutting tests can be traced from at least as far back in time as 1962. Since then, many rock cutting tests have been conducted for different cutting tools all around the world. But, traditional rock cutting tests do not attempt to determine the optimum production cost under given cutting conditions as these tests can not express tool wear quantitatively as a function of operating parameters.

Although the diamond wire sawing method was invented in 1968, it was not until 1983 that it was accepted for cutting harder stones like granites, mainly due to the improvements on the wire achieved by Diamant Boart. Today most of the European stone quarries and many others elsewhere, rely on the diamond wire to boost output and cut costs. What is more significant is the wire saw's usage growth within the construction, building and civil engineering industries. An excellent example, in fact, is that this technique could be transferred from the surface to underground mining activities. Recently, a mining method called Kerf and Rip Mining which combines the use of diamond wire saw and impact rippers was proposed[1], as shown in Figure 1.1. In this method, a diamond wire saw is used to cut a kerf on at least one

side of orebody, then the impact ripper is used to break out the ore. It is suggested that the breaking efficiency of the ripping machine will be significantly enhanced by the introduction of additional free faces to which the tools can break. It means that the rock will be split most effectively when it is in the form of an isolated boulder.

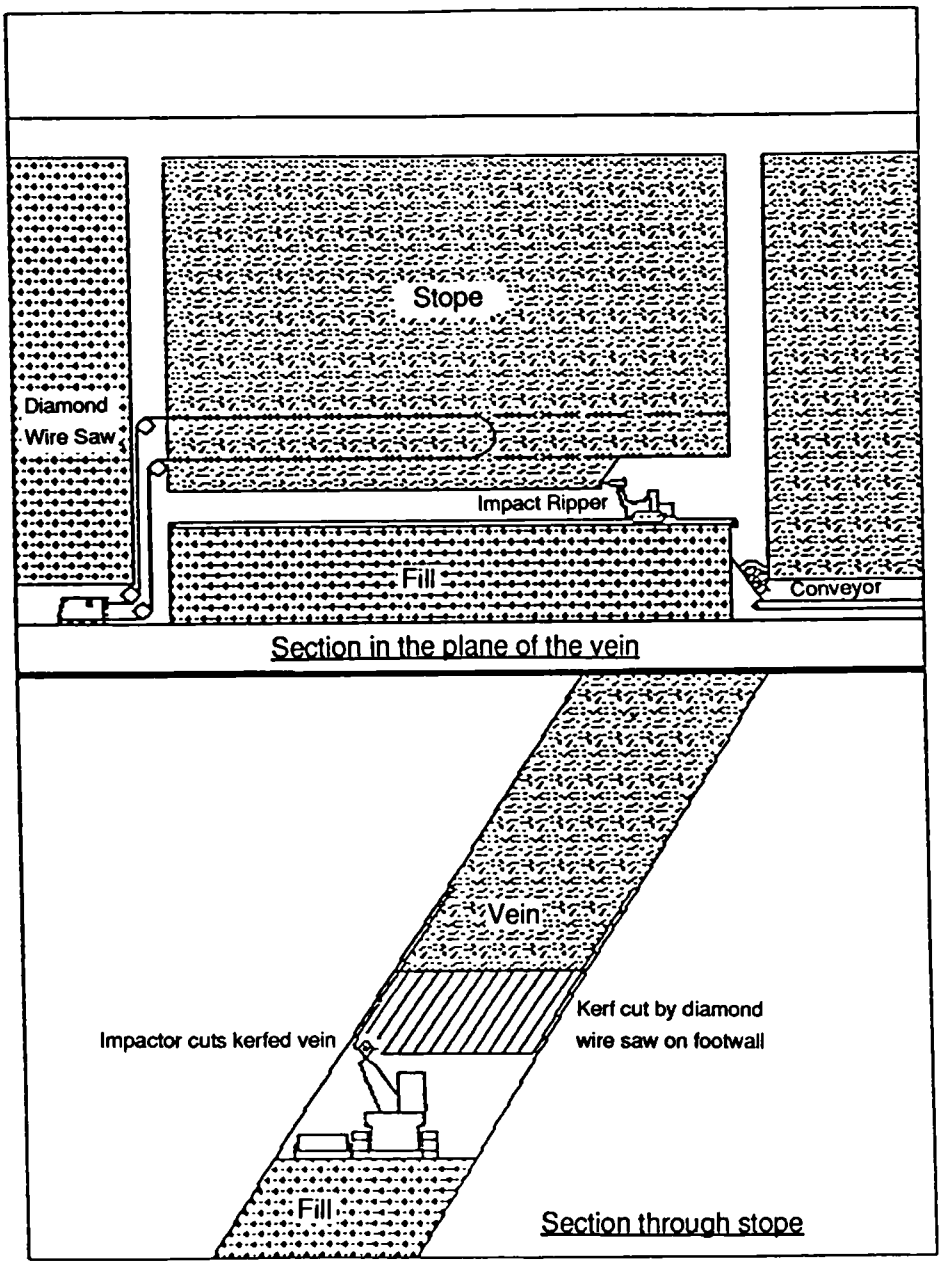


Figure 1.1: The proposed Kerf and Rip Mining method (After Shaw *et al*, 1991)

1.2 RESEARCH OBJECTIVES

In general, the main objective of this research is to form a theoretical basis for diamond abrasive rock cutting and provide a practical approach for the optimization of the use of diamond abrasive tools, in particular diamond saws. The research is also aimed at looking into one aspect of the potential development of methods of mining which do not require the use of explosives.

The main objectives of this research can be listed as follows:

(1) To develop models for quantitatively describing the stone cutting processes and to provide a practical approach to the optimization of the use of diamond abrasive tools for hard rock cutting. For the purpose of putting the theories into practice, develop a user friendly computer program to help the operators and engineers in making the right choice of machining conditions, such as the optimum sawing rate and tool life.

(2) To consummate the concept of machinability of stone and provide a standard for sawability tests. This includes descriptive definitions and the evaluating methodology.

(3) To find the relationship between the rock properties and the defined sawability and clearly indicate the function and limitations.

(4) To set out the mining methods which would allow the mechanization of ore production with the use of diamond wire saws and to develop the theories of wire tension.

In order to achieve these objectives (1) and (2), research was carried out on the cutting and wear mechanisms of diamond cutting tools. The influence of operating parameters of feed speed, depth of cut and sawing speed to the tool wear and cutting forces were also investigated by means of theoretical studies and actual sawing trials in Diamant Boart's pilot station in Brussels. Based on the conventional rock tests carried out at the Rock Mechanics Laboratories of Imperial College, objective (3) was investigated. According to objective (4), in-situ test were carried out in the Milldam Mine of Laporte Minerals.

1.3 THESIS STRUCTURE

In Chapter 2, the state-of-the-art knowledge on rock cutting is reviewed. The different models on cutting mechanisms, in particular the so called cutting and friction model are observed. The correlations between rock properties and the machining performance for various cutting methods are presented to show the different opinions on the subject. Some theories closely related to this research on metal cutting are also reviewed in this chapter.

Chapter 3 presents the specific features of diamond abrasive cutting process and the cutting tool. A useful knowledge is given on the diamond relative wear and particle wear. The main results obtained in the past on the diamond abrasive cutting including the "sawability" are reviewed.

The techniques of diamond sawing are summarized historically and technologically in Chapter 4, especially diamond wire sawing. These studies indicated that this technique can be transferred from surface to underground based on the considerations of technical characteristic, cutting efficiency and economics.

Chapter 5 introduces the experimental programme for diamond circular sawing tests on six rock samples. The developed theories on diamond abrasive cutting such as the optimization, diamond wear and force pattern are given.

In-situ tests of a diamond wire saw underground is presented in Chapter 6. The development of the wire tension equation is also discussed in this chapter.

Chapter 7 presents a comprehensive theory on sawability of rock. A standard sawability test is recommended in this chapter. The relationship between the rock properties and the defined sawability is discussed based on the analysis of the experimental results obtained from the conventional rock tests.

Finally, the contribution made by the author in the field of rock cutting by the use of diamond abrasive cutting tools is listed in Chapter 8, and proposals for further research is made. The computer program developed is described in the Appendix.

CHAPTER 2

GENERAL STUDIES ON ROCK CUTTING

2.1 INTRODUCTION

From the inception of productive applications of modern processes of rock fragmentation, their use has been essential to the process of civilization due to the efforts made by mechanical engineers, tool makers and scientific researchers. The machine development has lead to a rapidly increasing use of mechanical rock breaking using different types of machines in different applications. Generally speaking, the rock can be fragmented by the use of mechanical ways of cutting, drilling, sawing and ripping from large block extraction to secondary breaking. In spite of different mechanical methods, any force that is applied to the rock will result in an equally large force in the machine. However machines have been built sufficiently strong to withstand such forces by the mechanical engineers nowadays.

The tool maker has also played his part, with improvements in tool materials and manufacturing techniques. Nowadays, various tool shapes and tool materials are used for the purpose of rock cutting, e.g., tungsten carbide rotary cutter, PDC (Polycrystalline Diamond Compacts) drag bit, diamond abrasive segment and bead.

The theories of rock cutting are probably more important to improve the overall techniques and have been investigated experimentally and analytically in the world for a rather long time. There is a large amount of information in the literature concerning models of rock behavior and cutting mechanisms. Various attempts have

been made to correlate the rock properties with machining performance in order to make judgements on machinability. In this chapter, those achievements will be briefly described.

2.2 MECHANISMS OF ROCK CUTTING

Much research has been conducted trying to develop models relating to the mechanism of rock cutting. Such models are very important for understanding the processes of cutting. Although they contain some simplifications, they often describe reality quite well. It may be useful to divide those models into three: pure cutting models, numerical models and cutting and friction models.

2.2.1 Pure cutting models

Probably, one of the first models for rock cutting with picks was developed by Evans[2]. Based on his early experimental work, he showed that during the penetration of wedges normal to the surface in certain types of coal, cracks attributed to tensile breakage radiate from the tip of the wedge. Later on, he further developed the theory from the ploughing of coal by a sharp wedge to take into account blunting of the wedge[3]. His model was based on the assumption that the rock breakage is tensile in character and the assumed geometry is shown in Figure 2.1. From this model, it is possible to calculate peak forces on the cutting tool:

$$P = \frac{2\, t\, a_p \sin\theta'}{1 - \sin\theta'} \qquad (2.1)$$

Where, t = tensile strength of the coal

a_p = depth of cut

θ' = semi-angle of wedge

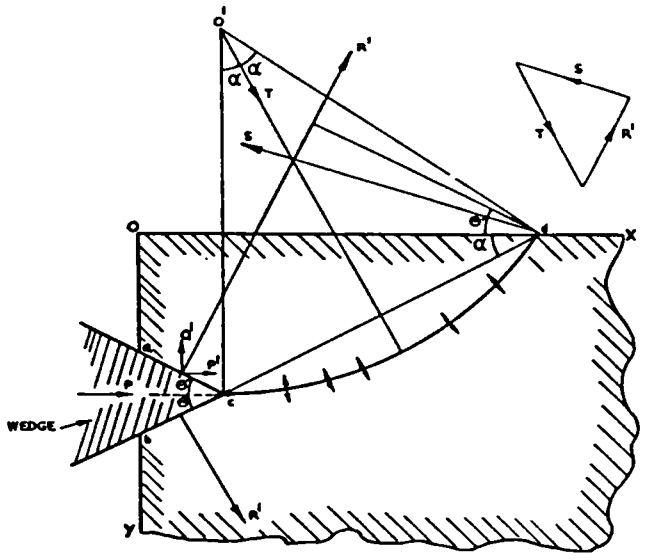


Figure 2.1: Tensile breakage theory proposed by Evans (1965)

Nishimatsu[4] observed the process of orthogonal rock cutting in a plane state of stress as schematically shown in Figure 2.2.

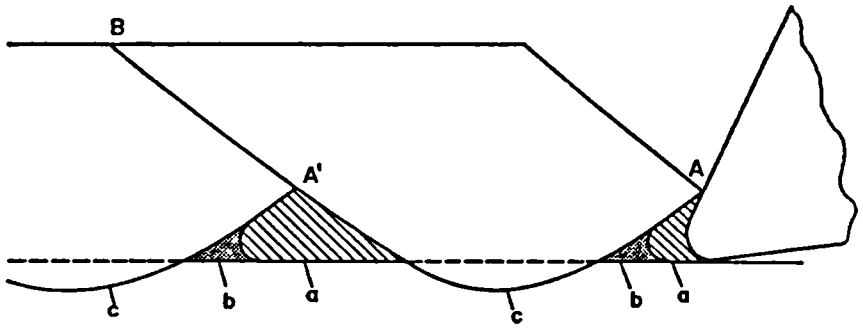


Figure 2.2: An illustration of the rock failure process during cutting as proposed by Nishimatsu (1972)

He described the rock cutting as a cyclic fracture process:

(1) Formation of the primary crushed zone. As soon as the tool edge is pushed into the buttock, a crushed zone is generated about the tool edge. The material is recompacted and sticks to the tool edge (see zone **a** in Figure 2.2).

(2) Formation of a coarse cutting chip. As the tool goes on deeper, a critical value of penetration generates a state of stress which allows the propagation of a macroscopic failure crack.

(3) Formation of the secondary crushed zone. As the tool goes on forwards, a peak remaining in the lower part of the initiation point of the macroscopic failure crack is crushed to a fine cutting chip (see zone **b** in Figure 2.2).

Following the last step of the cutting process, the tool goes on into the overcutting zone (zone **c** in Figure 2.2) without any substantial resistance, until the tool edge is forced against the next buttock which is formed by the macroscopic failure crack mentioned above. Thus, a new cycle of the process of rock cutting starts again.

Based on his observation and some assumptions, a theory on the mechanics of rock cutting was developed. In this theory, the resultant cutting force can be calculated from Figure 2.3.

$$F = \frac{2}{n' + 1} S a_p \frac{\cos k'}{1 - \sin(k' - \alpha' + \phi')} \qquad (2.2)$$

Where, n' = the stress distribution factor

S = the shear strength of specimen rock

k' = the angle of internal friction

α' = the rake angle of cutting tool

ϕ' = the angle of friction of rock cutting

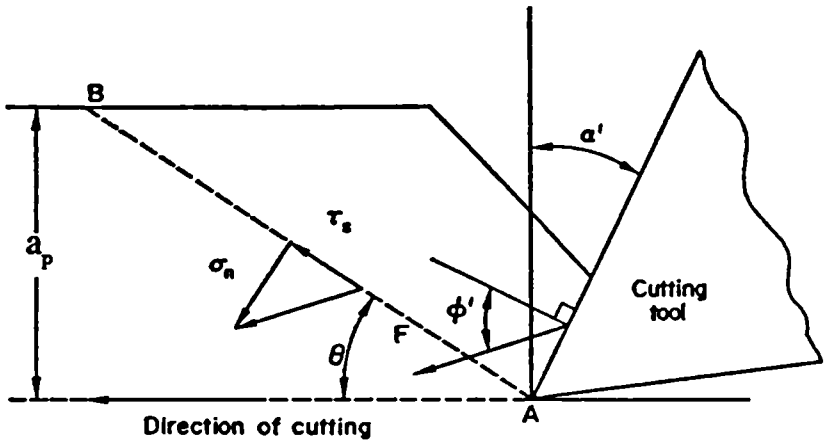


Figure 2.3: Stress and cutting forces for orthogonal cutting (After Nishimatsu, 1972)

Roxborough and Phillips[5] developed analytical models for describing rock cutting with discs. He assumed that the resistance to penetration is essentially compressive and that the force is equivalent to a compressive stress acting over the projected area of disc contact and the cutting force can be calculated according to the model by knowing the compressive strength of the rock.

It is noted that in Evans model the cutting force is calculated in relation to tensile strength of the rock and in Nishimatsu model the force is calculated in relation to shear strength.

2.2.2 Numerical models

With regard to numerical models, the best known application is the finite element method for calculating stresses in complicated structures.

Wang and Lehnhoff[6] attempted several computations with indentation models for different bit geometries. A typical result is presented in Figure 2.4. The purpose of their study was primarily to develop a general mathematical rock failure model and along the available finite element techniques to establish a computer code, which will allow the simulation of the sequence of penetration mechanisms and provide a better description of the failure phase - initial cracking, crushing, and chipping.

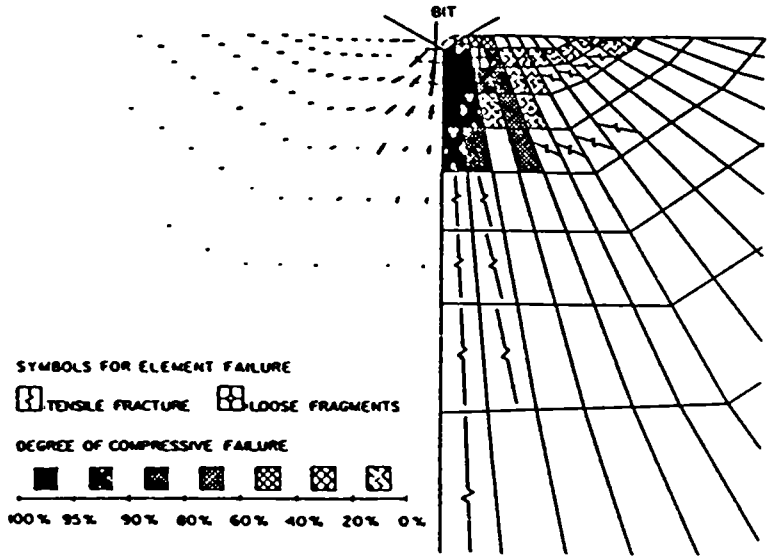


Figure 2.4: Sharp wedge bit penetration (After Wang *et al*, 1976)

Ingraffea[7] studied crack propagation with a fracture mechanics approach using finite element methods to model fracture propagation in rock. He presented an example problem (Figure 2.5) that simulates "in a very simplified manner" a plane strain analysis of chip formation under a cutter.

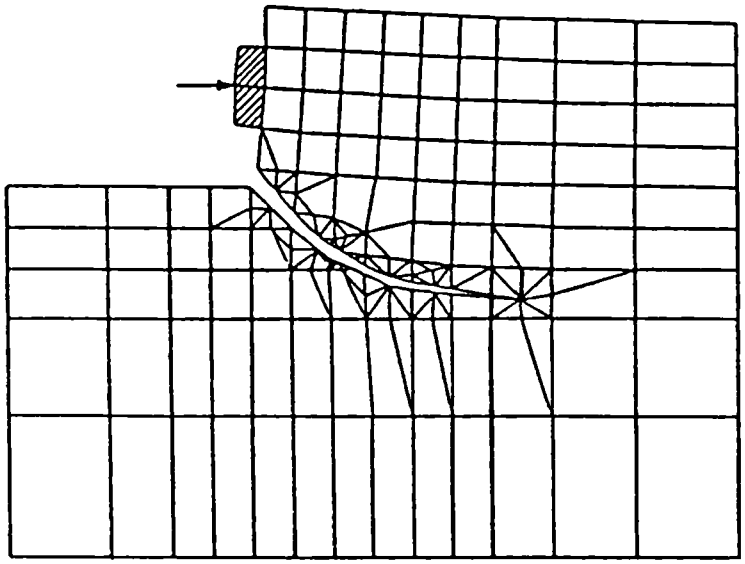


Figure 2.5: Final deflected shape and crack trajectory (After Ingraffea, 1987)

2.2.3 Cutting and friction models

A new model for the forces on the cutting tool was published by Detournay and Detournay[8], based on the investigation of the performance of PDC bits. It considers the basic cutting process as combination of "pure" cutting and frictional contact underneath the cutter. It assumes a constant cross-sectional area of cut and friction at the tool/rock interface. As this model will be used for determining the friction coefficient between rock and cutting tool, it is of interest to introduce this model here.

The model firstly considers a perfectly sharp cutter which creates a groove of constant cross-sectional area, A, when it is moved across a horizontal rock surface at a constant depth of cut. This cutter can only transmit a force through the contact of its cutting face with the rock. Let $\mathbf{F}_c$ denote this force and $\mathbf{F}^c_s$ and $\mathbf{F}^c_n$ represent its components in the parallel and normal directions to the rock surface respectively

(see Figure 2.6). They assumed that the forces in the horizontal and vertical directions are proportional to the cross-section area, **A**:

$$F_s^c = \varepsilon' A \tag{2.3}$$

$$F_n^c = \xi \varepsilon' A \tag{2.4}$$

Where, the constant ε' is the intrinsic specific energy, and ξ is the ratio of the vertical to horizontal force acting on the cutting face, which implies that there is friction at the rock-cutter interface. If the failed rock flows upwards along the cutting face and assuming that there is no transverse component of the cutting force, and the ratio ξ takes the particular maximum value ξ^*.

$$\xi^* = \tan(\theta_1 + \psi) \tag{2.5}$$

ψ denotes the interfacial friction angle and θ_1 the back rake angle of the cutter.

When a cutter with a wear flat is considered, the model was extended by assuming that two force vectors $\mathbf{F_c}$ and $\mathbf{F^f}$ act on the tool during cutting. The first force vector, $\mathbf{F_c}$ is transmitted by the cutting face, while the second one, $\mathbf{F^f}$, acts across the wearflat area of the blunt cutter (see Figure 2.7). This second force vector can be decomposed into a horizontal and normal components, $\mathbf{F^f_s}$ and $\mathbf{F^f_n}$, that are related by the friction law:

$$F_s^f = \mu_c F_n^f \tag{2.6}$$

where μ_c is the coefficient of friction between tool and rock.

From these basic equations, a linear relation between F_s, F_n and A can be written:

$$F_s = \varepsilon' A + \mu_c F_n^f \qquad (2.7)$$

Writing F^f_n as $F_n - F^c_n$ and using Equations 2.4 and 2.7, this equation becomes:

$$F_s = (1 - \mu_c \xi)\, \varepsilon' A + \mu_c F_n \qquad (2.8)$$

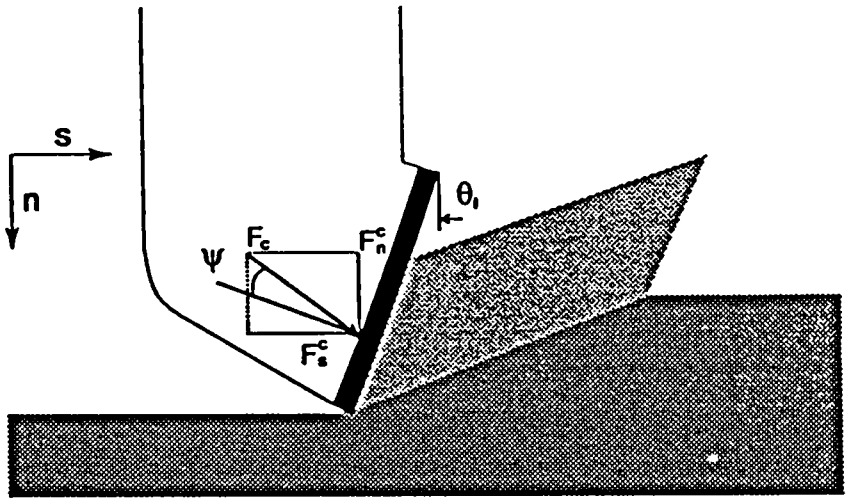


Figure 2.6: Forces acting on a sharp cutter (After Detournay *et al*, 1992)

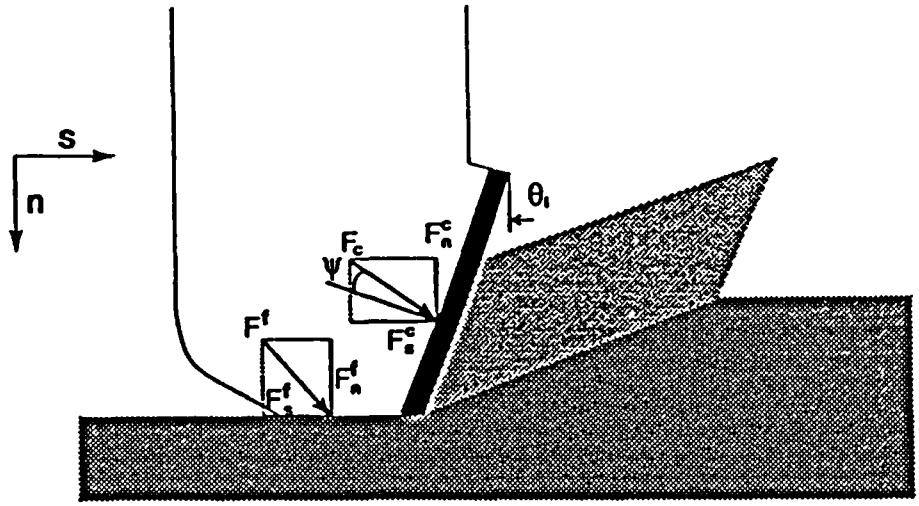


Figure 2.7: Forces acting on a blunt cutter (After Detournay *et al*, 1992)

One concept introduced here is the ε - S relation. Firstly, they introduce two quantities: the specific energy, ε, defined as,

$$\varepsilon = \frac{F_s}{A} \tag{2.9}$$

and the drilling strength S,

$$S = \frac{F_n}{A} \tag{2.10}$$

Noted that ε is the energy spent for drilling, irrespective of the state of the cutter (sharp or blunt), while ε' is meaningful only for the cutting action. Therefore, for a blunt cutter (cutting and friction model), there exists a linear relation between ε and S, which is obtained by dividing Equation (2.8) by A:

$$\varepsilon = \varepsilon_o + \mu_c s \tag{2.11}$$

where the quantity ε_o is defined as:

$$\varepsilon_o = (1 - \mu_c \xi)\varepsilon' \tag{2.12}$$

Actually, Equation 2.11 represents a constraint on the response of cutter. Three parameters appear in this equation: two for the cutting ε' and ξ, and one for the frictional contact, μ_c. Equation 2.11 is represented graphically in the ε - s diagram (see Figure 2.8) by a line with slope μ_c, intercepting the ε-axis at ε_o. This line is defined as the friction line. All the admissible states of the response of a cutter lie on the friction line above and to the right of the cutting point. The cutting point is the point at the intersection of the friction line with the cutting locus, the line that goes through the origin with a slope of ξ^{-1}.

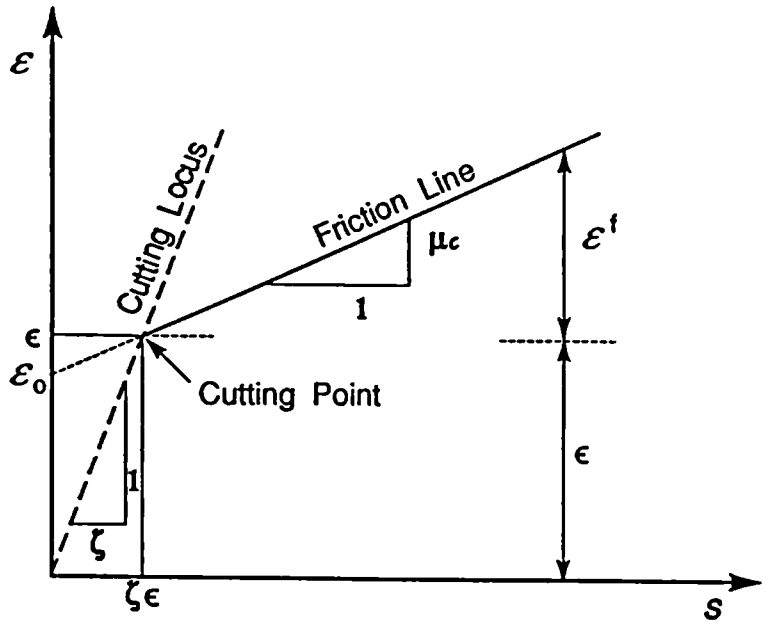


Figure 2.8: ε - s diagram (After Detournay *et al*, 1992)

2.3 CORRELATIONS BETWEEN ROCK PROPERTIES AND MACHINING PERFORMANCE

In the field of rock cutting, much research has been conducted trying to correlate machining performance with rock properties in different rock cutting methods. One could easily find a lot of references related to this area. It is almost impossible to give the different methods a rating with respect to quality or accuracy. The value of a specific test is different to every user. The value depends, to a large extent, on the experience of this test that the user has. This is the reason why most machine manufacturers and many universities and other research institutions often have a test of their own.

A project was undertaken to investigate the relationship between a Dosco SL-120 roadheader performance and rock mass and rock material parameters at Curraghinalt Mine by Royal School of Mines, Imperial College[1]. The rock consists of quartz-rich psammites and graphitic and pelitic schists. Roadheader performance data which was recorded and used as the basis for this comparison consisted of picks used per meter and meters advanced per shift. These factors can be considered to relate to tool wear and machining rate. Prediction equations have been formed for roadheader by relating its in-situ performance to rock parameters. The analysis of the linear regression confirmed that the RMR (Rock Mass Rating) is the strongest indicator of machine performance. In the case of the machining rate, it would appear that the Intact Rock Strength as measured by the Schmidt Hammer may be usefully included with the RMR in the developed equation for predicting this parameter. In the case of tool wear, it was found that the RQD (Rock Quality Designation) is a second factor worth including in another equation used to predict the pick consumption.

McFeat Smith and Fowell[9] used a multiple regression program to analyze the data collected from Dosco roadheader performance to laboratory cutting indices, in order to determine the petrographic, mechanical and physical properties of importance in explaining the cutting characteristics, tool wear rates and debris size produced by mechanical excavation systems. They measured 23 different rock parameters from mineralogical composition to hardness and compressive strength. They also performed liner cutting tests and obtained the specific energy of cut for each type of rock. Their analysis showed that the most relevant parameters for the specific energy were cone indenter hardness and plastic deformation. For the case of wear on the tool, they concluded that quartz content, cementation coefficient and the Shore rebound hardness were the parameters that gave the best correlations. The results were then given as predictive equations.

Misra[10], in his work, "drillability studies of rotary-percussive drills", used a large number of rock parameters to find a relationship to machine performance. He found many correlations between drillability and uniaxial compressive strength, triaxial testing results, static Young's modulus, Shore scleroscope hardness, impact hardness, apparent density and apparent porosity. The most important of these is the correlation between drillability and the so called rock impact hardness number. This may be due to the fact that test failure is similar to the mode of failure during excavation. The impact hardness test is a form of incremental crushing test.

Nelson *et al*[11], after an analysis had been made of the cutting mechanism, reached the conclusion that rock fracture and chip formation is a process in which energy is consumed in the creation of new surface area. They studied the relation between fracture toughness, fracture energy and the field penetration index of two case history tunnels. They arrived at the conclusion that for massive, brittle materials, the

critical energy release rate can be correlated with machine performance. That the correlation is consistent with the formation of rock chips because of the fracturing process. The correlations were made for only four types of rock so that results were speculative but promising. They also concluded that the critical energy release rate can be correlated with TBM performance and that this correlation is consistent with the formation of chips by fracture process.

Many other correlations have been proposed in the literature between measured rock properties and machining performances[12-15]. However, it is not necessary to review all of them here.

2.4 SOME RELATIVE THEORIES ON METAL CUTTING

There is no doubt that the progress of rock cutting has been greatly affected by the developments of metal cutting. The history of metal cutting dates from the latter part of the eighteenth century. Since the now-famous paper by Taylor[16] was published in 1906, empirical and fundamental work on metal cutting has gradually increased in volume. Most of the fundamental work has been carried out since the publication of the well-known paper by Ernst and Merchant[17] in 1941, dealing with the mechanics of the metal cutting process and in which the so-called "shear-angle solution" was first presented. Furthermore, Merchant[18] found that the shear strength of the material increases linearly with an increase in normal stress on the shear plane. It is this oldest model of the cutting mechanism that has served as a basis for the development of other models, such as Evans model and Nishimatsu model for rock cutting.

One of the most important theories in metal cutting is the Taylor Tool Life Equation. About that time, Taylor reported the results of 26 years of research investigations and experience. He was interested in the application of piece-work systems in machine shops, where a time allowance was set for a particular job and a bonus was given to the workman performing his task in the allotted time. To assist in the application of such a system, Taylor investigated the effect of tool material and cutting conditions on tool life during roughing operations. The principal object was to determine the empirical laws that allow optimum cutting conditions to be established. The mathematical form of Taylor's equation was given as:

$$T_t = \frac{C_t}{v^z} \tag{2.13}$$

Where: C_t - a constant taking into account the influence of all factors not appearing separately in the formula. In the physical sense the constant C_t is equal to the tool life T_t period for cutting speed v=1 m/min; z - exponent determined empirically.

Although Taylor connected tool life with cutting speed, feed and depth of cut in separate equations, he never attempted to combine them together. This was done and is known as the Extended Taylor Equation[19],

$$v\, T_t^m\, f^n\, a_p^p = C'_t \tag{2.14}$$

or, can be given in a more convenient form[20].

$$T_t = \frac{C''_t}{v^{1/\chi}\, f^{1/\delta}\, a_p^{1/\rho}} \tag{2.15}$$

In general, the exponent $1/\chi$ related to cutting speed v (m/s) is very much larger than the exponent $1/\delta$ related feed rate f (mm/r) which, in turn, is generally larger than the exponent $1/\rho$ related to depth of cut a_p (mm), i.e. tool life will be least affected by changes in depth of cut and most affected by changes in cutting speed.

It should be noted that in metal cutting, the definition of the tool life T_t in the above equations is the cutting time under constant cutting conditions until conventional dulling of the tool point occurs. Each tool point may be used several times for cutting by resharpening. The sum of all the tool life periods which can be obtained from a given tool point, is another definition called the total tool life.

In abrasive machining of plane metal surfaces, Tarasov[21] presented an interesting paper in which the abrasive machining characteristics of a class 40 gray iron were studied. Tests were made at different feed rates and the volume of stock removed and volume of the wheel consumed were accurately determined. The ratio of the volume of work removed to volume of wheel consumed (grinding ratio = G_g) was determined for a variety of feed rates f. It was found by Shaw and Farmer[22] that the test curves made by Tarasov strongly resemble curves of turning tool life versus cutting speed when plotted on rectangular co-ordinates and obey a Taylorlike equation for abrasive machining of metal.

$$f\, G_g^{\,k} = C_g \qquad (2.16)$$

The tool life equations have played a very important role in metal cutting. In studying the optimization of machining processes, it is necessary to know the relationship between tool life and cutting parameters for the conditions under examination.

2.5 SUMMARY

The models related to the mechanism of rock cutting were studied by various researchers in the past years. These models were divided by the author into three parts as: pure cutting models, numerical models and cutting and friction models. The pure cutting models can be reviewed as the classical theories that use the rock strength properties to describe the rock breakage mechanism. In order to provide a better description of the rock failure process, Finite Element Method was widely used for calculating stresses generated in rock cutting. The cutting and friction models which consider the basic cutting process as combination of "pure" cutting and frictional contact underneath the cutter were introduced in detail.

The main points on the subject of correlating machining performance with rock properties in different rock cutting methods can be summarized as follows:

- It is difficult to find a single rock parameter to precisely predict machining performance. As Morrel *et al*[23] stated: the compressive strength of the rock is not fundamentally related to the rock breaking mechanism and therefore cannot be used as a reliable method of predicting machinability. Rad and Olson[24] did find that compressive strength could be used to predict some of the cutting characteristics of independent grooves in rock.

- It is almost always possible to find some parameters that give a reasonable mathematical correlation with machinability. As Tarkoy and Hendron[25] stated: a coefficient larger than 0.7 for any rock test implies a good correlation between the machine performance and rock parameters. With that criterion one

can always find rock parameters which correlate well with machine performance.

- Rock parameters related to elastic properties have little influence on the actual breaking of rock. As Ranman[26] stated: at the time of fracture, the elastic properties mostly determine how much elastic energy is stored in the rock. This will certainly affect the crack propagation and thereby the final result, but no reported investigation has indicated that this should have any significant influence in rock cutting.

In rock cutting, the theoretical basis for the optimization of operating parameters is lacking. Therefore, a very important fundamental concept used in metal cutting known as the Taylor Equation and its extended forms are introduced. Furthermore, a Taylorlike relationship also exists in abrasive machining of metal.

Diamond abrasive cutting, as a branch of rock cutting, has its own specific features. Therefore, the next chapter concentrates on the studies of the abrasive cutting process and cutting tools. A relevant literature review will also be given.

CHAPTER 3

DIAMOND ABRASIVE CUTTING AND THE CUTTING TOOL

3.1 DIAMOND ABRASIVE TOOLS

An abrasive tool is a porous solid of a determined shape and dimensions, containing in its volume abrasive particles held in a sufficiently permanent manner by a binding material called the bond or matrix. The following properties of the cutting tool should be known.

- type of abrasive material,
- particle size and concentration,
- properties of bond (matrix) and diamond segment.

The abrasive tool features listed above influence the course and results of abrasive processes. Therefore a good knowledge of those features is the basis for optimization of abrasive process conditions.

3.1.1 Diamond type

De Beers Industrial Diamond Division produces a wide range of diamond particles, both synthetic and natural, to suit the individual machining requirements of all stone materials. These diamond abrasives can broadly be categorized into the following areas:

(a) SDA range

This is a range of synthetic diamond abrasives, all coarser than 60 US mesh size. Individual particles have a blocky, regular shape with a predominance of cubo-octahedral crystals, the ideal shape for maximum strength and wear resistance.

(b) MDA range

These particles are similar in shape and strength to the SDA range, but are available in sizes below 60 US mesh.

(c) Natural grits

Natural diamond abrasive has many advantages over synthetic diamond abrasive such as greater bond retention, sharper cutting edges (useful for free-cutting tools), higher thermal stability and greater suitability for electroplating. EMB and EMBS are produced by crushing natural bort and grading to sizes above 60 US mesh. SNDMB is similar in shape and strength to EMB/EMBS but is available in sizes finer than 60 US mesh. EDC is a crushed synthetic particle which exhibits similar shape characteristics to EMB, resulting in excellent bond retention and free-cutting action. In certain applications, this range of grit may be preferred to SDA.

3.1.2 Diamond size and concentration

For stone working tools, the diamond sizes used are between 0.15 and 0.9 mm average particle diameter (FEPA D181- D1001 or 80/100 - 16/20 US mesh) except in the case of polishing applications where vary fine powder is used[27].

The diamond concentration in an abrasive tool is defined as: a concentration of 100 is conventionally defined as having 0.88g (4.4 carats) of diamond grains per cm^3 of

impregnation, or approx. 25% by volume. All other concentrations are proportional. It, in conjunction with the diamond particle size, governs the number of cutting points per unit area, which is proportional to the concentration and inversely proportional to the mean particle size.

3.1.3 Properties of bond and diamond segment

The effective use of diamond abrasives in metal bond tools, such as diamond saws, depends to a large extent on the materials that are used to hold and support the diamond particles while they do their work. The technique for maximizing this relationship includes atomic bonding at the metal/diamond interface, proper mechanical support, and degradation rate control. Nowadays, tungsten and tungsten carbide together with suitable bond alloys (frequently copper/nickel/zinc) are extensively used in metal bond tool manufacture[28].

A toolmaker has also played his part, with improvements in bonding matrix composition and manufacturing techniques, such as laser welding of the segments to the sawblade blank which can be used with or without coolant, thus enabling better diamond blade cutting efficiency to be achieved[29].

In general, the long useful life of a diamond impregnated product is derived from the wear resistance of the metallurgical bond. The diamond tool manufacturer should design a matrix in accordance with the wear characteristics of the diamond, taking into account the material to be cut, so that diamond and bond wear proceed in parallel. Without toughness and durability, the bond will wear faster than the diamond resulting in the possibility of the diamond "falling off". On the other hand, an extremely wear-resistant bond will wear very slowly compared to the diamond,

causing the bond surface to "glaze-over"[30]. The sound production should be the result of a collaboration between the diamond producer, the diamond tool maker and the end-user of a diamond product.

3.1.4 Selection of diamond tools

Diamond type

It is very important to select the most efficient diamond type for various sawing applications. For example, comparing SDA with SDA100 on hard Georgia granite, tool life was increased 100% by providing a more wear resistant bond with the improved diamonds[31]. A selection of diamond types is listed in Table 3.1.

Table 3.1: Selection of diamond type

Diamond types	Sawing conditions
SDA+, SDA	relatively soft materials, such as hard marbles and limestones
SDA85+, SDA85	wide range of industrial sawing applications in both natural stone and concrete
SDA100+ SDA100	exceptionally hard material, such as hard granite, refractories, concrete containing tough aggregates
MDA	grinding and milling operations, with a finer finish

Synthetic diamond is now the preferred type of abrasive used in the stone industry, since controlled manufacturing conditions enable the diamond types to be produced for specific purposes and with the guarantee of product consistency. SDA is superior to any other available particle for hard stone sawing, especially for granite.

Diamond particle size

The size of a diamond particle determines its protrusion above the bond surface and also regulates the clearance of swarf from the cutting zone. In general, hard materials require a smaller diamond size than softer stones. This is because the load per particle is not as high for softer materials and a greater clearance is required for swarf. If the speed of the blade remains constant and the sawing rate increases, then an increase in diamond size will be necessary, since each individual particle has to remove a larger volume of rock material per blade revolution and consequently demands a greater clearance to optimize swarf ejection[32].

The generally recommended sizes are as follows: 40/50 US mesh - for hard grained materials (e.g. granite, basalt); 30/40 US mesh - for medium hard materials (e.g. marble); 20/30 US mesh - for relatively soft materials (e.g. limestone, sandstone). The main advantage of using coarser particle is a faster cutting rate. However, if such a particle is used on hard materials, the penetration of each diamond particle is limited and either excessive pull-out occurs or large wear flats appear on the diamonds.

Diamond concentration

A concentration between 20 and 40 will suffice for sawing practically all natural rocks. In general, the softer and more abrasive the stone, the higher should be the diamond concentration. In order to gain the most benefit from the diamond abrasive, it is obvious that high concentrations must be used, because for a given set of parameters, high blade life can be expected from high concentrations[33]. However, when applying high concentration to increasing the tool life, a sufficiently high cutting power must be available. Otherwise the load on an individual particle is correspondingly low, i.e. the particle penetration depth is shallow, which results in

polishing the diamond. In such a case, little or no cutting action is observed and the blade requires redressing.

Segment type

The so-called "sandwich" segment type is recommended for rock cutting. The sandwich is a three or more layer segment in which the outer layers differ from the inner one(s) in their susceptibility to wear, as shown in Figure 3.1[34]. Due to the relatively lower abrasion resistance of the inner layer(s), a desirable self-sharpening wear of such a segment is observed at work.

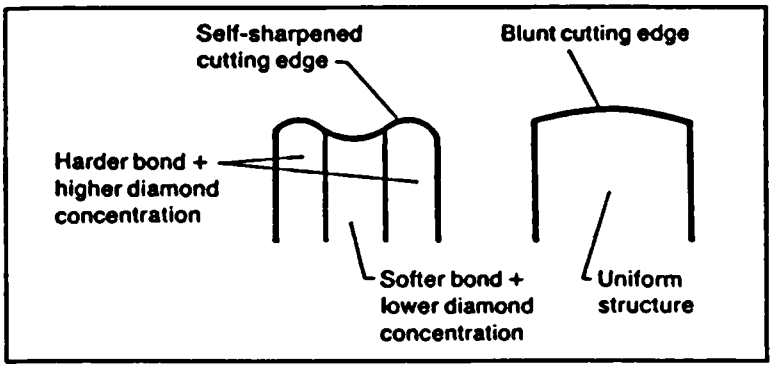


Figure 3.1: Wear patterns of the sandwich (left) and conventional (right) diamond impregnated segments (After Konstanty, 1991)

3.2 CUTTING PROCESS AND SPECIFIC FEATURES

Diamond tools for stone cutting are generally made up of the diamond abrasive, the bonding matrix, and the steel blade or center to which the segments are attached. Figure 3.2 shows the typical conditions under an impregnated segment works. Approximately, one-tenth of the diamond particle size penetrates the material being cut, three-tenths is exposed to provide room for the cuttings and circulating fluid,

and six-tenths is held in the matrix[35]. Therefore, diamond exposure is needed more for the cuttings than for penetration.

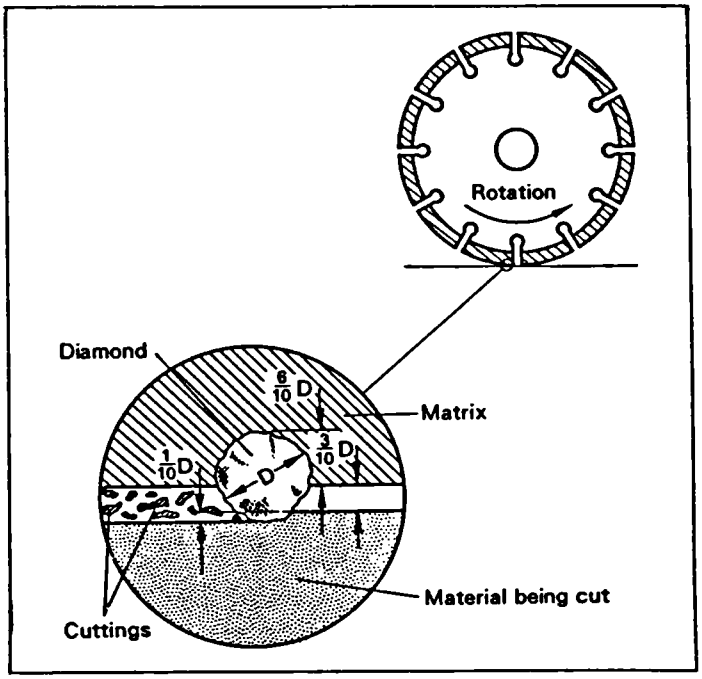


Figure 3.2: Typical cutting conditions under a saw blade segment
(After Bridwell *et al*, 1974)

The cutting edge of a diamond abrasive tool is composed of a large number of minute cutting edges on the matrix surface. Each diamond particle has its own individual life span. Initially the diamond particle is covered by the bonding matrix. Due to wear and tear, the matrix level is eroded to a point where the diamond particle is exposed, and thus contact is made between the diamond particle and the stone. In the following phases the diamond particle takes part in the cutting process, when it is subjected to wear.

The size and volume of the undeformed chip cut by a single abrasive particle is very small. As abrasive particles penetrate the material to a depth of the order of

micrometers to hundreds micrometers, a considerable number of particles may not cut at all. Since particle corners are rounded off at the top, a certain minimum penetration of the particle into the material is necessary for the cutting process to begin. The minimum tool penetration depth $\mathbf{h_{min}}$ may depend on the properties of the rock material. When the penetration depth reaches to $\mathbf{h_{max}}$, the particle remains mainly intact and wears at a rate equal to the erosion rate of the blade matrix until the particle breaks down. Further erosion of the matrix will result in the particle either being lost or coming back into contact with the rock material and subsequently being lost due to matrix erosion. The slight decline in the height of penetration coincides with cleavage on the side of the particle and progressive wear on the top surface.

A tabulated description of the development of wear progression of two diamond particles were given by Wright[36]. Figure 3.3 shows the height of penetration by those two particles when sawing Cornish grey granite.

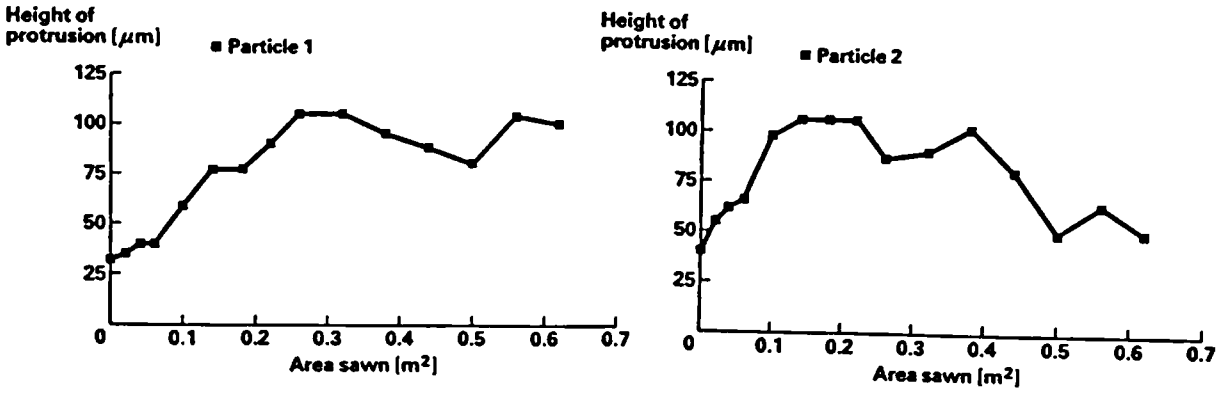


Figure 3.3: Height of penetration of diamond particles versus cumulative area sawn (After Wright, 1988)

The graph in Figure 3.3 shows that, for particle **1**, matrix erosion took place around the particle at a reasonably constant rate until 0.26 m^2 had been sawn. At this stage, the particle had reached a height of protrusion of 105 μm. After a sawn area of 0.32 m^2, the slight decline in the height of protrusion coincided with cleavage on the side of the particle and progressive wear on the top surface. Unlike particle **1**, the rate of increase in the height of protrusion of particle **2** was rapid. Again, a penetration of between 100 μm and 110 μm was achieved. This level was maintained until a sawn area of 0.38 m^2 had been reached. Having broken down to certain level, the particle remain at a constant height of protrusion until the end of the test.

There lies here a difference between frame and circular saws. With circular sawing, the blade rotates in a constant direction at high speeds, usually in excess of 30 m/s. The wear on the diamond particle and matrix is therefore also constant in one direction. This leads to the development of a 'trail' of matrix behind each individual diamond particle which acts as a support during cutting as shown in Figure 3.4[37]. So for hard stone cutting, the diamond particle itself must be strong and blocky to withstand the constant one directional impact force.

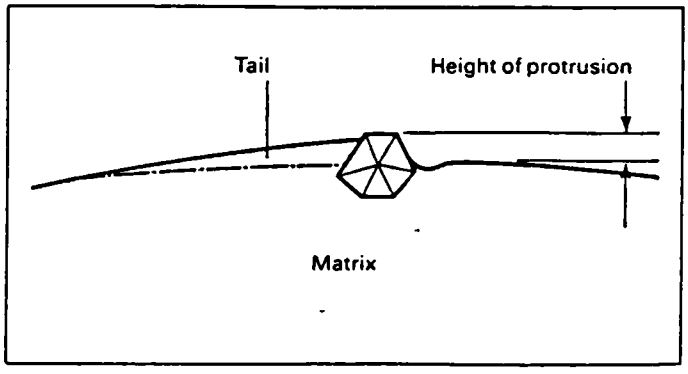


Figure 3.4: Diamond particle protrusion (After Jennings, 1988)

Frame sawing, on the other hand, involves a reciprocal sawing action where the forces act in alternate directions with each stroke of the cutting tool. Consequently there is no build-up of a matrix 'tail' and in many cases it is advantageous to use a diamond particle more irregularly-shaped than that used in circular sawing, to ensure greater bond retention.

In summary, sawing of stone with impregnated diamond tools can be characterized as bonded abrasive processes and the following characteristic features of abrasive processes should be noted:

(a) as a result of different point forms situated in random positions, only a part of them carry out the actual cutting work, another part plastically scratches the work material surface, while still other part rubs against this surface causing only elastic deformations,

(b) the size of the undeformed chip cut by a single point is very small and varies from point to point,

(c) the vertical cutting force is higher than the horizontal cutting force and in turn the thrust force is higher than the tangential force,

(d) the abrasive tool is the only cutting tool which has the ability of self dressing i.e. restoration of the cutting surface through fracture of blunt grains and formation of new cutting edges as a result of cutting forces developed during the process.

3.3 DIAMOND RELATIVE WEAR AND PARTICLE WEAR

The diamond impregnated sawblade is an abrasive cutting tool. In order to determine objectively, and to evaluate, the definitions of abrasive tool wear, the notion of relative wear and particle wear have been introduced.

Generally speaking, change of the original shape and dimensions of abrasive tools, connected with a loss of their mass (volume reduction) as a result of cutting work is called abrasive tool wear. As described by Atkinson and Cassapi[38], the three generally accepted modes of abrasive wear are indicted as follows (rock cutting by diamond abrasive tools belongs to mode 2).

(1) Two body, low stress abrasion, caused by gouging or shearing action of the abrasive particles sliding over surfaces and removing wear debris, without reducing the size of the abrading material.

(2) Two body, high stress abrasion, with the effect of impact causing gouging, deformation and material loss.

(3) Three body, high stress abrasion, caused by an abrasive solid present between two surfaces in relative motion that wears the surfaces by a grinding action, through gouging, deformation and fracture.

Abrasive tool wear is expressed by relative wear dimensionally and shown in different terms as in the following relationships:

- Relative volumetric wear:

$$G = \frac{V_t}{V_m} \tag{3.1}$$

Where, V_t is volumetric loss of the abrasive tool, V_m is volumetric loss of the rock material.

- Relative superficial wear:

$$G_A = \frac{V_t}{A_m} \tag{3.2}$$

Where: A_m is the machined surface area.

- Relative linear wear:

$$G_B = \frac{L_t}{A_m} \tag{3.3}$$

Where: L_t is the linear loss of tool.

It should be noted that the relative wear is described as the tool wear related to the effect on cutting work. For a better understanding the abrasive cutting process, the wear occurring on the individual diamond particle must be known. The assessment of the characteristic diamond particle wear in the saw is confined to microscopic studies. Typical wear features are illustrated in Figure 3.5. The following classifications of the worn diamond particles were widely accepted by the diamond cutting industries[39,40].

(a) Good crystals without significant wear. Those particles are protruding above the surface of the matrix and doing work, whilst retaining their crystal shape and exhibiting no evidence of surface damage.

(b) Flattened particle surface. Such particles display a worn area which is not one of the original crystallographic faces, and which has most probably been caused by abrasion.

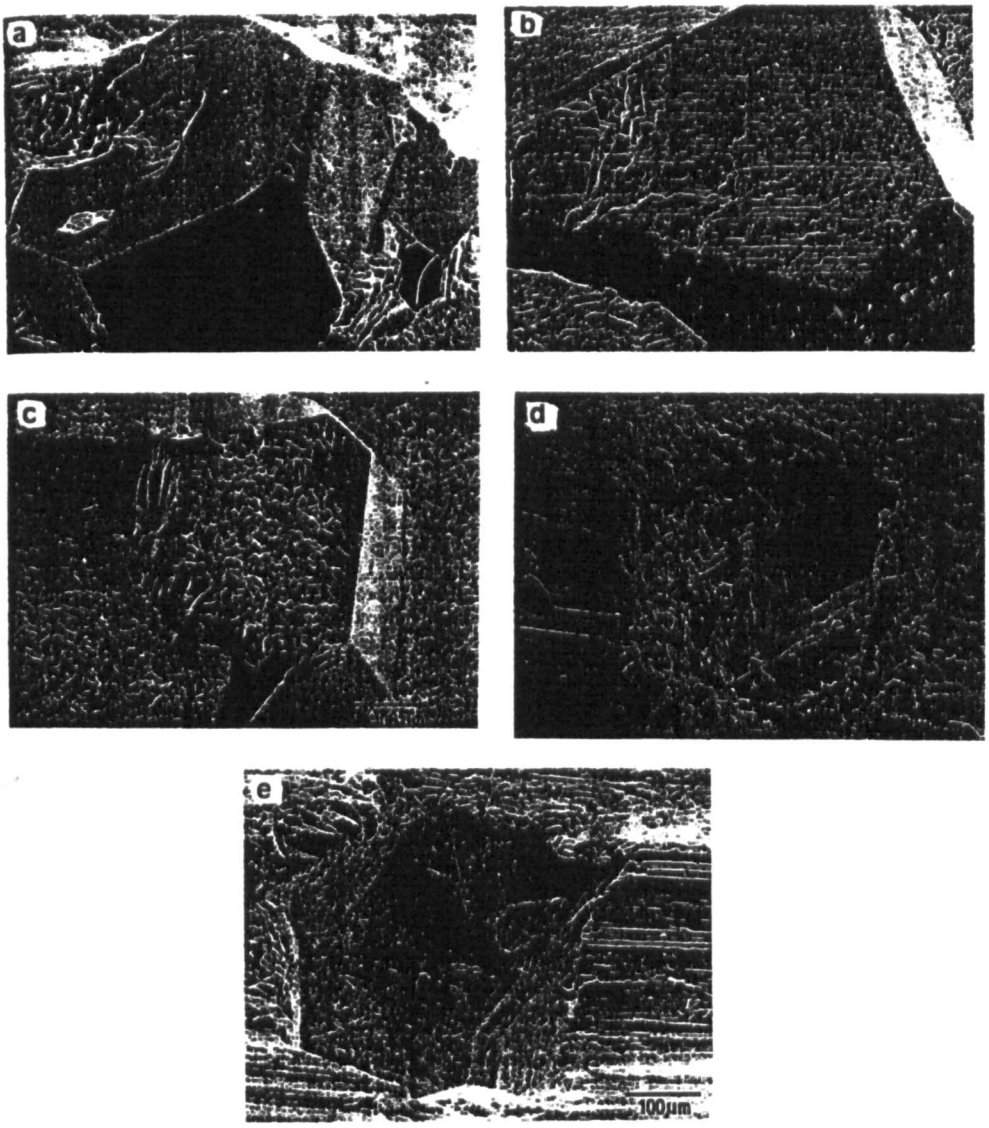


Figure 3.5: Wear patterns on diamond particles (After Miller *et al*, 1990)

(c) Cleaved microfracture surface. Such particles have well-defined wear flats but, as a result of repeated impact with the rock material, these are no longer smooth.

(d) Broken diamond surface. This is probably a progression from the previous classification, whereby repeated impact has caused further damage to the surface of the diamond particle, with the result that no smooth area remains.

(e) Particle pull-out. The worn surfaces holes formed when diamond particles have disappeared from the tool face.

However, definite classification in to these five types was not always possible. Therefore, intermediate types, such as "microfracture/broken" or "flat diamond surface with microfracture", etc., were included.

3.4 REVIEW OF THE MECHANISMS OF DIAMOND ABRASIVE CUTTING

Diamond abrasive cutting is a very complex machining process. Although various researchers have tried to define the mechanisms which should be included in the cutting mechanism and wear mechanism, the answer is still not clear.

Miller and Ball's suggestion[40]

A test drilling a rock type, Bushveld norite, with impregnated diamond microbits was conducted by Miller and Ball and a mechanism of diamond abrasive cutting was suggested based on the assumption that the rock breakage is shear in character. According to his suggestion, the rock fracture mechanism is principally one of indentation of the rock by the diamond particles and subsequent fracture by shear to the free surfaces. The path of fractures is strongly influenced by the cleavage of the constituent minerals and the bonding between adjacent grains. The diamond particles are generally small with respect to the size of the crystal grains in the rock, so that the mechanism of rock fracture is largely determined by the microfractures of the rock.

Nakajima's suggestion[41]

Nakajima used a single point diamond disk to cut stabilized zirconia. The main conclusions related in the studying the cutting mechanism were: (1) There are three different regions varying with depth of cut; elastic, plastic and cutting regions. (2) There are critical depths and critical normal forces at the beginning point of plastic deformation and cutting. (3) In the transitional cutting process, there are three types of interference with maximum depth of cut: elastic region through the contact length; elastic-plastic-elastic; elastic-plastic-cutting-plastic-elastic; (4) Surface generation of a groove is performed by plastic deformation as well as brittle fracture.

Bienert and Lutz 's suggestion[42-43]

According to Bienert and Lutz, there are two principle mechanisms by which diamond particle wear may occur when in sliding contact with a hard non-metallic material such as stone (Figure 3.6).

- When high cutting forces are acting on a sharp diamond point as it first engages the rock, fragments split off, thereby producing sharp new cutting edges and reducing the depth of penetration of the diamond. Linear wear of the segment ultimately brings these cutting edges into renewed contact with the work, and further microfracture occurs. After repeated microfracture of the diamond and erosion of the bond, the diamond particle is finally dislodged from its anchorage;

- With lower cutting forces or a higher abrasive action of the rock, the cutting edge of the diamond particle becomes progressively rounded. A wear flat is formed on the flank of the diamond and the clearance angle is reduced.

The cutting forces acting on the particle increase until the bond can no longer hold the particle, when pull-out occurs.

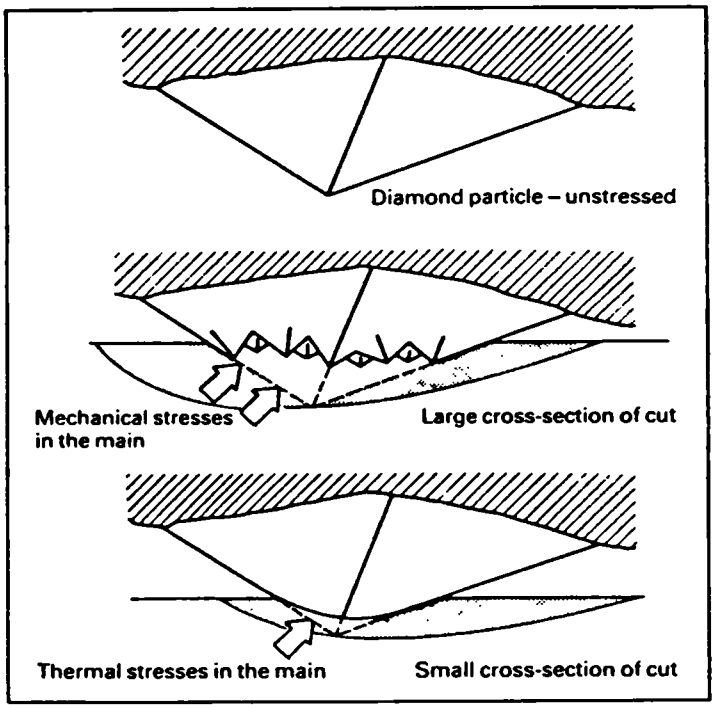


Figure 3.6: Diagram illustrating the effect of material removal rate on the principle mechanism of diamond particle wear (After Ertingshausen, 1985)

Ertingshausen's suggestion[44]

Ertingshausen has monitored relative wear around the whole blade periphery. Two hypotheses were suggested as explanations of the observed relative diamond wear:

- Freshly exposed diamond particles develop wear flats as sawing progresses. This causes the cutting forces to increase and the diamond particles begin to break down. Parts of the particles are then dislodged from the bond in the form of splinters;

- The points of freshly exposed diamonds break off after initial engagement with the rock. These particles then develop wear flats and are pulled out of the bond wholesale by the high cutting forces which exceed the strength of the anchorage.

Bailey and Bullen's suggestion[45]

Based on observations of an actual operation wear characteristics, they suggested that as the rotational speed of the blade is varied, wear may be considered to be the result of two mechanisms:

- impact of the diamond particles on the rock,
- direct mechanical loading as the particles remove the rock material.

3.5 PREVIOUS RESULTS ON DIAMOND ABRASIVE CUTTING

3.5.1 Sawability predictions

A literature review given on machinability in Section 2.3 is related to the various machining processes of rock except diamond abrasive cutting. Many researches studied "sawability" of rocks and methods of predicting rock sawability were investigated due to similar research objectives discussed in that section.

Test work carried out by Wright *et al*[46,47,32]

During 1985-1988, serious sawability tests were carried out at the De Beers Technical Service Center. Test procedures and results were published in three different publications[46,47,32]. The method of this research was to examine standard rock tests including petrological and mechanical examination of the rock properties

and then comparing these results with practical sawing tests in order to determine the rock's suitability for predicting sawability.

In these tests, eight samples were chosen to cover a broad spectrum of stone types. These samples were Grey granite, Pink granite, Larvekite, Red granite, Diorite, Gabbro, Red granite and Sandstone. The coarse grained Red granite was considered to be one of the most difficult natural stones to cut. The sandstone although considered abrasive, was generally regarded as the easiest to cut. The mean Mohs hardness and percentage content of the main minerals (quartz, plagioclase and orthoclase) and the size of the grains were obtained from a study of the petrological properties of the rock. The mechanical properties of the rock were also investigated. The following are the tests carried out:

(a) The Shore scleroscope hardness test: This test is basically a rebound test which measures resistance to penetration.
(b) The NCB cone indenter: The NCB (National Coal Board, UK) Cone Indenter measures the residual penetration of a tungsten carbide cone under a predetermined normal load.
(c) The Cerchar abrasiveness test: This apparatus basically consists of a sharp conical steel stylus mounted in a swinging arm. The stylus is scratched over the rock surface for a distance of 10mm under a normal load of 7kg. Abrasiveness is determined by the resultant wear flat at the point of the stylus, measured on a travelling microscope.
(d) Uniaxial compressive test:Uniaxial compressive strength tests are conducted on a special compression test machine in which specimens are loaded to failure.

(e) Tensile strength test: Tensile strength measurements are also conducted on a compression test machine. The method employed was the Brazilian disc indirect tensile strength test.

Sawing tests were carried out on a Gregori bridge circular saw. During testing, the specific mean linear wear (mm/m^2) and data on power and cutting forces were measured and recorded. The test results showed that when examining the blade wear figures, it is difficult to establish any correlation between petrographic analysis and mechanical properties. The NCB cone indenter test, Cerchar abrasiveness test, compressive strength and tensile strength tests are not very meaningful with respect to blade wear for sawing these hard rocks. The Shore scleroscope measurements appear to correspond closely to the wear results. However, as pointed out, even when taking 100 measurements on each rock type, two samples (Gabbro and Grey granite) of the total 8 samples do not correlate; hence, this test can only be used to give a general guideline on the prediction of sawability. The test also showed that the quartz content alone can not be used as a guideline of sawability. Referring to these test results, the quartz content is far higher for Sandstone than for Red granite, but the wear figures show 90% less wear on the Sandstone. However, the ranking of the samples according to cutting force follows exactly that produced by blade wear. Therefore, an accurate assessment can be made of the sawability of a stone by measuring the vertical force generated during the sawing process.

Test work carried out by Birle *et al*[48]

In 1988, another sawability prediction test was carried out by Birle and a regression equation was obtained. Ten stone types ranging from easiest to most difficult to saw, based on previous empirical testing and field experience, were selected for the study. Petrographic analyses were carried out and the abrasion resistance and average Shore

sceleroscope hardness of each were determined. The wear performance in m^2/mm (square meters of stone per millimeter blade wear) was then entered into a stepwise multiple linear regression analysis against each of the measured properties. Of the seven variables, only two proved to be significant in the regression: Abrasion Resistance and Quartz Content. The resulting regression equation (R=0.84) was:

$$Y = -0.13B - 0.17C \qquad (3.4)$$

Where, Y = Wear performance in m^2/mm

B = Quartz content in %

C = Abrasion resistance (measured using an apparatus according to ASTM Designation C241-51(1958))

Hausberger's suggestion[49]

In 1990, Hausberger[49] claimed that mineralogical analysis can be used to assign a stone to a machinability class without a costly sawing test. According to his analysis, there are numerous criteria which can be used to explain the differences in sawability:

- Owing to its high hardness and absence of cleavability, quartz is difficult to cut. A large proportion of quartz usually means low sawability.

- Thanks to their pronounced cleavability, micas, hornblendes and pyroxenes assist cutting. With these minerals, size of grain and distribution have a greater influence than the quantity. Most favorable to sawing are coarse minerals accumulated in wedges of feldspars and quartzes.

- The plagioclases are easier to machine than the alkali feldspars thanks to their better developed cleavability. In the feldspars it is primarily the composition and state of the minerals which are important. Alkali feldspars with microcline latticing or perthitic intergrowths are more difficult to machine. Increasing sericitization also renders cutting more difficult.

- Plagioclases become more difficult to machine as sericitization increases. The cause of this behavior may well stem from the loss of natural cleavability.

- Sawability can also be affected by grain boundary formation. Minerals with marked interfingering occur more frequently in rocks which are difficult to machine.

3.5.2 Diamond relative wear

Buttner[50] reported test results as shown in Figure 3.7 on sawing Impala granite with a ϕ600 mm diamond circular sawblade at a peripheral speed of 41 m/s, and has shown that the linear wear rises at a uniform rate with increasing cutting rate from 200 cm^2/min to 650 cm^2/min. It was also reported that wear will increase rapidly above a sawing rate of 650 cm^2/min.

Busch and Warker[39] carried out a test on plain cured concrete using a diamond segmented sawblade with a peripheral speed of 50 m/s and found that: as the sawing rate increased from 150 cm^2/min to 600 cm^2/min, blade wear increased gradually as shown in Figure 3.8. It should be noted that in their test, the tool life was inappropriately defined as the area of sawing. In fact, tool life is a time concept,

which is widely accepted in the field of metal cutting and also should be applied to stone cutting.

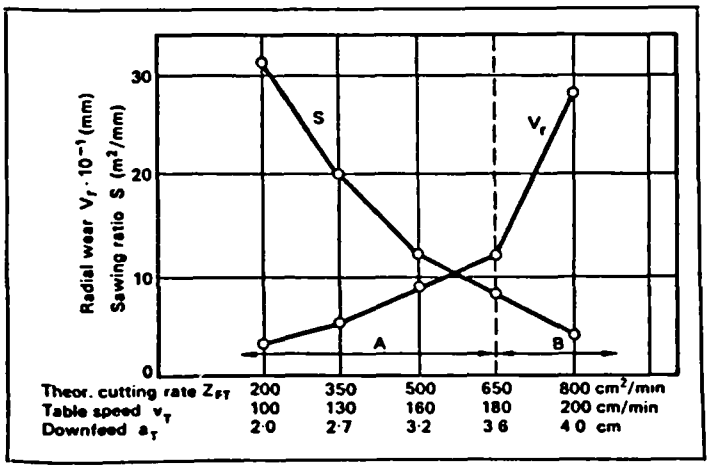


Figure 3.7: Blade wear in sawing hard rock depending on the sawing rate (After Buttner, 1972)

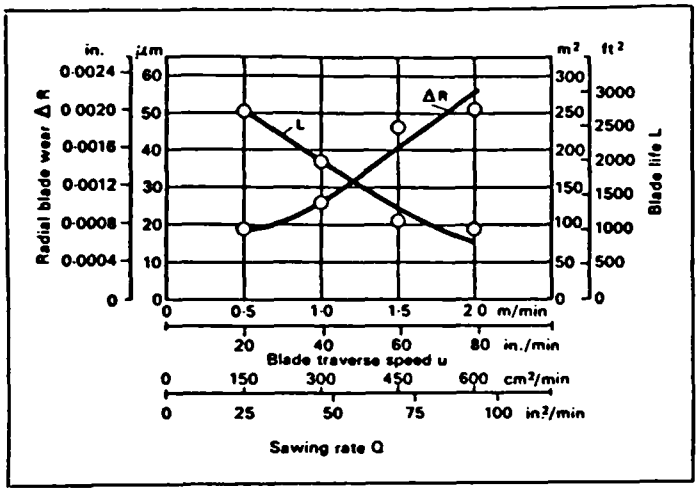


Figure 3.8: Blade wear relative to sawing rate when sawing concrete (After Busch *et al*, 1973)

Jennings[37] proposed a graphical relationship for tool life against sawing rate as shown in Figure 3.9 without giving any details. However, there was no attempt to further define the relationship between tool life and sawing rate in numerical terms.

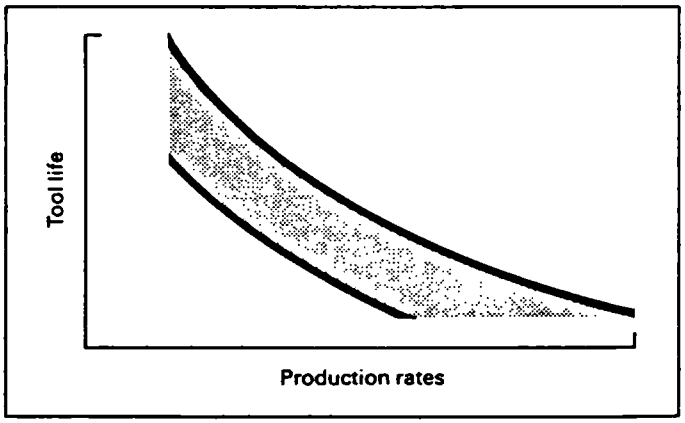


Figure 3.9: The graphical relationship between tool life and production rate (After Jennings, 1988)

3.5.3 Optimum sawing speed

The principle which suggests that different rock materials respond better to different blade peripheral speeds which optimize tool life has been accepted for a long time. Figure 3.10 shows typical results obtained by Bailey and Bullen[45], when sawing a South African black granite (Impala), using 40/50 US mesh SDA85. At a cutting rate of 200 cm^2/min, the optimum blade speed was found to be 35 m/s.

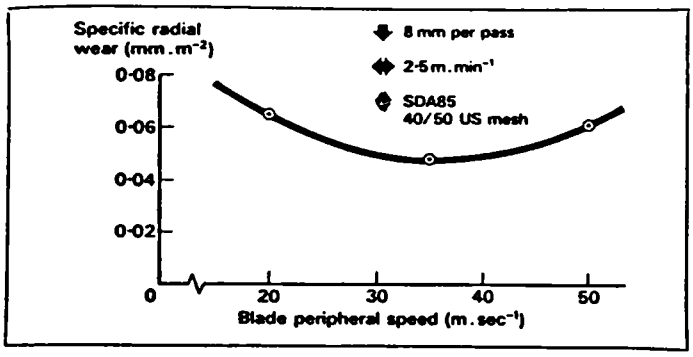


Figure 3.10: Effect of blade speed when sawing Impala (After Bailey *et al*, 1979)

Figure 3.11 shows results obtained by Busch and Warker[39], when sawing two kinds of concrete.

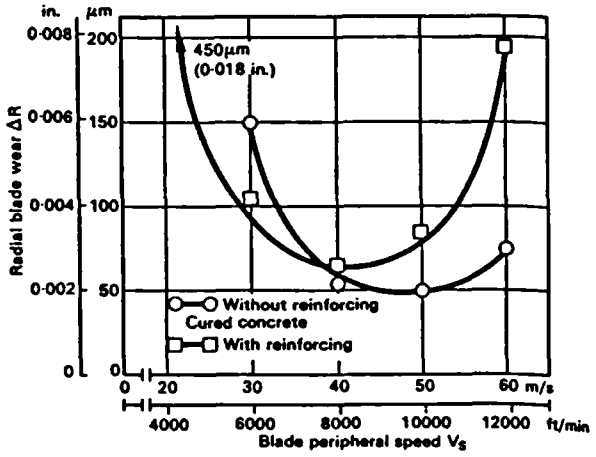


Figure 3.11: Blade wear relative to blade peripheral speed when sawing concretes (After Busch *et al*, 1973)

The results in Figure 3.11 showed:

(a) An increase in blade wear at blade peripheral speeds $v < 40$ m/s and $v > 55$ m/s in plain cured concrete. Lowest wear rates occur in the speed range $40< v <55$.

(b) In reinforced concrete the lowest wear rates were in the speed range $35< v <45$.

The explanations of this phenomenon given by Bailey[45] and Busch[39] have shown different opinions: In the low sawing speed range, they supposed that the wear increase is due to the mechanical load on each diamond particle being increased at decreasing sawing speeds. Beyond the optimum, the wear again increases rapidly. Busch suggested that a rise of sawing temperature would be a dominating factor affecting the wear. Bailey suggested that the impact forces may be sufficient to set up shock waves within the diamond particles causing them to shatter.

3.5.4 Sawing forces

It is well recognized that, increasing the sawing rate by increasing feed speed whilst maintaining the same depth of cut has little effect on cutting forces. Alternatively, maintaining feed speed and increasing depth of cut leads to a substantial increase in cutting forces[32,37].

Test results obtained by Mamalis *et al*[51] discussed the effects of operating parameters on the force components.

(1) The depth of cut has a marked effect on the normal force. For deeper cuts with decreasing feed speeds the normal force increases linearly.
(2) The behavior of the tangential cutting force is different to that of the normal force. With increasing depth of cut and decreasing feed speed the tangential force for sawing Colombo granite decreases considerably. But the tangential cutting force for sawing Impala remains almost constant. As he explained that anisotropy and a difference in the fracture strength of the test material as well as different blade conditions are the probable factors influencing the force values.
(3) The axial force due to lateral contact of the blade with the rock material was found to be negligible.

3.6 SUMMARY

SDA (Synthetic Diamond Abrasive) is now superior to any other particle available for hard stone cutting, especially for granite. The generally recommended abrasive sizes for cutting hard rocks are 40/50 US mesh with a diamond concentration between 20 and 40. Cutting of stone with impregnated diamond tools can be

BL LONDON UNIV

characterized as bonded abrasive processes and the abrasive processes have been analyzed in this chapter. In order to determine the definitions of abrasive tool wear objectively, and to evaluate the diamond segment wear and particle wear, the notion of relative wear and particle wear have been introduced.

A review on the previous test results in the field of diamond abrasive cutting can be summarized as follows:

- At present, "sawability" studies are very limited in their application to the technology of natural rock machinability. The literature review showed that different test results were obtained by different researchers.
- Although several theories on the mechanisms of diamond abrasive cutting were suggested, there are still not definitive as abrasive cutting is a very complex machining process.
- Previous tests suggested graphical relationships for tool relative wear against operating parameters. However, there was no attempt to further define the relationship between tool life and operating parameters in numerical terms.
- Despite the limitations of the previous test configurations, the opinion that different rock materials respond better to different blade peripheral speeds which optimize tool life has been accepted for a long time.
- It is well recognized that, increasing sawing rate by increasing feed speed whilst maintaining the same depth of cut has little effect on cutting forces. However, maintaining feed speed and increasing depth of cut leads to a substantial increase in cutting forces.

Nowadays, diamond saws are the main types of diamond abrasive cutting tools with the potential of underground use for mining purpose. Therefore, the state of the art in diamond saws will be discussed in the next chapter.

CHAPTER 4

STATE OF THE ART IN DIAMOND SAWS

4.1 INTRODUCTION

During recent years, the development of diamond tools for the stone industry has proceeded at a rapid pace, both in areas of traditional usage such as circular sawing for stone block cutting and the application of diamond wire for stone extraction.

The familiar well-tried methods still used today for cutting stone blocks in the plant are the framesaw, circular saw, bandsaw and diamond wire saw. When smaller blocks are cut, circular sawing would be the simple, effective and economic method, although it was announced that hard rock could be cut more efficiently and more economically with a suitably designed bandsaw in some cases. When larger blocks are cut, the diamond wire is more and more popular nowadays, although when sawing smaller blocks the cost of the diamond wire remains more expensive than a circular saw.

All over the world, quarry operators have been eagerly awaiting a better method for the extraction of granite and other hard stones. Now, at last, Diamant Boart, whose purpose-built machines and diamond wires have transformed extraction techniques for marbles, slates, sandstones and limestones, have introduced a cost-effective system for the winning of hard stone blocks. In the diamond wire extraction system, there are several cutting techniques. The mixed technique may be a promising way, to give maximum output from smooth faced large blocks. In this technique, a chain

saw or circular saw is used in conjunction with the diamond wire for stone extraction.

4.2 DIAMOND CIRCULAR SAW

The first diamond circular saw blades for cutting stone were developed in France in 1885 by the research worker Felix Fromhole. Blades from 2-3 meters diameter were frequently employed in the period 1900-1910 for cutting medium-hard stones[52]. These early diamond saw blades consisted of steel discs with a number of cast steel sockets around the periphery. The sockets were fitted into dovetail slots and attached by pins or rivets. Diamond stones up to 0.8 carats in size, or, as stated at that time, "the size of peas", were individually hand-set into each socket. A hole just large enough to take a diamond was drilled in the socket and the diamond was positioned in the hole. The socket was gripped in a special vice with insulated copper jaws, which was then tightened, whilst applying an electric current for a few seconds, thus solidly embedding the diamond. At this stage, approximately 0.75 mm of the diamond protruded from the socket. Diamonds were alternately spaced on either side of the sockets to achieve the required side clearance and they could be re-set in new sockets two or three times.

This led in the late 1930's to the development of matrices formulated from metal powders, which were mixed with the diamond and then sintered to produce a segment. Until synthetic diamond became commercially available in 1959, all diamond used in the manufacture of diamond circular saw blades was natural material from Africa or Brazil. Synthetic diamond now enjoys the largest share of the diamond tool market. Instead of mechanically fixing the segments to the steel disc, the natural progression was to use a brazed joint. The industrial use of laser

equipment now allows segments to be laser-welded to the steel blank. Nowadays, for cutting small blocks of stone to size in a workshop, the diamond circular saw has virtually taken over from all competitors.

Here, the sawblade's structure and the various applications will not be introduced in detail, but the particular applications of using circular saws for mining will be briefly introduced. As investigated by Bracken[53], it was found that circular saws can be used to cut the face from three different principle axes. These are parallel cut to the face, horizontal and vertical cut to the face as shown in Figure 4.1. However, a combination of horizontal and vertical cuts is the best approach as the footwall is left smooth and jamming difficulties are reduced.

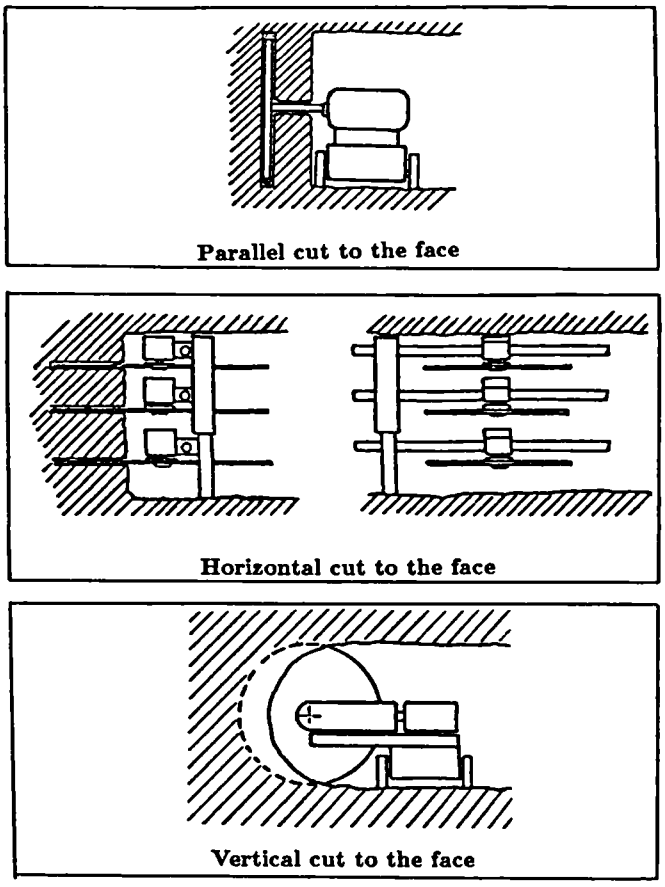


Figure 4.1: Diamond circular saw used for mining purpose (After Bracken, 1988)

4.3 DIAMOND WIRE SAW

The so-called diamond wire comprises a stainless steel cable made up of twisted strands (for higher flexibility) on which the diamond cutting elements (commonly termed 'beads') are placed, together with the spacers and the positioners. The wire may be in one continuous piece or made up of several lengths closed with a joint or joints.

Since the idea using diamond electroplated beads on a wire for the cutting of stone was proposed by the British inventor Prowse in 1968[54], the structure of the diamond wire has undergone, during a relatively short period of time, constant evolution due to field testing under production conditions. The first paper on "sawing marble with diamond wire" was published in January 1971 by Hallez[55]. The main structure of diamond wires before 1983 was the multi-strand, high strength steel cable carrying electroplated diamond beads, 6-10 mm long, linked by specially designed sleeves. A most important advance in 1983 was the introduction of impregnated beads in place of the original electrodeposited design[56]. Developed to overcome the latter's drop-off in performance when cutting harder materials, the impregnated bead comprises a cylindrical hollow steel support surrounded by a diamond-impregnated annulus whose composition is similar to that of traditional diamond segments and with the diamond particles distributed evenly throughout the impregnated annular volume. This feature lends the tool a uniform cutting ability over its entire life. On the other hand, the wire was designed with injection moulded plastic spacers fixed between impregnated diamond beads. The plastic spacers inhibit the ingress of abrasive slurry to the wire core. Thanks to the above developments made by Diamant Boart, a new field of diamond wire cutting was opened up at that time - granite sawing using of diamond wire. Another application

of the diamond wire nowadays is to cut reinforced concrete. This type of wire incorporates beads impregnated with a mixture of two high strength diamond abrasives, developed by De Beers[57].

Nowadays, the general specifications of diamond wire for sawing hard rock like granite include:

- impregnated beads: ϕ11mm x 6mm long, on ϕ9mm steel support;
- diamond: SDA 100, 40/50 US mesh;
- pitch: 25 mm (40 beads/meter);
- plastic spacers: 8.5 mm injection moulded between the diamond beads in order to keep beads apart when sawing and also to protect the carrier cable against abrasion from the high-quartz cutting slurry;
- joints: the ends of a wire loop may be joined either by means of a brazed threaded tip which screws into a female threaded coupling, or by means of copper tubes crimped by hand using a special hydraulic clamp device.

For sawing soft rock like marble, electroplated diamond beads and spring spacers are still widely used on the wire. This is the main difference in the specification of diamond wires used for sawing soft rock and hard rock. Figure 4.2 shows the diamond wire machine for stone extraction and two kinds of diamond wires (left: electroplated diamond wire; right: impregnated diamond wire).

The main advantages of using diamond wires was suggested by Daniel[58]. The former extraction techniques were blasting, thermic cutting, and helicoidal wires. Now the basic constraints of designing a diamond wire system for hard rock cutting provides the following advantages:

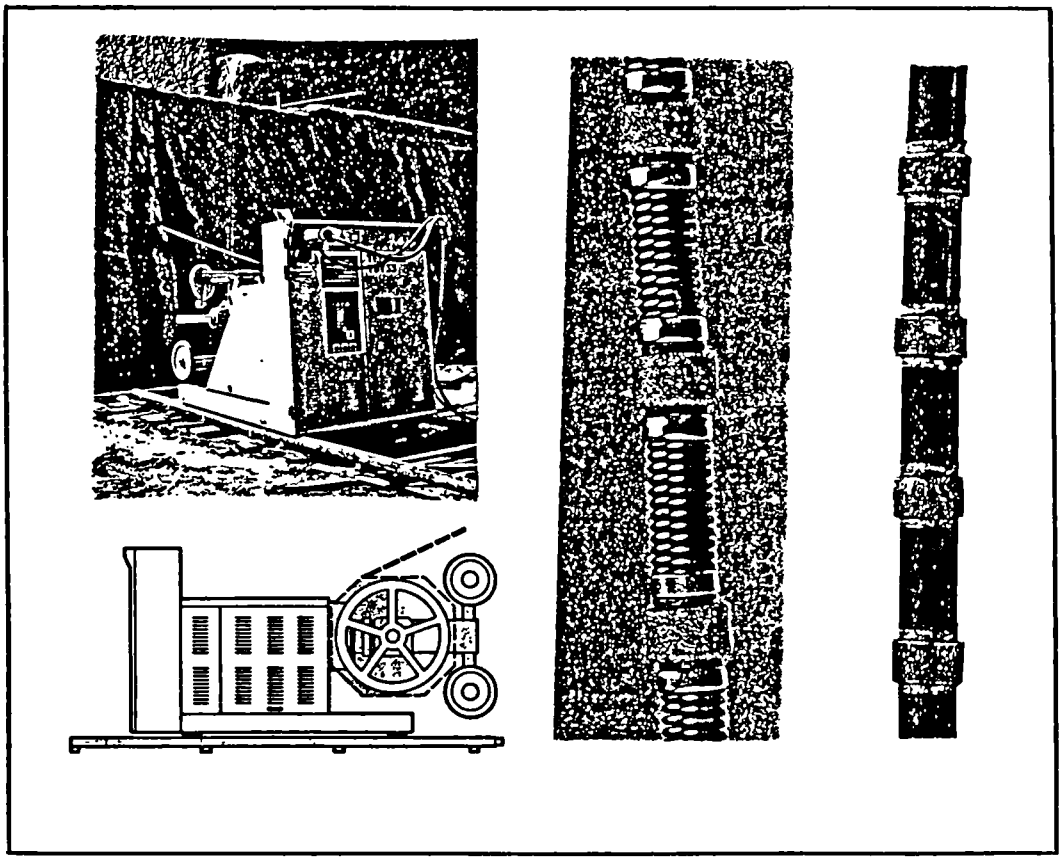


Figure 4.2: TDV 55 Diamond wire machine and diamond wires

- virtually 100% of blocks recovered can be used to produce useful slabs or panels;
- minimum material wastage: the width of cut is only about 12mm with no thermal damage at either side of the kerf;
- minimal set-up time due to the ease of transportation and installation of the system;
- wide range of applications: the technique can be used to square the rock face prior to block extraction; for block extraction by vertical, horizontal or oblique cutting, or for trimming blocks to ideal dimensions for transport or subsequent machining operations;
- low labour costs: only one operator required once sawing is in progress.

4.3.1 Cutting techniques employed using diamond wire saws

Stone block cutting

The diamond wire was first used in 1968 for squaring blocks in the workshop. As regards granite block cutting, one of the most common methods employed was as shown in Figure 4.3[59]. The method used high-speed wire and the entire frame around which the wire rotated moved. With this method, it is possible, at least in theory, to have a constant pre-tensioning value since the length of wire remains the same in all cases. The curve angle of the wire due to the cut varies from 0° at the beginning of the cutting operation to a increased value when all the wire has entered the block. Then it can be increased again depending on how difficult it is to cut the material. The curve angle can not be varied very greatly in that the horizontal and vertical cutting forces always form wide angles. In this method, the wire, which is very much directed by the pulleys, could turn on its own longitudinal axis with less difficulty.

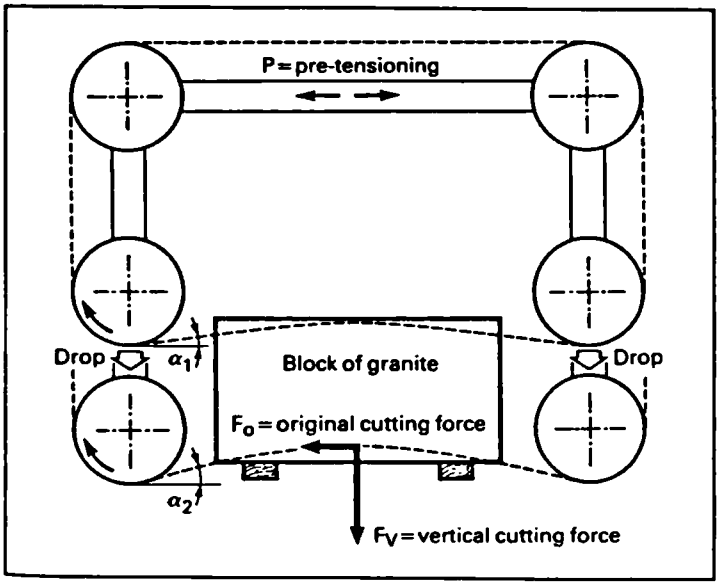


Figure 4.3: Diamond wire sawing method with descending pulleys
(After Cai *et al*, 1988)

At present, research concentrates on the possibility of constructing a multi-wire machine with the cutting line in a sub-vertical position, able to cut at least 5 slabs at a time, as shown diagrammatically in Figure 4.4[59].

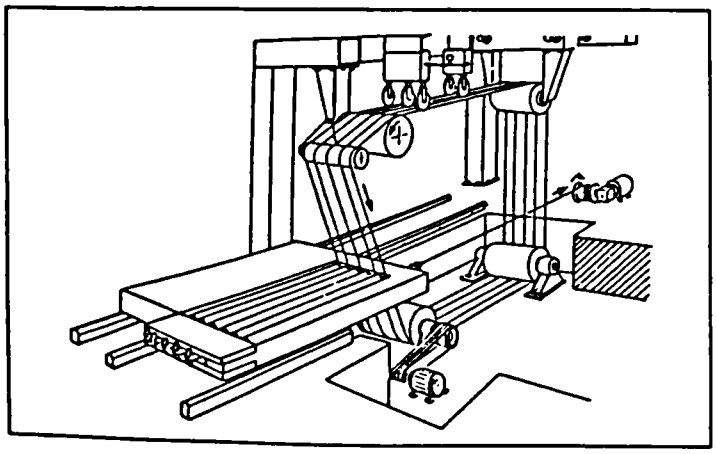


Figure 4.4: Multi-diamond wire block slabbing machine (After Cai *et al*, 1988)

Stone extraction

The original idea for stone extraction using the diamond wire was introduced for the first time in 1972 by Diamant Boart in a Swedish quarry and involved closing the diamond wire around the mass of stone to be cut and pulling the loop back through the stone by means of a large diameter pulley. The use of wire saws requires the drilling of intersecting horizontal and vertical holes to define the block. Blocks can be freed from the face by splitting along cleavage planes using wedges or small charges of black powder. Today, the cutting technique in quarries almost universally used is the "loop" technique. There are several possibilities for using diamond wire in stone extraction from a quarry.

(1) Vertical sawing

The loop cut (Figure 4.5[60]) is the primary technique used when cutting into the rock face. This technique has made it possible for the diamond wire to acquire its present dominant position in the quarries. It is used when two surfaces are free and available, for instance, two holes are drilled, one vertical and the other horizontal, so that the diamond wire may pass through them along the cutting plane. The wire is then joined around the pulley and the cut is initiated after ensuring an adequate water coolant supply.

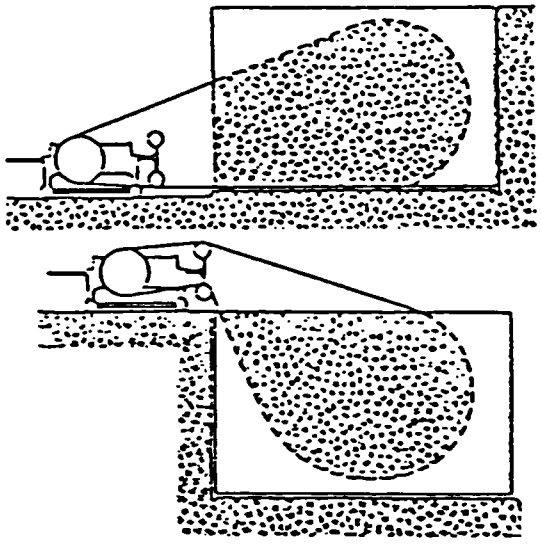


Figure 4.5: Vertical bench sawing (After Pinzari, 1983)

Another technique shown in Figure 4.6[60] requires the drilling of a single large diameter (240-320mm) hole in which a pulley is sunk. The pulley guides the wire. This technique seems to find its application in the case of large-dimension blocks, where the meeting of the two smaller holes is more uncertain.

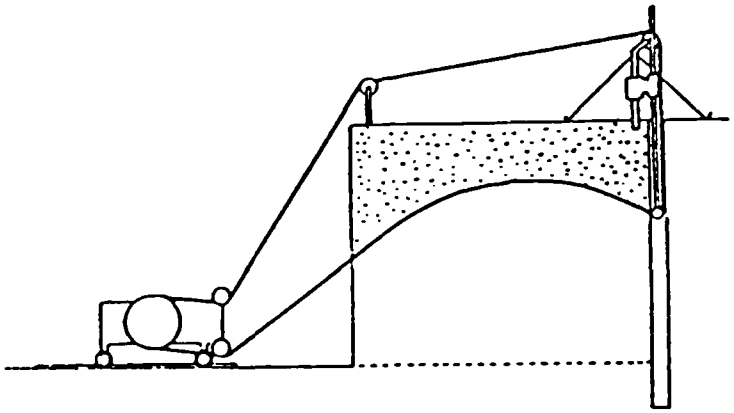


Figure 4.6: Vertical bench sawing with a sunk pulley (After Pinzari, 1983)

(2) Horizontal sawing

The diamond wire machine can be used not only in the vertical, but also in the horizontal plane as shown in Figure 4.7[61].

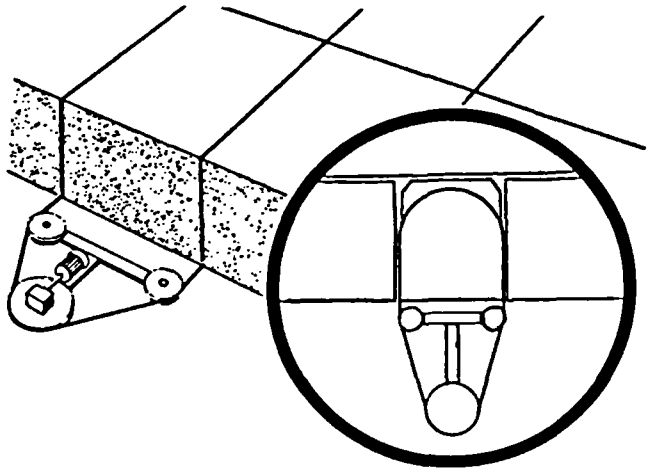


Figure 4.7: Horizontal bench sawing (After Decroly, 1981)

Furthermore, the line of cut can be at a different level to the plane of drive pulley as shown in Figure 4.8[57].

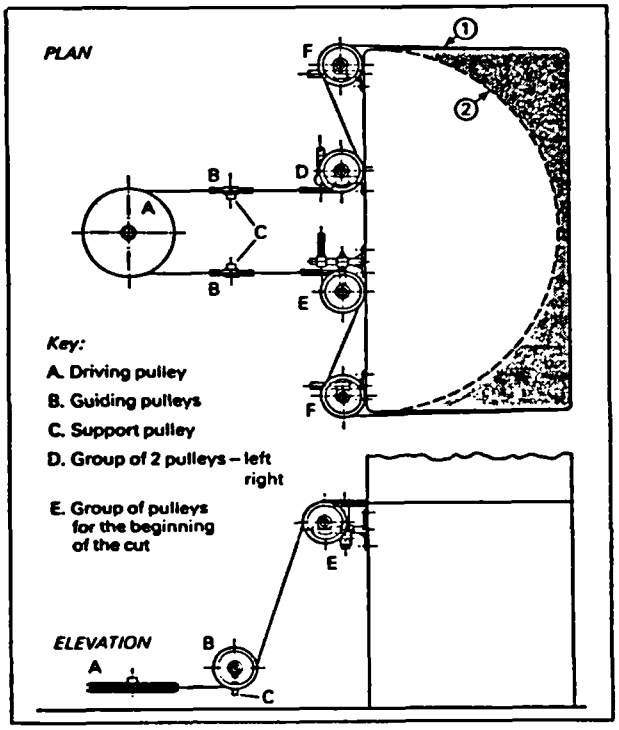


Figure 4.8: Horizontal sawing at different level (After Herbert, 1989)

(3) Opening cut

The traditional technique for the opening cut is shown in Figure 4.9[60]. Two free pulleys, each equipped with an automatic sinking mechanism, guide the wire inside two large (240-320mm) diameter holes and press the wire against the stone.

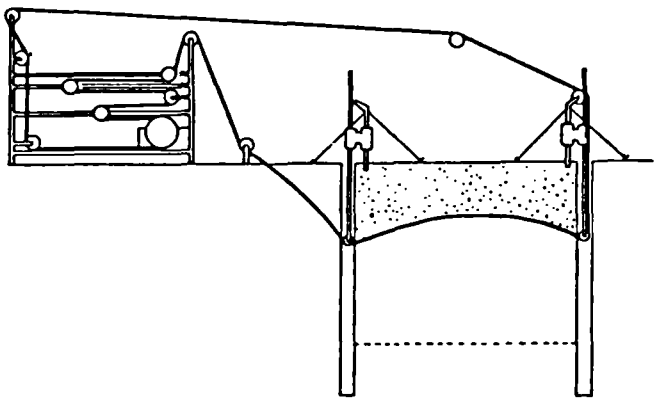


Figure 4.9: Traditional method of opening cut (After Pinzari, 1983)

Another method for the opening cut is called the mixed technique. In this method, a diamond wire cutting machine is used in conjunction with a chain saw machine as shown in Figure 4.10[61], or with a circular saw blade.

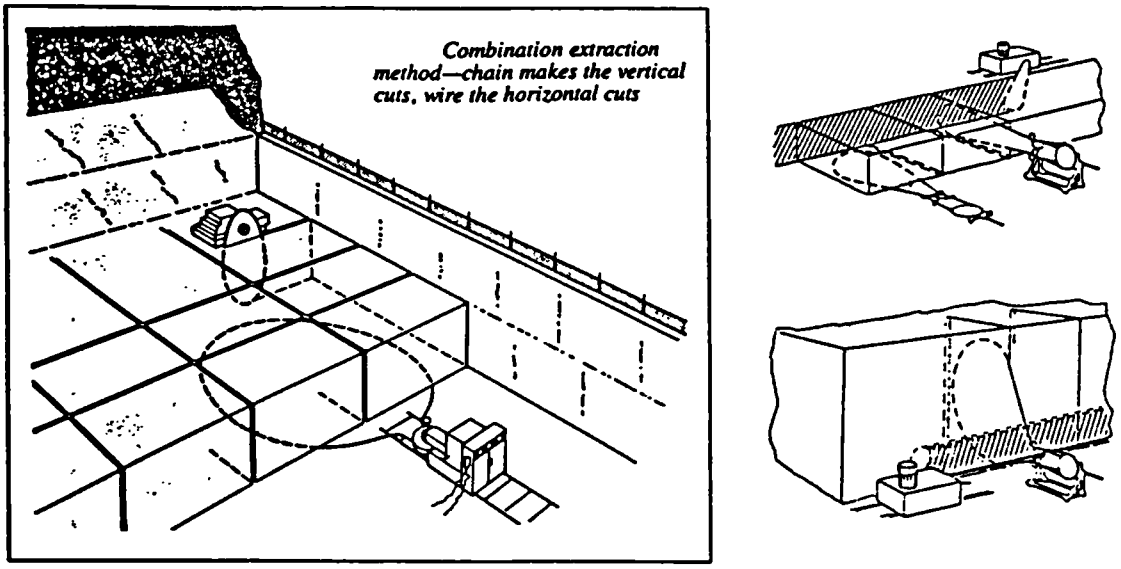


Figure 4.10: Combination extraction method of opening cut (After Decroly, 1981)

In this case the diamond chain saw has proved its true worth. It is designed for quarrying operations and versions are available which are capable of cutting to 3 m depth and more in a single pass. The mixed diamond wire-chain saw cutting technique deserves special attention inasmuch as in working the quarry, the number of wire-guiding holes is reduced to zero or to one for each face. For example, the chain makes the vertical cuts, the wire the horizontal cuts, or first a bottom cut is obtained by means of the chain saw, consequently the vertical holes are drilled down to the bottom cut, the diamond wire technique used is the same as that of the loop.

4.3.2 Technical considerations for cutting hard rock

When considering the destruction of the rock on a macroscopic scale like blasting or on a microscopic scale like drilling or cutting, there is a great difference between soft rock and hard rock. For example, when excavating a tunnel, approximately 50% more explosive is used when working through granite than through marmoreal limestone. According to Cai *et al*[59], a comparison of marble and granite cutting shows that it should be possible to cut granite at the same speed as for marble if 10 times more stress can be placed on the beads and on the wire, with local load variations which are many times greater than the mean value, and consuming, per unit of time, approximately 5 times more energy.

The following aspects for sawing hard rock with diamond wire such as granites should be particularly considered:

The rotation of beads and wire

From experiments, there is absolutely no doubt that the beads must not rotate around the cable, because this would contribute to damaging wear between the hole and the cable. If the methods of assembly which were employed were not watertight, there was the possibility of slurry from the cutting operation filtering in between the internal diameter of the hole and the external surface of the steel cable. In fact if, because of the abrasive slurry and the concomitant action of the rotation of the bead on the cable, the external diameter of the cable itself were to become worn and the hole of the bead were to be excessively enlarged, this would make it very difficult for the diamond to penetrate the rock material, causing rapid wear and leading to a disastrous effect on the diamond wire. To solve this problem, injection moulded

plastic spacers are used in diamond wires for cutting granite. Furthermore, the operators feel that to make the plastic spacers more flexible would be desirable.

To ensure that the diamond beads wear around their periphery, the easiest way is to use screw-type couplings to enable the wire to be joined after it has been looped[62]. Prior to joining, the wire is rotated axially at each of its two free ends in order to induce a spiralling action when the wire is cutting. Thus the running wire rotates about its axis (through 360° every 2 m of cut) and with it the diamond beads. An additional effect of the spiral motion is a self-tightening action at the threaded couplings. Future solutions may include cutting machines employing methods which actually make the wire rotate on its own longitudinal axis. Actually, this is a big problem worthy of being solved by the machine designer of the future.

The assembly of the spacer

The adoption of a method for assembling the wire using spacers between the beads which, while ensuring good transmission to the cable of all the cutting forces due to the diamond, allowing the wire to remain very flexible, preventing the infiltration of slurry between the hole and the cable and finally providing good resistance to wear caused by friction produced from slurry resulting from the cutting operation is very important. On the other hand, the distance between the beads should allow an available space for the discharge of debris and an efficient flow of coolant into the cut. From this point of view, the material sawn has a greater influence on the choice of the distance. When sawing very abrasive and hard materials, the problem of cable wear is encountered. The general rule may be that the more abrasive the material to be sawn, the wider the distance should be. Future research could look into finding a way of attaching the diamond beads to the cable without needing spacers which reduces the space available for the discharge of cutting debris.

Loop length, sawing speed and water supply

About the loop, one should try to cut the largest face area that the stone layout allows, since if the wire forms a short loop - a greater incidence of 'corners' - it will have a shorter life. According to Daniel[63], the ideal size to be extracted for operations would be a 5 m^3 block.

A high cutting speed leads to a greater number of "destructive" actions on the stone per unit time. On the other hand, it is important to contain the costs incurred per square meter sawn which is influenced mainly by the wear on the diamond tools. A reasonable cutting speed of the cable, from 40-45 m/s typically employed nowadays when sawing marble to 30-35 m/s for sawing hard rock should be provided. A still slower speed, say 15-16 m/s might reduce fatigue of the cable, although this may necessitate a change in the specification of the diamond beads[63].

Whereas sawing with electroplated diamond wire can be performed with a limited coolant flow, impregnated beads require a higher minimum flow rate (about 40 liter/min) so as to provide the necessary cooling of the tool in service.

Stress on the wire

Methods of reducing the stress on the diamond wire should be based on studies of how it is produced. The total stress on the wire, is calculated by:

$$\sigma_w = \sigma_x + \sigma_y + \sigma_z \qquad (4.1)$$

Where, σ_x is the stress produced by tensile loads acting on the wire. σ_y is the stress due to the run of the wire onto the driving pulley. σ_z is the stress produced by curving the wire onto the cut rock surface.

Referring to the previous studies on this aspect, equations given by Tonshoff[64] and Cai[59] may be inadequate. In their equations, the term σ_z was not mentioned, and the single straight core wire was considered only with regard to σ_x.

Consider that the diamond wire is a single twisted strand and this strand is composed of **m** layers of wire wrapped around either a fibre core or a steel wire core. Referring to the studies of wire ropes, Hruska[65] has shown that the tensile stress σ_x in the strand can be calculated by the following equation:

$$\sigma_x = \frac{S_t}{\sum_{i=c}^{m} n'_i A'_i \cos^3\alpha_i} \qquad (4.2)$$

Where: S_t = Wire tension (tight side tension)

n' = Number of wires in one layer

A' = Wire cross section area

α = Wire lay angle

There are several equations for the calculation of stress σ_z produced by curvature changes. This stress in a wire of diameter $\mathbf{d_w}$ could be presented by the popular Czitary's formula[66]:

$$\sigma_z = \frac{d_w}{2\rho} E_w \qquad (4.3)$$

ρ is the actual radius of wire bending on the rock. E_w is the modulus of elasticity of the wire material.

The stress σ_y can be computed according to the following equation[64]:

$$\sigma_y = \frac{2S_t \tan\beta}{A'} \sqrt{\frac{E\,A'}{S_t}} \qquad (4.4)$$

The definition of angle β (in Equation 4.4) is given in Figure 4.11.

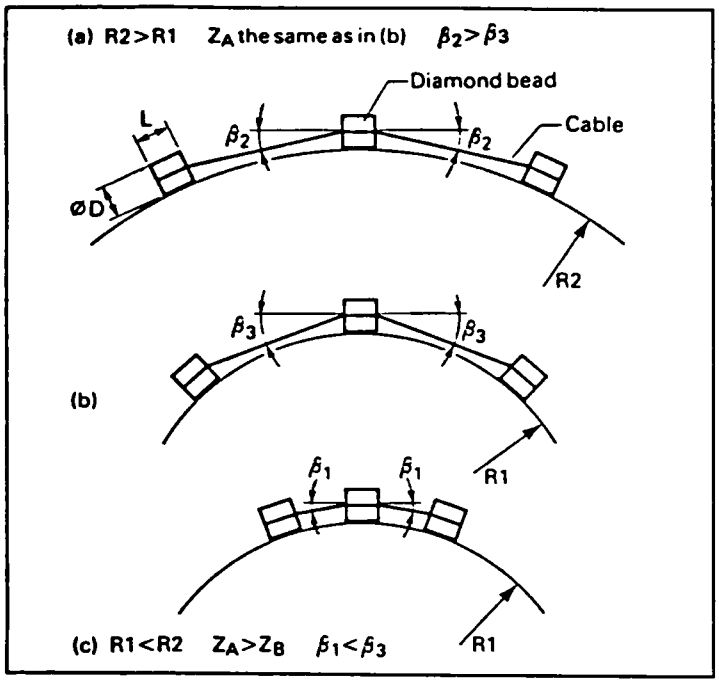


Figure 4.11: How to reduce stress σ_y on the wire (After Cai *et al*, 1988)

Basically, the diamond wire stresses can be analyzed and calculated according to the above formulae. In practice, pre-tensioning remains unchanged (or tends to increase on account of the cutting forces). The winding angle β takes on different values according to the cutting method. The diagrams in Figure 4.11 illustrate how it is also possible to reduce the stress on the cable which passing into the hole through the

beads, which are rigid and have their own rectilinear length, force the cable to assume a shape which resembles a polygonal and not a round piece. A reduction in the distance between the beads (decreasing the winding angle), could increase the life of the wire (Equation 4.4) or the use of wider diameter pulleys would have the same effect.

4.3.3 Wire performance evolution

Marbles cut by diamond wire

When the electroplated diamond wire was used in 1971 for block squaring, sawing speed reached 25 m/sec and the sawing rate of 2 m^2/h was achieved.

From 1980, diamond wires were widespread in quarries for marble extraction, due to the development of the "loop" technique. Typical results achieved in 1980 in quarries were cutting rates of 3-4 m^2/h with tool lifes of 10-20 m^2/m[61]. Regarding the cutting rate only (high cutting rate usually means short wire life), the highest figure achieved was 14 m^2/h on the white Carrara marble of the Luchetti quarry at Fantiscritti in Italy[60].

After 1983, a most significant advance was the development of the impregnated beads. The tool life is about 60% longer than that of electroplated wire cutting marbles[56]. The life of the diamond wire, therefore, became an all-important factor. According to Diamant Boart reports in 1985[62], the diamond impregnated wire system achieved the most significant performance figures. Those figures over seven different materials are reproduced in Table 4.1.

Table 4.1: Impregnated diamond wire life and performance (After Herbert, 1985)

Materials	Country of origin	Cutting rate (m^2/h)	Life of a 20m length of wire (m^2)
Carrara Marble	Italy	7	500
Tivoli travertine	Italy	7	600
Pierre Blue	Belgium	3	400
Boulonnais Marble	France	4	400
Pink and White Marbles	Portugal	4	400
White Marbles	Greece	6	400
Cambrian Green Shale	U.K.	3	300

Granites cut by diamond wire

Granite blocks can be squared by diamond wire machines. For example, a wire saw machine specially designed and built by Ets Salagnac France for granite cutting in 1988[67], had a cutting rate of 0.8 - 2 m^2/h with a tool life of 11.1 m^2/m when sawing different granites. According to Ets Salagnac, tool costs with the conventional wire with carborundum abrasive system and with the diamond wire system are approximately similar. However, with the diamond wire machine, cutting is 50% faster. It was said that seven different types of diamond wire to cut the various types of granite blocks were produced by Milano Manufacturing Co Ltd in Japan[68]. One of those machines is Milano's DW-1L double pulley diamond wire saw, fitted with two 2100 mm diameter pulleys driven by a 30 h.p. motor. The wire is designed to run at a speed of 35m/s. Cutting rates of 1.2 m^2/h with a wire life of 2.6 - 5.5 m^2/m were achieved.

For granite extraction using the loop technique, a cutting rate of 2.5-3.0 m^2/h and a wire life of 4-5 m^2 per meter length of wire was obtained in Vosges Grey granite at the Petitjeam quarry which was a very considerable achievement in 1986[63]. The main results for sawing granite with diamond wire in Europe, up to the end of July

1986, included the five quarries in the Valle d'Ossola and Valle Antigorio north of Lake Maggiore in Italy, were summarized by Daniel[58]. His report showed that more granites can be cut economically by diamond wire at a cutting rate of 2 - 5 m^2/h with a wire life of 2 - 7 m^2/m. A 90's result was reported from the Saga Pearl quarry in Norway[69]. The machine recommended for this application is a Pellegrini mobile wire saw, the Telediesel TDD100 Super, specifically developed for cutting granite, sandstone and shale. For cutting Blue Pearl, a wire speed of between 22 and 25 m/s is used, and the saw cuts through the granite at a rate of about 4.5 m^2/h. The life of the wire is normally 5 m^2 of cut per linear meter of wire.

Whilst the practical advantages of diamond wire sawing compared with alternative techniques for hard rock extraction are today indisputable, there is still the very important question of costs. As reported by Herbert[70] in 1986, a diamond wire costs around £100 per meter. According to Thoreau quoted by Daniel[58], diamond wire costs (1986) work out at about \$US 44/m^2, with variations depending on the granite class, or in other words its sawability rating. For block squaring of granite using diamond wire, according to Milano's results[68], at present the cost of diamond wire remains more expensive than a circular diamond saw. At the same cutting rate, the diamond circular saw of 1-2.5 m diameter cost about \$US 20/m^2 in 1988, half of the cost of using diamond wires.

Concrete cut by diamond wire

The first Italian application that cut concrete by diamond wire was reported in 1986[71]. The cutting of 22 m^2 of concrete together with 300 steel reinforcing rods 30 mm in diameter was completed in 26 hours using two partly worn diamond wires. Diamond wire consumption was about 1 m per m^2 cut.

In 1988, Holemasters Limited cut out more than 150 tones of heavily reinforced concrete in England[57]. In cutting rate terms, the hydraulically-driven wire saw achieved an average of around 1 m^2 /h. The incorporated beads were impregnated with a mixture of two high-strength diamond abrasives, specially developed by De Beers for applications such as the cutting of reinforced concrete.

4.4 CHAIN SAW

It is perhaps surprising to learn that chain saws with tungsten carbide segments were first used around 1945, and eventually proved relatively successful in soft limestones. An experimental machine for block slabbing, using a chain fitted with diamond impregnated segments, was installed as long ago as 1948 in the USA. The progression from tungsten carbide to diamond, the hardest and most wear resistant tool material, is logical enough. However, in the event, it is not in block slabbing but in block extraction from the quarry that the diamond chain saw has proved its true worth (see Figure 4.10). Chain saws designed for quarrying operations are available for cutting to 3 m depth and more in a single pass. The advent of tool blanks comprising a layer of polycrystalline diamond (PCD) bonded to a tungsten carbide substrate stimulated new ideas, and the first practical tests using PCD cutters on a chain saw were performed in a Belgian limestone quarry in 1977.

Nowadays, the chain saw is mainly used for soft rock cutting. During 1986, superior results when chain sawing in several Italian marble quarries were obtained with De Beers Syndrill PCD rock cutters[72]. Compared with alternative PCD inserts, the Syndrill rock cutters are holding their edge longer, with no evidence of edge chipping. All Syndrill products from De Beers consist of a 0.7 or 1.0 mm thick layer of polycrystalline diamond which is integrally bonded to a tungsten carbide

substrate. The PCD layer is bonded to the tungsten carbide substrate during the sintering process while the wear resistant layer, an extremely tough, intergrown mass of randomly orientated fine diamond particles, is produced at very high temperature and ultra-high pressure. Syndrill rock cutters thus combine the extreme hardness and wear resistance of diamond with the strength of tungsten carbide[73]. It has been found that an average rate of advance of 5 cm/min (giving a cutting rate of 5.25m/h) provides the optimum balance between output and tool life in Arabescata marble, said to be somewhat harder than the Carrara marbles. The chain is run at a speed of 0.4-2 m/s. Kerf width with the chain saw is 38 mm. The chain has total of 77 Syndrill rock cutters - 55 "round" and 22 "squares", as shown in Figure 4.12. Working in Arabescata marble, with a chain cost of 14 million Lire, tool costs thus work out at 4666 lire/m^2 ($US 2.77/$m^2$). It is cheaper than cutting with diamond wire (7500 Lire/m^2)[73].

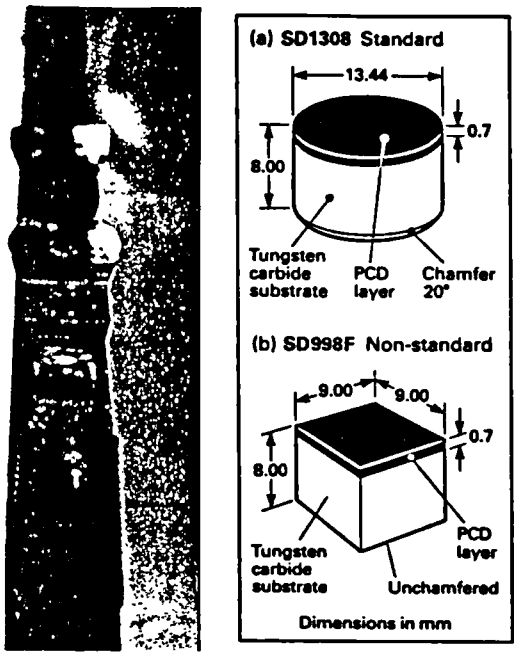


Figure 4.12: Dimensions of round and square Syndrill as used on chain saw (After Daniel, 1986)

It was announced that chain saws fitted with diamond impregnated cutting segments also could be used for hard stones such as granite sawing[74]. From tests, it was found that chain links with diamond segment as shown in Figure 4.13 had produced the best results. Unfortunately, tool life and cutting rate were not given.

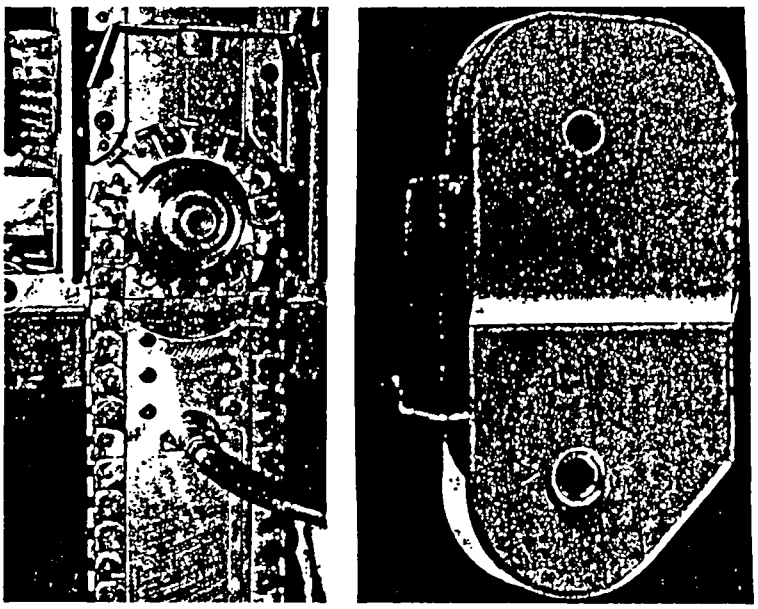


Figure 4.13: Chain link with diamond segment (After Meier, 1983)

4.5 BANDSAW

Bandsaws have been successfully used for cutting softer natural stones for more than twenty years. In 1980, cutting rates of 4.8-7.2 m^2/h with proportionate tool costs of \$US 1.5-2/m^2 had been achieved when sawing marble. Furthermore, hard rock could be cut more efficiently with a suitable bandsaw than with a circular saw as Gerhauser pointed out[75]. He gives details of discussions with Carl Meyer KG, the firm that built a special bandsaw in accordance with the design proposals made. This saw was installed at Marmorwerk Gerhauser KG, Sinntal. Cutting rates of 1.2-3.85

m^2/h were achieved with six types of granite. With the cutting areas stated, proportionate tool costs worked out in the range of \$US 7-8/m^2.

According to the reference, a well design bandsaw called Canali Mach 1 natural stone bandsaw appeared on the market in 1982[76]. The machine features a closed bridge construction with attachments for the two saw pulley bearings. The machine frame is guided on four columns. The diamond saw band runs over two pulleys each 2 m in diameter and performs a vertical feed movement controlled via an infinitely variable drive. Blocks measuring 2.8x1.5x1.7 can be cut into slabs of any thickness. A sawing rate of 1.7 m^2/h for material rich in quartz and 2 m^2/h for a mixture of materials with high and low quartz contents can be anticipated. However, the design of a bandsaw machine and diamond blades for sawing hard stone must meet special requirements, which have been realized only in a few cases to date.

4.6 FRAME SAW

Diamond blade frame saws have been used since the mid-fifties for cutting natural stone. Nowadays, there is no problem in cutting marble into slabs on a frame saw. Granite cannot yet, however, be frame sawn on a regular production basis on conventional frame saws[77]. Due to the reciprocating action of the frame saw, conventional synthetic diamond saw grits are not generally acceptable in a frame sawing application. Alternative, EDC synthetic diamond abrasive was successfully used in frame sawing[78]. However they have the advantage of being able to deal with blocks of any width and make continuous feeding easy. Generally their fields of application are medium-size marble works.

4.7 SUMMARY

The familiar and well-established tools still used today for cutting stone blocks in the plant are circular saw, framesaw, bandsaw and diamond wire. When smaller blocks are being cut, circular sawing would be the simplest, effective and economic method. When larger blocks are cut, diamond wire is more effective, although when sawing smaller blocks the cost of diamond wire remains more expensive than a circular saw.

The diamond wire saw is already established as a practical tool in marble quarries and block squaring by use of both the electroplated and impregnated diamond wires. Sawing rates of 3-7 m^2/hr with a wire life of 20-30 m^2/m are achieved for sawing marble. The diamond wire also provides a cost-effective system for the winning of hard stone blocks like granite since the development of impregnated beads and the injection moulded plastic spacer by Diamant Boart in 1983. Sawing rates of 2-4.5 m^2/hr and a wire life of 3-6 m^2/m was obtained in an ideal combination of the above two factors. There are several cutting techniques of diamond wire extraction system. The mixed technique may be a promising way, to give maximum output from smooth faced large blocks. In this technique, a chain saw or circular saw is used in conjunction with the diamond wire for stone extraction.

Although there has been vast improvements in granite cutting by the application of current technology, many technical and theoretical problems still remain unsolved.

CHAPTER 5

DEVELOPMENT OF THE THEORIES OF DIAMOND ABRASIVE CUTTING

5.1 INTRODUCTION

This chapter concentrates on the study of machining mechanisms of diamond cutting and the influences of engineering parameters on the cutting processes. It is also aimed at developing these theories. Based on large scale experimental work, the two most important factors of diamond cutting, diamond wear and cutting force were studied, because it had been found that a comprehensive theory for diamond abrasive cutting had not yet evolved.

The tests were performed on six samples including five granites and one limestone. Sawing tests were carried out at Diamant Boart's pilot station in Brussels, using the 18 kW Van Voorden bridge circular saw machine.

Sawing these samples gave very promising results for developing theories on diamond cutting. Based on the studies of the wear mechanism, a balanced wear region was clearly defined. A tool life equation has been established for diamond cutting and is presented in a very practical form. The quantitative description of the sawing process enables the development of an optimization approach for diamond cutting to be undertaken, which has resulted in the new concept of the **R-C** curve. Sawing forces and diamond particle wear were analyzed and a theory on the force

patterns and diamond wear mechanism has been developed in order to form a basis for understanding the nature of the diamond tool wear.

5.2 CUTTING PARAMETERS AND CHIP CROSS-SECTION

In circular sawing, blade peripheral speed **v**, saw feed speed v_f and depth of cut a_p are the parameters in the sawblade operation as shown in Figure 5.1. The cutting rate A_s at which a rock material is sawn is governed by v_f and a_p. A traditional method for understanding of the cutting operation under the influence of these parameters was provided by considering the load on an individual diamond particle during cutting. The load on a diamond particle, given by the average chip cross section which the particle has to remove, was established in Equation 5.1 as an analogy and is widely adopted by stone cutting industry[39,44].

$$F_q = \frac{v_f \sqrt{a_p}}{v \sqrt{D}\, N_d} \qquad (5.1)$$

Where,

F_q = Undeformed chip cross-section which an individual diamond particle has to remove when using a circular sawblade

v_f = Saw feed speed (traverse speed)

v = Blade peripheral speed (sawing speed)

a_p = Depth of cut

D = Diameter of the sawblade

N_d = Number of diamond particles per unit area of segment surface (proportional to concentration)

It can be seen from Equation.5.1 that chip cross-section increases with decreasing sawing speed, and the mechanical stress on each diamond particle is thus increased. This can lead, unless a force point is reached which exceeds the strength of the bond anchorage, to high degrees of particle pull-out or premature splintering-off of parts of the diamond particle, which in turn results in a reduction in the number of diamond particles in the segment, and consequently an increase in the cross-section of the chip to be removed by each individual diamond particle.

A deeper cut causes increasing mechanical load on the diamond particles, it also follows that increasing the blade feed speed has a stronger influence on the enlargement of the undeformed chip cross section than a corresponding increase in the depth of cut (F_q - v_f; F_q - $\sqrt{a_p}$).

However, the predictive results do not give a correlation with the actual test results. For example, as indicated in Section 3.5.4., it has been established from tests that the cutting forces are minimized by employing a shallow depth of cut and a high feed speed, which is opposite to the prediction obtained from Equation 5.1.

This equation was introduced by Busch[39] and Ertingshausen[44] quoted from Buttner[79] and Lindenbeck[80]. The author believes that the equation is incomplete. A similar formula can be derived from the diagram shown in Figure 5.1.

Supposing that the diamond particles are well-distributed in the surface of the saw segment and the total circumferential length of segments is equal to 4/5 of the sawblade girth. As shown in Figure 5.1, during sawing, the point C will move to point B, as point A is rotated to point B. Then a layer of rock material with the cross

section of **ABC** will be removed. So the maximum thickness of the undeformed chip cut by a single diamond particle is equal to:

$$t_{max} = \frac{\overline{BD}}{(\frac{4}{5} AB)\, N'_d} \qquad (5.2)$$

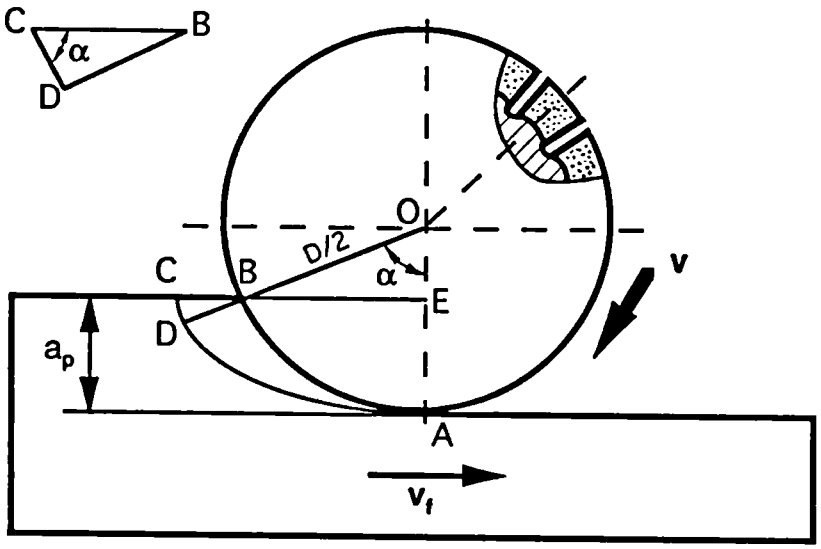


Figure 5.1: Undeformed chip thickness in diamond circular sawing

Where, N'_d is the number of diamond particles per unit length of segment along the sawblade girth.

Supposing that **BDC** is a right triangle, therefore:

$$BD = BC \sin \alpha \qquad (5.3)$$

As the sawblade is rotated with the peripheral speed **v** from point **A** to point **B**, at the same time, the rock material will be moved from point **B** to point **C** with the feed speed v_f. It is given by:

$$\frac{\overline{BC}}{\overline{AB}} = \frac{v_f}{v} \tag{5.4}$$

$$\cos\alpha = \frac{OE}{OB} = \frac{(D/2) - a_p}{D/2} = \frac{D - 2a_p}{D}$$

Then,

$$\sin\alpha = \sqrt{1 - \cos^2\alpha} = 2\sqrt{(a_p/D) - (a_p^2/D^2)}$$

It may be considered that:

$$\sin\alpha = 2\sqrt{\frac{a_p}{D}} \tag{5.5}$$

Submitting Equations 5.3 - 5.5 to Equation 5.2, the following equation is obtained:

$$t_{max} = \frac{2.5\, v_f \sqrt{a_p}}{v\sqrt{D}\, N'_d} \tag{5.6}$$

Therefore, the maximum undeformed chip cross section can be given as:

$$F_{qmax} = \frac{2.5\, v_f \sqrt{a_p}}{v\sqrt{D}\, N_d} B_w \tag{5.7}$$

Where, B_w is the width of saw segment.

5.3 EXPERIMENTAL PROCEDURE

5.3.1 Equipment and testing materials

The experimental work was carried out at the pilot station of Diamant Boart S.P. in Brussels. Sawing tests were performed using the 18 kW Van Voorden bridge saw machine, as shown in Figure 5.2, equipped with a force table (quartz force transducers for decomposing dynamic force in three orthogonal components). The hydraulic feed system was steplessly adjustable and monitored by a flowmeter. The depth of cut was accurately controlled by an electric motor and gear transmission.

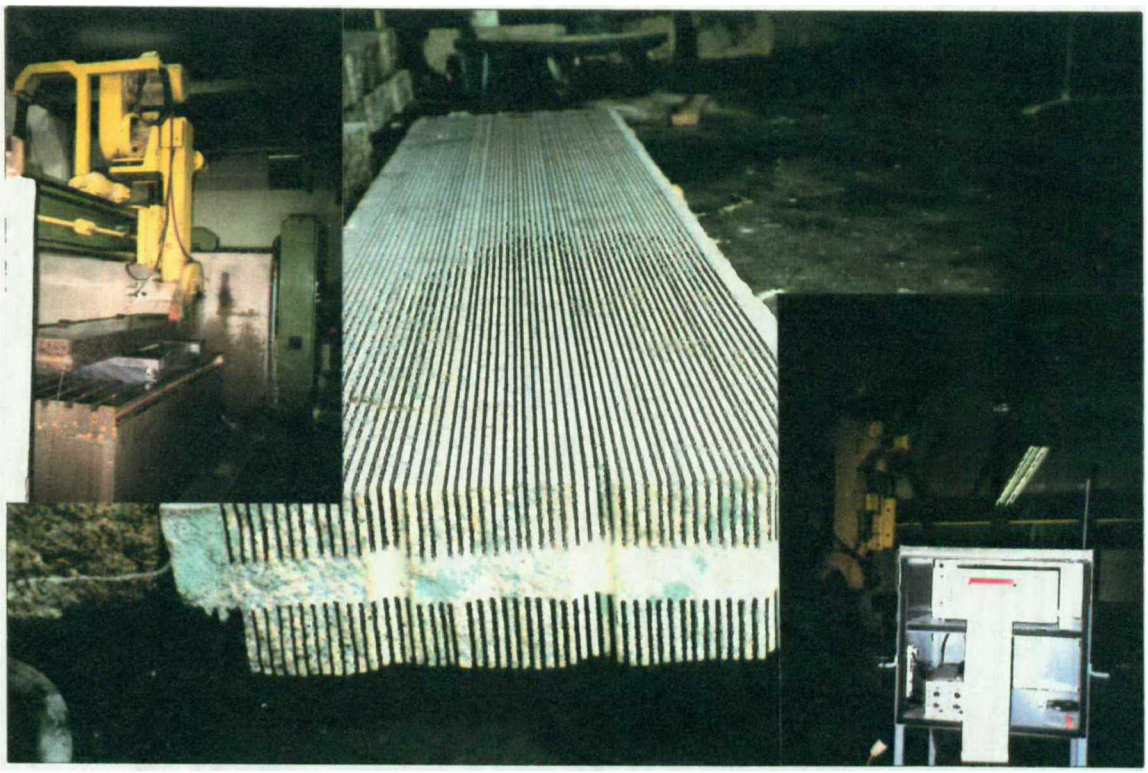


Figure 5.2: Bridge saw for the tests

DTA ϕ600mm impregnated diamond sawblade with 36 segments was used for the tests. The synthetic diamond particle size was 40/60 US mesh and the diamond concentration was 20 (0.88 Carat/cm^3).

A selection of sample materials was supplied by Diamant Boart, five granites and one fine grey limestone was supplied by Laporte Minerals of England. The granites were representative of the most difficult rock material to be sawn by stone cutting machines fitted with diamond impregnated tools. The limestone was chosen as an easily machinable rock and was used to show the degree of variation in tool wear rate and sawing forces when compared with the most difficult granite type of rock. In hand, all the sample material was found to be competent and in good condition, with no obvious evidence of weathering or chemical alteration. The rocks used for this experimental programme are as follows:

(1) Marlin granite (South Africa)

(2) Rose De La Clarte granite (France)

(3) Celtic granite (France)

(4) Lanhelin granite (Northern Ireland, U.K.)

(5) Balmoral granite (Finland)

(6) Laporte Limestone (England, U.K.)

5.3.2 Sawing test arrangements

The overall sawing test for six samples can be divided into three steps. In Step 1, Rose De Clarte granite was tested. The test was carried out at three different conditions relating to high, medium and low peripheral sawing speeds. At each sawing speed, a constant cutting rate of 300 cm^2/min was applied, using different combinations of depth of cut and feed speed as show in Tables 5.1 - 5.3.

Table 5.1: Sawing parameters for test Step 1 (v=20m/s, Rose De La Clarte)

Depth of cut(mm)	3	5	10	20	30	40	50	60	70
Feed speed(cm/min)	1000	600	300	150	100	75	60	50	43

Table 5.2: Sawing parameters for test Step 1 (v=31m/s, Rose De La Clarte)

Depth of cut (mm)	3	5	10	20	30	40	50	60
Feed speed (cm/min)	1000	600	300	150	100	75	60	50

Table 5.3: Sawing parameters for test Step 1 (v=47m/s, Rose De La Clarte)

Depth of cut (mm)	3	5	10	20	30	40
Feed speed (cm/min)	1000	600	300	150	100	75

In Step 2, a constant depth of cut of 10 mm, and a blade peripheral speed of 30 m/sec were applied. Feed was step by step increased from a small speed to a maximum depending on the rock samples. The combinations of each cut are presented in Tables 5.4 and 5.5.

Table 5.4: Sawing parameters for test Step 2 (v=30m/s, Rose De La Clarte)

Depth of cut (mm)	10	10	10	10	10	10
Feed speed (cm/min)	150	300	400	450	500	600

Table 5.5: Sawing parameters for test Step 2 (v=30m/s, Balmoral and Celtic)

Depth of cut (mm)	10	10	10	10
Feed speed (cm/min)	200	300	400	450

In Step 3, a constant peripheral speed of 30 m/sec was applied. The sawing rate was increased by increasing the feed and depth of cut simultaneously as shown below.

Table 5.6: Sawing parameters for test Step 3 (v=30m/s, Marlin)

Depth of cut (mm)	12	15	18	18.5	19	10
Feed speed (cm/min)	166	200	222	243	263	500
Sawing rate (cm^2/min)	200	300	400	450	500	500

Table 5.7: Sawing parameters for test Step 3 (v=30m/s, Lanhelin)

Depth of cut (mm)	12	15	18	18.5
Feed speed (cm/min)	166	200	222	243
Sawing rate (cm^2/min)	200	300	400	450

Table 5.8: Sawing parameters for test Step 3 (v=30m/s, Limestone)

Depth of cut (mm)	15	18	24	18	15
Feed speed (cm/min)	200	222	250	444	600
Sawing rate (cm^2/min)	300	400	600	800	900

5.3.3 Sawing force, relative wear and particle wear examinations

Test were performed with a reciprocating movement. Therefore, both the down and up-cutting methods were used in the test, which means the samples were cut by the movement of the sawblade in both directions on the force table. The cutting forces were measured using a 3-component dynamometer platform to which the rock material was clamped. A recording instrument produced a continuous trace of the

force signals with the reference system connected with the machine. Therefore, the axial component, vertical component and horizontal component were recorded.

The relative wear of the sawblade or change in radius of the wheel was measured at the same points of four segments on the total 36 segments equilaterally spaced round the circumference, using a specially designed micrometer. For each test combination, an area of 2 m^2 was sawn, in order to get the significant values of the relative linear wear of the sawblade. For the purpose of increasing measuring accuracy, four readings of cut to 0.5 m^2, 1 m^2, 1.5 m^2 and 2 m^2 were taken and averaged.

Diamond particle wear was examined under a binocular microscope (Figure 5.3). Individual abrasive grains on the wheel surface per unit area were counted and classified as five types according to their worn shapes. For every type of worn grain, the count was taken as an average from 5 different areas of 2 mm width on one segment surface repeated for 10 segments equilaterally spaced round the total 36 segments.

According to the conventional classification used in diamond cutting, the worn particles are classified as follows:

(a) Good crystals without significant wear
(b) Flattened particle surface
(c) Cleaved microfracture surface
(d) Broken diamond surface
(e) Particle pull-out

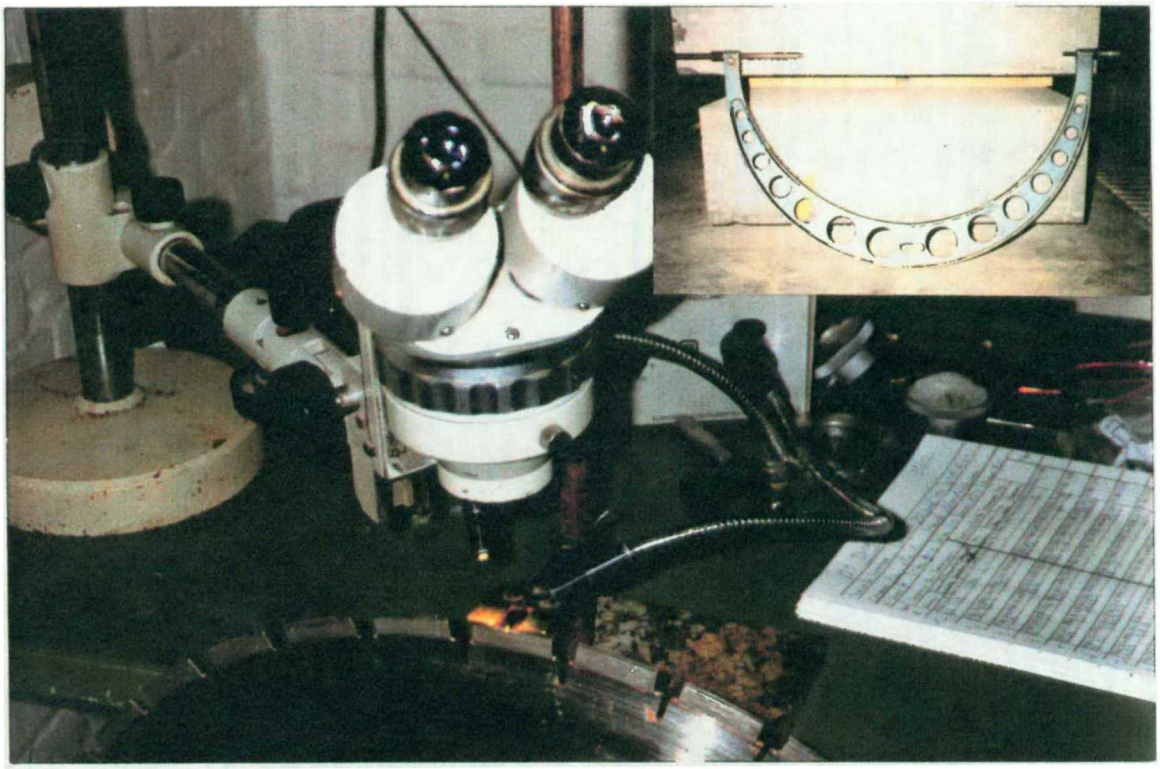


Figure 5.3: Segment surface was examined under a binocular microscope

5.4 BALANCED WEAR REGION, TOOL LIFE EQUATION AND R-C CHARACTERISTIC CURVE

Of vital interest to the manufacturing engineer are production costs and production rates. When discussing costs, it is of great importance to consider all the factors involved. Nowadays, in hard rock sawing, diamond tool costs are a significant factor in the overall cost. Therefore it is necessary to study the wear mechanism of diamond cutting and find out how the cutting parameters affect the tool wear, so that the inter relationship between tool costs and machining costs can be established. In general, the total cost of an operation can be expressed by the formula:

$$C_T = K_M + K_T \qquad (5.8)$$

Where, C_T = Total costs; K_M = Machine time costs; K_T = Tool costs.

When the sawing rate is increased while the other conditions are held constant, the actual machining time will be reduced, and the tool wear rate will increase. Very low sawing rates will result in low tool wear, but the machining time will be increased. Clearly, an optimum condition will exist giving minimum production cost. The importance of establishing the inter relationship between tool costs and machine time costs for rock cutting has been appreciated by many researchers for a long time. For example, this relationship was expressed graphically in Figure 5.4 by Buttner[27], without going into any detail.

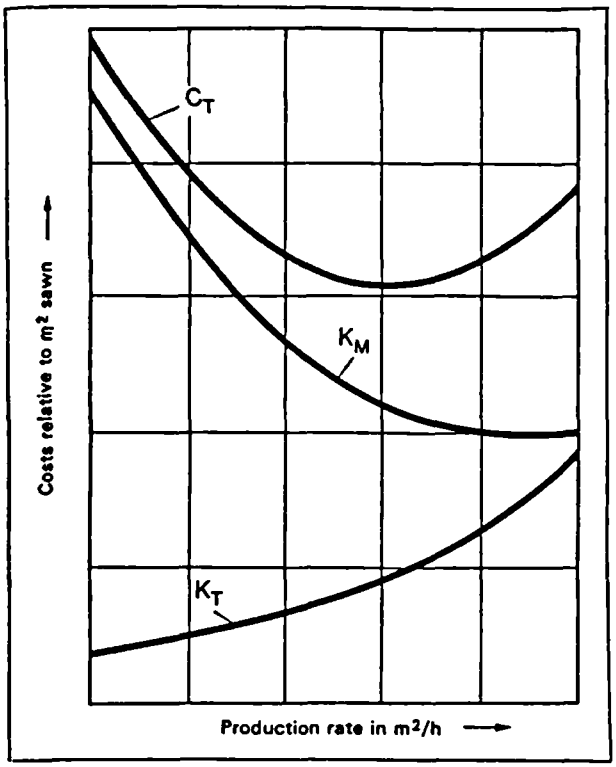


Figure 5.4: Production rate in relation to costs (After Buttner, 1974)

However, this research will lead to the development in which this relationship can be described quantitatively.

5.4.1 Wear mechanism of diamond cutting

Previous studies of diamond wear as reviewed in Section 3.4 may indicate only the apparent nature of the wear rather than the actual mechanisms. Therefore, two hypotheses are given below by the author, which suggest themselves as explanations of the diamond relative wear:

The wear on a diamond segment is caused by: (a) the plowing (cutting) action of the diamond particles on the rock, which induces a higher cutting temperature and (b) the impact of sawing thrust, which induces a higher shock wave. Therefore, the principle wear process may be considered to be the composite result caused by "plowing" and "impact". Then two typical wear processes can be distinguished. The first type of wear which is caused by friction as a result of plowing and is called abrasive wear. The second type of wear consists of exceeding the local ultimate or fatigue strength as a result of impact and is called fracture wear.

In practice, plowing and impact occur together. However, in certain cases, depending on the operating parameters, rock and tool materials, one of them will distinctly prevail. The type of wear process can be indicated by the worn diamond particle classification as described in Section 3.3.

As discused above, the first type of wear which is caused by friction as a result of plowing is called abrasive wear. This wear will be reflected by particle wear patterns of good particles and wear flattened particles. The second type of wear occurs when

the local ultimate or fatigue strength is exceeded as a result of impact and is called fracture wear which may be reflected by particle wear patterns of microfractured, broken and diamond to pull out.

Table 5.9 shows the test result of diamond particle wear when Rose De La Clarte is sawn at a sawing speed of 30 m/s and a depth of cut 10 mm. From this table, it can be seen that the impact is the main function that affects the tool wear and therefore the fracture wear is the dominant wear pattern when sawing Rose De La Clarte using DTA sawblade. The percentage of microfractured, broken and diamond to pull out was from 60.1% to 77.4% as the feed speed was increased from 150 cm/min to 600 cm/min.

Table 5.9: Analysis of diamond particles after sawing Rose De La Clarte

Feed speed	Worn diamond particles category (%)				
(cm/min)	good	flattened	mic.fracture	broken	pull-out
150	27.1	12.8	31.5	4.4	24.2
300	33.5	2.7	41.1	4.3	18.4
400	28	0	52	5.1	14.9
450	29.6	0	31.5	17.9	21
500	22.3	0	35	18.3	24.4
600	22.6	0	15	48	14.4

The effect of sawing parameters to the functions of "plowing" and "impact" can be understood from the graphs as shown in Figure 5.5 and the curves may be interpreted as:

- as the feed speed increases, the increased impact forces may be sufficient to set up shock waves within the diamond particles, causing them to shatter.

Therefore the fracture wear by impact action is rapidly increased rather than the abrasive wear.

- as the depth of cut increases, the cross sectional areas of cut increases and the cooling for the sawblade becomes more and more difficult. Therefore cutting temperature is increased due to the increased mechanical load and the worse coolant conditions. The increased temperature leads to the particles becoming relatively "soft" and abrasive wear will be more easily developed rather than fracture wear.

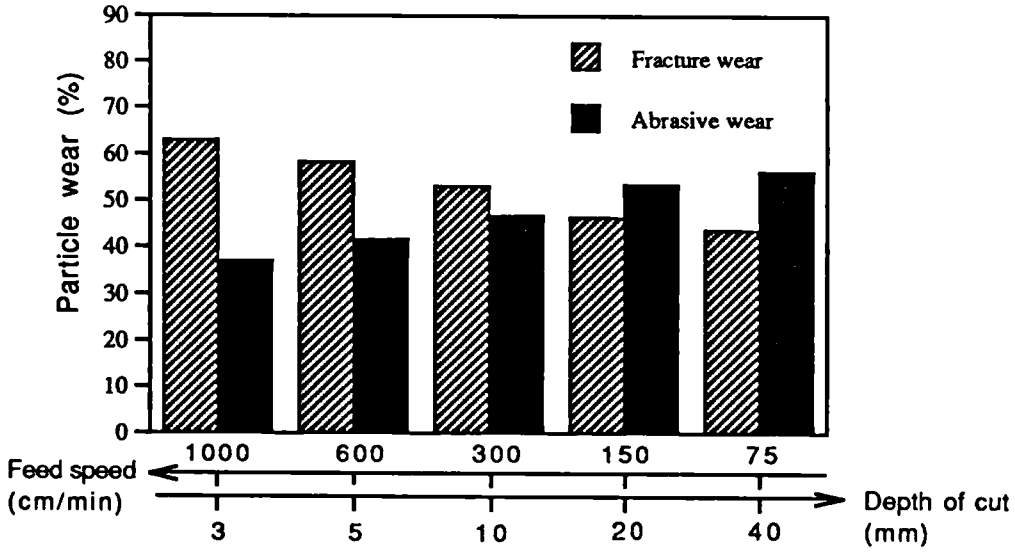


Figure 5.5: The variable behavior of the diamond sawblade for sawing Rose De La Clarte (v=47m/s)

Based on the re-analyses of previous results on the aspect of coolant-lubricants, the author's suggestion on the wear mechanism can be further evaluated. When impact is the main function to affect the tool wear and fracture wear is the dominant wear mode for cutting, coolant-lubricants should be used for the purpose of their cooling and washing effects. In this case, it can be assumed that the lubrication will lose its

function for the shock waves. Test results obtained by Tonshoff[81], and Buttner[82] showed that no reduction in diamond wear was observed with any oil on sawing Impala granite. The reason behind this can be explained by pointing out that the tool wear produced in their sawing test is dominated by fracture wear. Under this consideration, oil is not suitable as a coolant, because of its viscosity. It was also indicated that[81], the normal force was not reduced with oil when sawing Impala granite except at very low speeds. In this case, even plain water could be used as the coolant.

When the plowing is the main function to affect the tool wear and the abrasive wear is the dominant wear mode for cutting, the coolant-lubricants should be used for the purpose of their lubricating effect. Hence, oil has properties which greatly reduce frictional wear, which flattens the diamonds and which in turn makes the tool virtually ineffective. The evidence can be found from Tonshoff's result. He used tool WZ1 and WZ2 to saw hard stones. Tool WZ1 and WZ2 differ only in the nature of the synthetic diamond particles. WZ2 has about 10% more fracture resistance than the diamond particle type in tool WZ1. The results showed that tool life of WZ2 was longest with oil, whilst tool life was longest for WZ1 when a 2% aqueous solution of organic coolant was used. It appears that the abrasive wear is easier to occur when tool WZ2 was used. Furthermore, abrasive wear more easily occurred at very low cutting rates, however, the test results showed that the neat cutting oil had a profound effect on the reduction of normal forces at low cutting rates only.

5.4.2 The concept of balanced wear region

The effects of the operating parameters, feed speed, depth of cut and sawing speed on diamond wear are important in rock cutting. In the past, attempts to use Equation

5.1 to explain the effects of these parameters have failed. Without correctly designed test programmes and a deep understanding of the problem's nature, it is not possible to obtain a clear and meaningful answer. The tests were designed as discussed in Section 5.3.2, so that the effects of sawing speed, feed speed and depth of cut on the relative segment wear could be investigated. Test results are graphically shown in Figures 5.6 - 5.8.

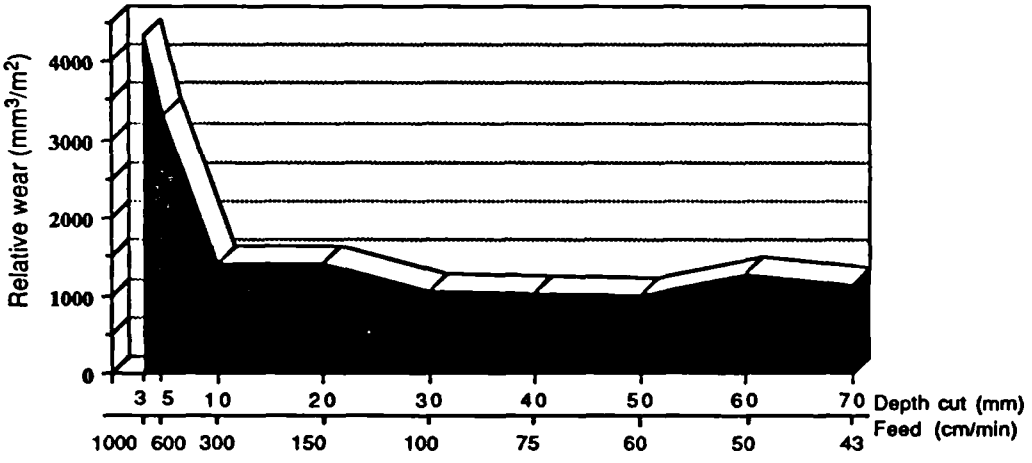


Figure 5.6: Relative wear versus feed and depth of cut at constant sawing rate at low peripheral speed (v = 20 m/sec, A_s = 300 cm²/min)

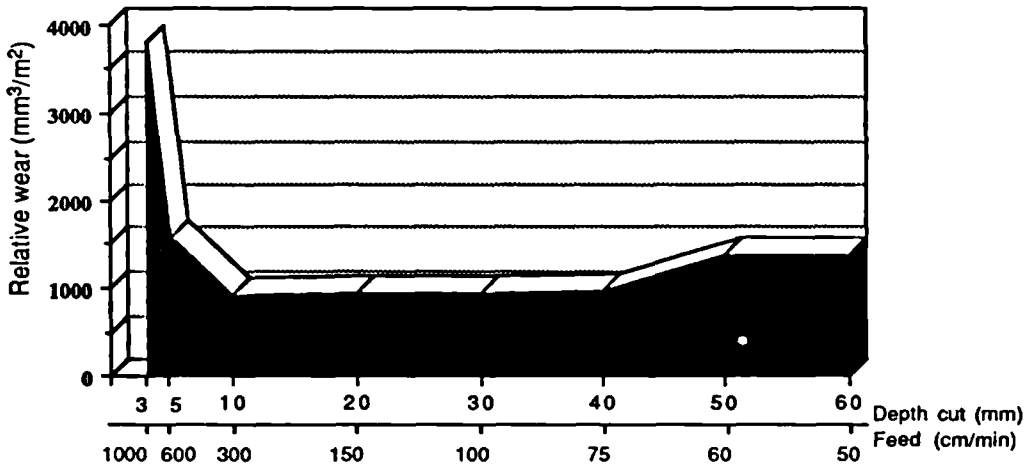


Figure 5.7: Relative wear versus feed and depth of cut at constant sawing rate at medium peripheral speed (v = 31 m/sec, A_s = 300 cm²/min)

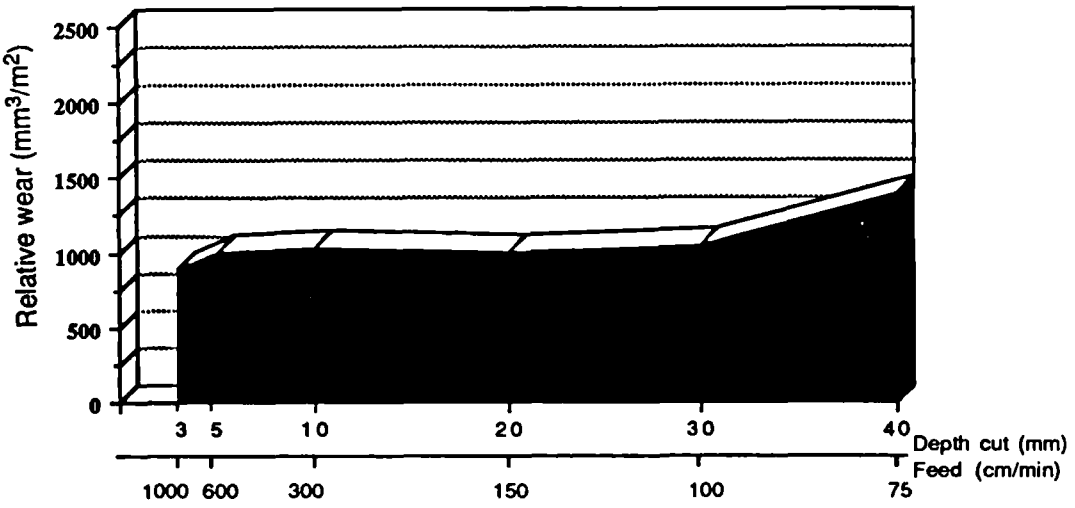


Figure 5.8: Relative wear versus feed and depth of cut at constant sawing rate at high peripheral speed (v = 47 m/sec, A_s = 300 cm^2/min)

From these figures, it is interesting to see that there is a balanced tool wear region in response to the different sawing speeds. Within this region different combinations of feed and depth of cut for a constant sawing rate has no significant effect on the segment wear, which, therefore, is defined as the balanced wear region by the author. For example, at the medium sawing speed, the balanced wear region is from depth of cut of 10 mm to depth of cut of 40 mm as shown in Figure 5.7. On the other hand, as the sawing speed increases, this region is shifted towards the shallower depth of cut as shown in the above figures.

The above test results can be correctly explained by the suggested wear mechanism of diamond abrasive tools for hard rock cutting. The results of the analysis of these worn diamond particles within the balanced wear region are shown in Figures 5.9 and 5.10.

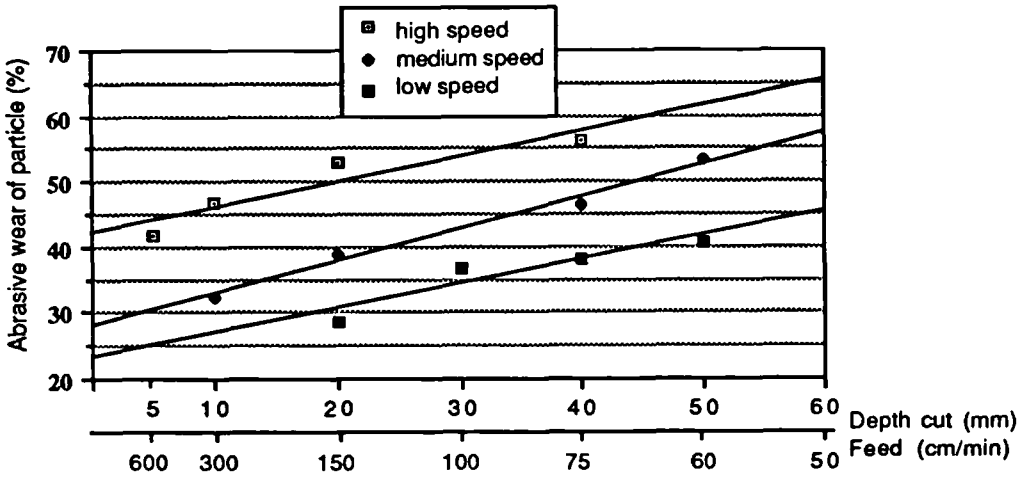


Figure 5.9: Abrasive wear relative to feed and depth of cut within the balanced wear region

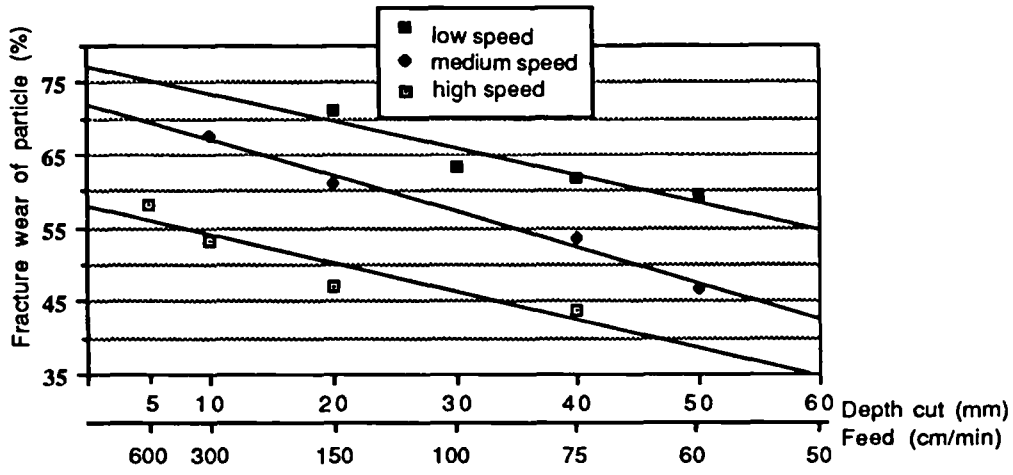


Figure 5.10: Fracture wear relative to feed and depth of cut within the balanced wear region

These figures clearly indicate that: As feed speed increases, the fracture wear is gradually enhanced and abrasive wear is reduced due to increasing impact action. As depth of cut increases, the abrasive wear is gradually enhanced and fracture wear is reduced due to increasing cutting temperature. It is believed that the overall effect of increasing abrasive wear and decreasing fracture wear as a result of increased depth

of cut and decreasing feed creates a balanced wear region. In this region, the different combinations of feed and depth of cut for a constant sawing rate have no significant effect on the segment wear. Outside the balanced wear region, larger segment wear will take place due to:

- a very strong impact action sufficient to set up shock waves within the diamond particles, leading to the shattering of the diamond edges (at a very high feed speed),

- a very heavy plowing action sufficient to produce high cutting temperatures within the cutting zone, leading to the development of excessive flat diamond wear (at large deeps of cut).

In general, radial loss of the flattened diamond particles is smaller than the loss due to shattering. That is why the excessive wear on two sides of the balanced wear region are different as shown in Figures 5.6 - 5.8.

The balanced wear region defines the limit of feed and depth of cut to be selected. For example, when Rose De La Clarte granite is sawn at a medium sawing speed, the feed speed can't exceed 600 cm/min and depth of cut can not be in excess 40 mm. And it is found that such a balanced wear region provides very reasonable limits for practical selection of these parameters.

Sawing speed plays it's role on the aspect of transposition of the balanced wear region. Results in Figures 5.6 - 5.8 shows that the balanced wear region moves towards a shallower depth of cut and higher feed speeds as the sawing speed increases as:

- at low sawing speeds, or lower cutting temperatures, the starting point of the balanced wear region will appear at a deeper depth of cut and therefore at higher cutting temperatures. Here the excessive fracture wear of diamond particles is restrained,

- at high sawing speeds, or higher cutting temperatures, the ending point of the balanced wear region will appear at a shallower depth of cut and therefore at low cutting temperatures. Here the excessive abrasive wear can be restrained.

The balanced wear can be graphically illustrated with reference to a performance model based on the relationships between the relative wear and the engineering parameters of feed speed, depth of cut and sawing speed (Figures 5.11 and 5.12).

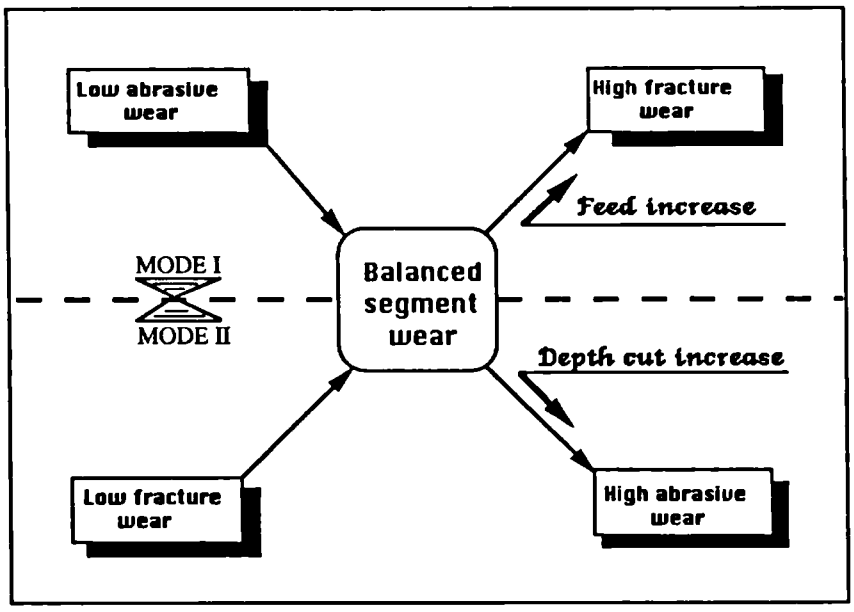


Figure 5.11: The affect of feed and depth of cut on the balanced relative wear under both modes of control

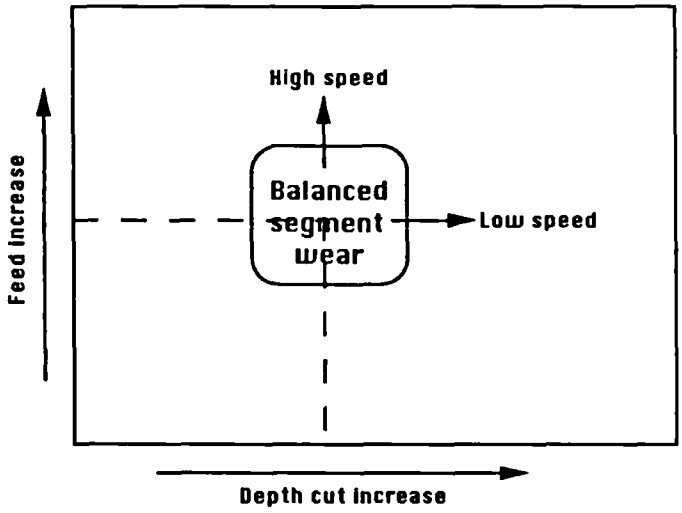


Figure 5.12: The affect of sawing speed on the balanced relative wear

5.4.3 The minimum tool wear and optimum sawing speed

During wear processes, abrasive particles gradually undergo abrasion or fracture and loose their cutting ability. The successive phases of this process may include the following phases:

The original shape of the cutting point, does not last long. From the very beginning of cutting there will repeatedly occur small losses, gradually increasing the total loss and changing the shape of the particle. The further course of wear may be twofold. In the first case, as a consequence of point shape change, the cutting force increases so much that exceeds the force retaining the particle in the bond and the whole particle is released together with a bond fragment, uncovering a new particle. Due to the pressure exerted by the tool, new particles situated in deeper bond layers now begin to work. As a result, the cutting performance of the abrasive tool practically does not change. Such a case of tool wear is called self-dressing. In the second case, although the cutting force increases as a result of particle shape change, the force

retaining the particle bond is greater and the particle becomes rounder and microchipped until it completely looses its cutting ability.

However, it is hoped that, both from technical and economic effects, the particles are released from the bond at the right moment. If this happens too early, then the relative wear of the abrasive tool increases exceedingly. If too late, the relative wear also increases, since the cutting performance is then greatly reduced. The condition under which the self-dressing process is economical is thus the occurrence of minimum relative tool wear G_{min} (Figure 5.13).

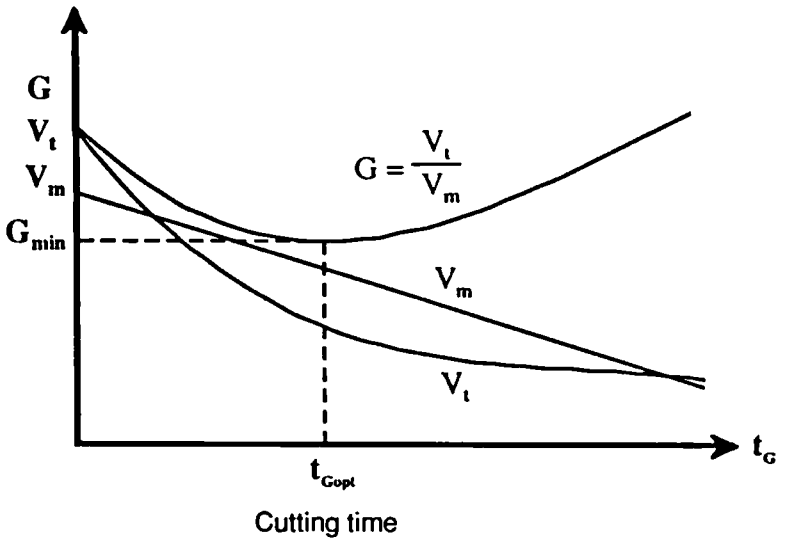


Figure 5.13: Diagram of the dependence of relative wear G_{min} during self-dressing on time of cutting by particles until torn out of bond t_G

There is no doubt that the minimum relative tool wear G_{min} is desired and test results show that the minimum tool wear is related to sawing speed. Figure 5.14 shows that the optimum sawing speed to minimize the tool wear is about 35 m/s when sawing Rose De La Clarte.

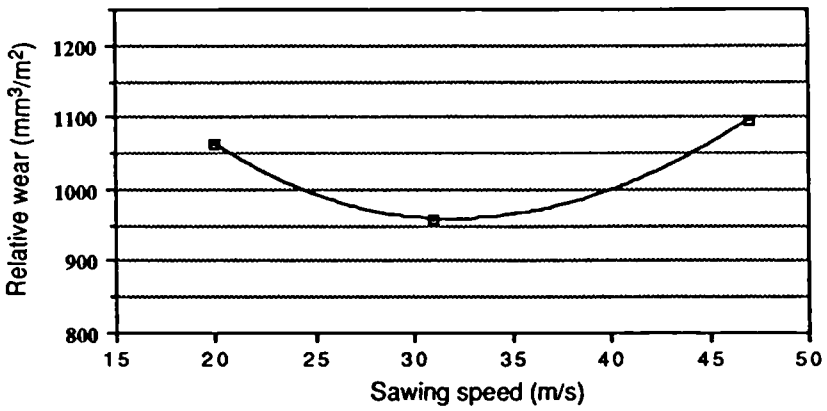


Figure 5.14: Optimum sawing speed for Rose De La Clarte
(a_p = 30 mm, v_f = 100 cm/min)

The opinion that different rock materials respond best to a specific blade peripheral speed has been accepted for rather a long time as indicated in Section 3.5.3. However, this research suggests that this view has limitations, due to the insufficient and not very carefully designed test configurations used in the past. Current work on diamond sawing optimization suggests that these tests may have been conducted within the balanced wear region related to different sawing speeds and therefore the optimum sawing speed was identified. In Figure 5.14 a depth of cut of 30 mm and a feed speed of 100 cm/min were chosen to demonstrate that the relative wear at different sawing speeds is within the balanced wear region. Figures 5.15 and 5.16 clearly indicate that there is no optimum sawing speed if the relative wear is not in the balanced region under the different sawing speeds.

In Figure 5.16, the value of relative wear corresponding to a sawing speed of 47 m/s with a depth of cut of 60 mm actually had the depth of cut at that point reduced to 40 mm. The depth of cut for this part of the test was reduced due to the fact that such a high sawing speed with 60 mm depth of cut could be harmful to the testing machine. However as the experience gained from previous tests (see Figures 5.6 and 5.7)

suggest, the relative wear at a depth of cut of 60 mm could not be less than at a depth of cut of 40 mm when a sawing speed of 47 m/s is applied.

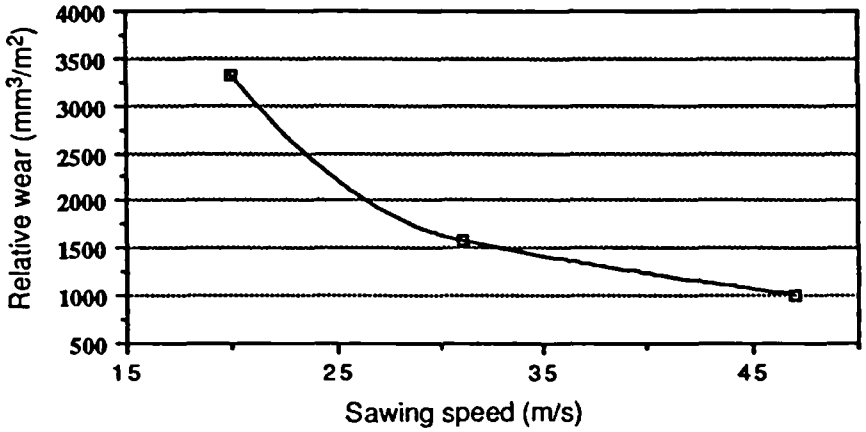


Figure 5.15: Effect of sawing speed on relative wear when sawing Rose De La Clarte (v_f = 600 cm/min, a_p = 5 mm)

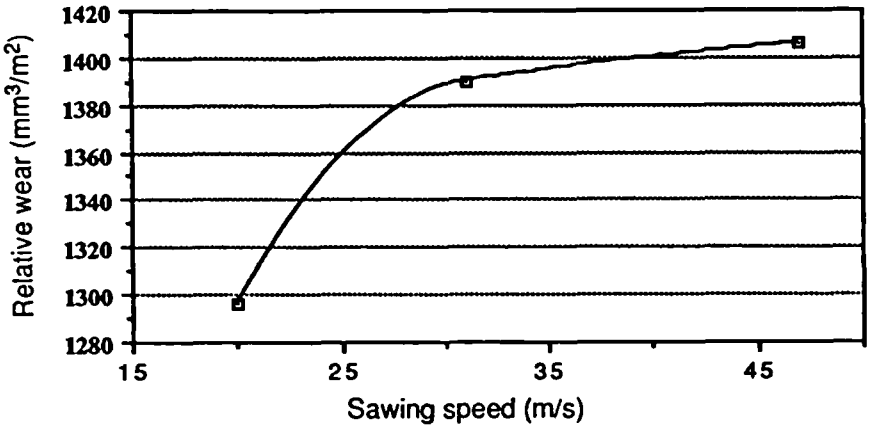


Figure 5.16: Effect of sawing speed on relative wear when sawing Rose De La Clarte (a_p = 60 mm, v_f = 50 cm/min)

The author suggests that the minimum relative tool wear may be related to the optimum temperature. The optimum temperature is defined as the temperature at which the diamond tool keeps an efficient strength and cutting superiority, while the rock becomes relatively "soft". According to experimental results by Dyer[83], a

significant reduction in the efficient strength of synthetic diamond grits is obtained at about 900°C. This indicates that one of the important mechanical properties of diamond is its efficiency at a high temperature. On the other hand, it has been found that, with respect to rock, the resistance of cutting and rock abrasiveness decrease with increasing temperature[84]. For example, test results obtained by Taljas[85] show that when cherty flint, granodiorite and limestone were cut, the cutting resistance measured at a temperature of 20°C was more than 180 - 252% when compared to that resistance at a temperature of 900°C. The results also showed that the abrasive index was reduced to 1/5 - 1/2 in the same time.

Therefore, it can be suggested that the lowest diamond wear under given conditions is related to the optimum temperature. The curve shown in Figure 5.14 then could be interpreted as: Since virtually all the work done in cutting is converted into heat, it could be expected that a sawing speed which increases the power consumed per unit volume of rock removed will increase the cutting temperature. It is suggested that as the sawing speed is increased, the temperature rises and this results in a softening of the rock material, therefore the wear curve is reduced. Beyond the optimum, the higher temperature results in a softening of the tool material as well, therefore the wear curve rises again.

5.4.4 Relative wear curve and tool life equations

Tool life in diamond cutting is defined as the time at which the useful volume of the diamond segments on a sawblade is brought to an end by gradual or progressive wear. During cutting, premature failure of a sawblade may occur at certain high sawing rates, depending on the tool and rock material. Although, after repairing, the failed sawblade could be used again, the premature failure of the sawblade should be

avoided. Therefore, tool failure is unpredictable and wear values obtained under these conditions should not be used as a measure to determine the tool life.

The relative superficial wear is taken as a measure of the diamond abrasive wear. Figure 5.17 shows the progress of relative superficial wear G_A with feed speed v_f, when Rose De La Clarte granite is sawn. It was found that this figure is very similar to the previous test results obtained by Buttner[50] on sawing Impala granite as discussed in Section 3.5.2. The wear curve of diamond cutting therefore can be divided into two regions:

-The uniform wear region where the wear progresses at a gradually increasing rate as the sawing speed increases.

-The rapid wear region where a very much larger proportions of relative wear takes place.

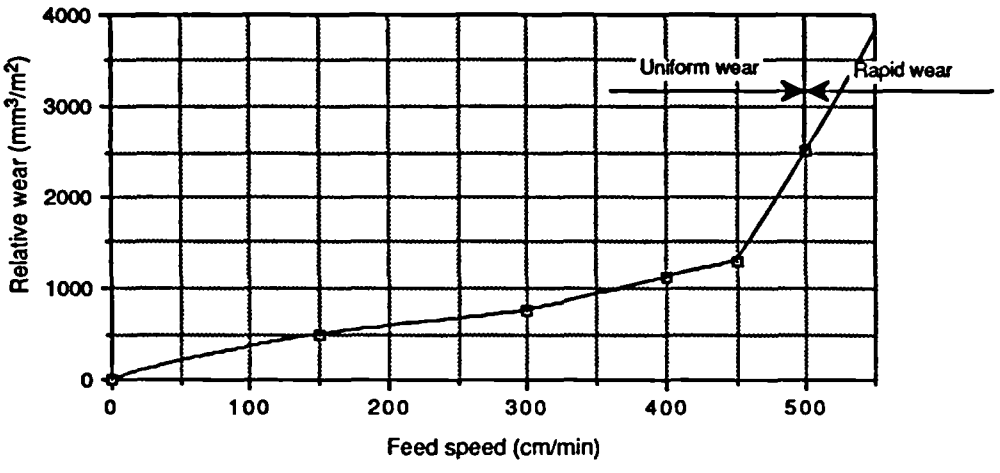
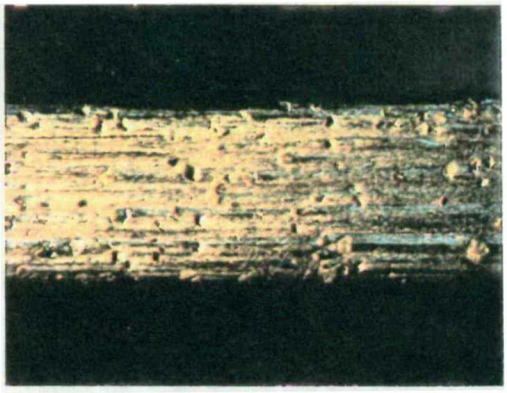


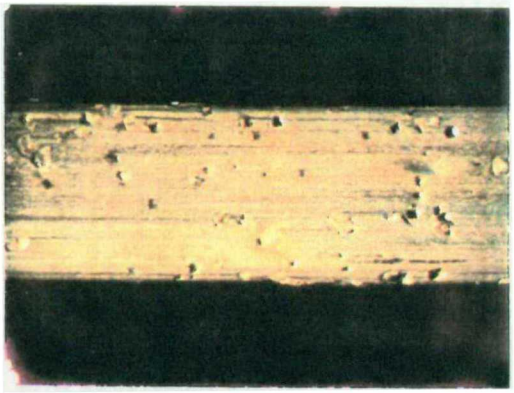
Figure 5.17: Development of the relative wear with feed speed

As shown in Figure 5.17, at very high feed speeds, the uniform wear region is ended because of the starting of the rapid wear region caused by excessive diamond

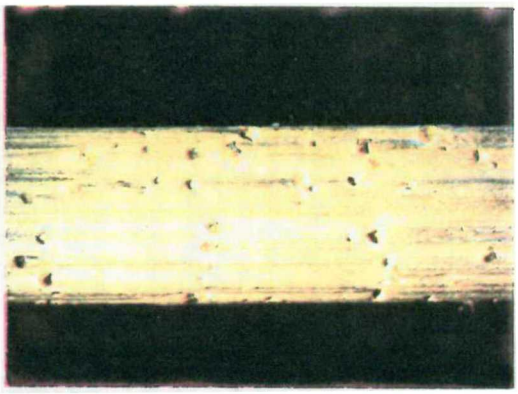
fracture wear. In the rapid wear region, the segment has become sensitive to the increased impact action and the cutting forces are also rapidly increased. Figure 5.17 shows that rapid wear has occurred at a feed speed of 450 cm/min with a depth of cut of 10 mm, when Rose De La Clarte is sawn. The premature failure of the sawblade occurred at a feed speed of 600 cm/min with the depth of cut of 10 mm. Figure 5.18 shows the cutting surfaces of a diamond segment from the uniform wear (Figures 5.18a and 5.18b) to rapid wear (Figure 5.18c) and the premature failure of the sawblade (Figure 5.18d).



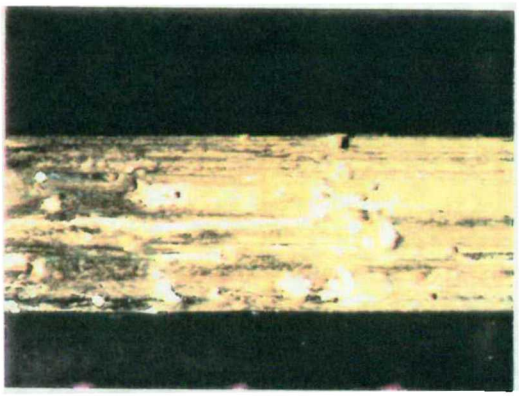
(*a*) v_f=150 cm/min, a_p= 10 mm



(*b*) v_f=300 cm/min, a_p= 10 mm



(*c*) v_f=500 cm/min, a_p= 10 mm



(*d*) v_f=600 cm/min, a_p= 10 mm

Figure 5.18: The worn segment surfaces at different conditions

The white portions in picture (*c*) and (*d*) are the stone particles inlaid into the segment being the hackly broken pieces of the diamond particles. It is noted that from the test the segments will be worn out after each sawblade failure. The segment radial wear due to failure was about 0.32 mm (just below the average size of the diamond particles), as most diamond particles were crushed or dislodged from their anchorage.

As discussed above, the practical tool life should be determined by the uniform wear rate rather than the rapid wear. The maximum feed speed before causing the rapid wear will give the minimum tool life. Referring again to Figure 5.17, the relationship between practical tool life and feed speed is presented in Figure 5.19.

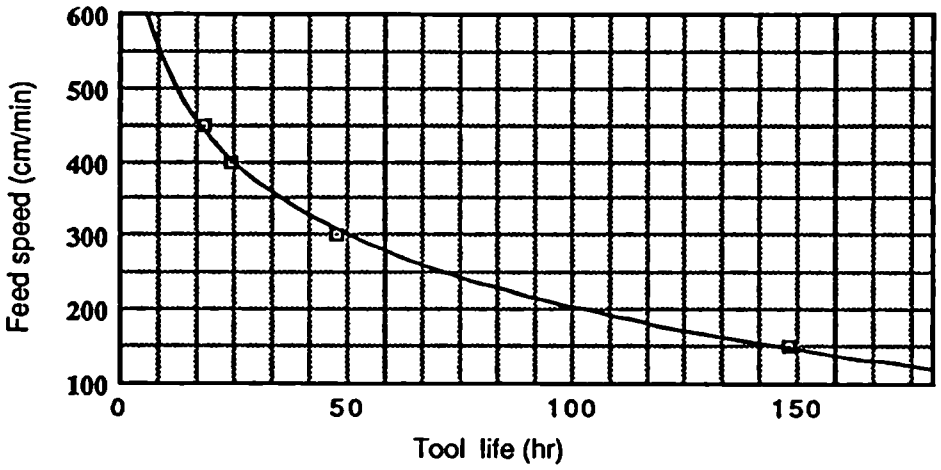


Figure 5.19: The relationship between tool life and feed speed

The curve in Figure 5.19 represents the relationship between the tool life T and feed speed v_f when plotted on rectangular coordinates. When double logarithmic coordinates are used, a straight line usually results, and that this straight line corresponds to the following equation (R^2=0.99):

$$v_f T^{0.529} = 2172 \qquad (5.9)$$

Where, v_f is the feed speed (cm/min)

T is the tool life (hr)

The above tool life equation was developed for Rose De La Clarte in the form of feed speed with tool life. This equation is very similar to the Taylor Equation for metal cutting as described in Section 2.4 except for the different definition of tool life. The definition of the tool life in metal cutting is the cutting time under constant cutting conditions until conventional dulling of the tool point occurs. Here, tool life in diamond cutting is defined as the total time at which the useful volume of the diamond segments is brought to an end due to the diamond abrasive tool wear in a self-dressing process. In the field of metal cutting, the so-called Extended Taylor Equation connecting tool life with cutting speed, feed and depth of cut provides a more convenient and useful form. This research is also aimed at developing this kind of relationship for rock cutting.

Based on the fact that there is an optimum sawing speed within the balanced wear region and that the sawing rate is governed by feed speed and depth of cut, such a relationship taking into account the effect of feed speed and depth of cut on the tool life will be particularly interesting. As indicated in Section 5.4.2., there is a balanced wear region if the depth of cut and feed speed are not too large to destroy this balance at a constant sawing rate. Also it is shown that the balanced wear region is a very practical selection range for feed speed and depth of cut. But is this finding applicable to different sawing rates? If so, a tool life equation then can be developed in the form of sawing rate with tool life so that the equation can be used more conveniently and practically.

The test for Marlin was designed in such a way that the feed speed and depth of cut were increased simultaneously with the sawing rate as shown in Table 5.6. Test results showed that the segment wear progress was also increasing at a progressive rate with increasing sawing rate, compared with the cuts of increasing feed speed only. The premature failure occurred at the sawing rate of 500 cm^2/min (263cm/min x 19mm) after sawing 1.0 m^2. Then the sawing parameters were changed to 500 cm/min x10mm at the same sawing rate of 500 cm^2/min, in order to investigate the effect of different combinations of feed speed and depth of cut on premature failure. Test results showed that failure also occurred (after sawing 1.2 m^2) with these cutting parameters and the amount of wear was almost the same as was developed with the cut of 263 cm/minx19mm, as shown in Figure 5.20.

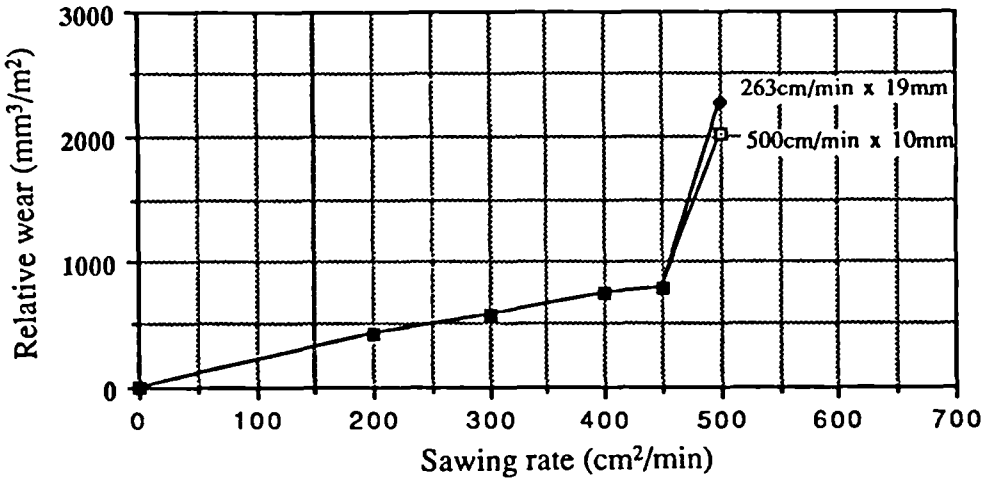


Figure 5.20: The development of the relative wear with sawing rate for Marlin

The test parameters designed for sawing Lanhelin and Limestone were similar to those used in sawing Marlin and also showed that the segment wear was at a progressively increasing rate with increasing sawing rate.

As discussed above, it is confirmed that under a defined sawing condition the different combinations of feed and depth of cut have no effect on the diamond relative wear or tool life in the whole sawing process. This means that the wear occurring within the uniform wear region belongs to the balanced wear zone. Therefore, the relative wear curves as shown in Figure 5.17 can be presented as the relative wear against sawing rate, irrespective of the different combinations of feed and depth of cut.

Figure 5.21 shows the relative wear against increasing of sawing rate for the five granite samples tested. It should be noted that the relationship between relative wear and sawing rate shown in Figure 5.21 represents the uniform region before premature failure of the sawblade occurs. The maximum sawing rate corresponding to the premature failure of the sawblade varied depending on the properties of the rock and probably on the tool material. For example, the failure happened at a sawing rate of 450 cm^2/min for Celtic, and at 500 cm^2/min for Marlin.

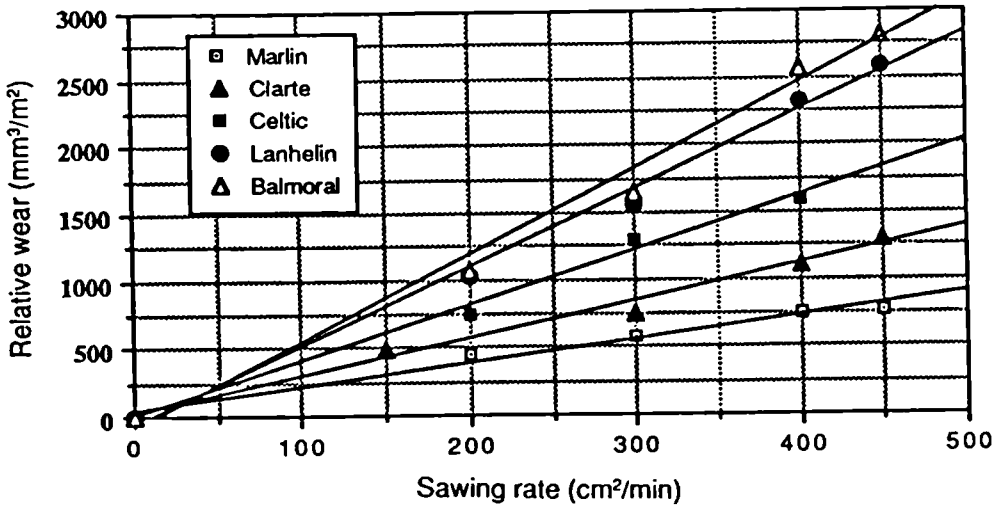


Figure 5.21: Development of the relative wear with sawing rate for five granites

Referring again to Figure 5.21, the relationship between tool life and sawing rate for these rocks are given in Figure 5.22.

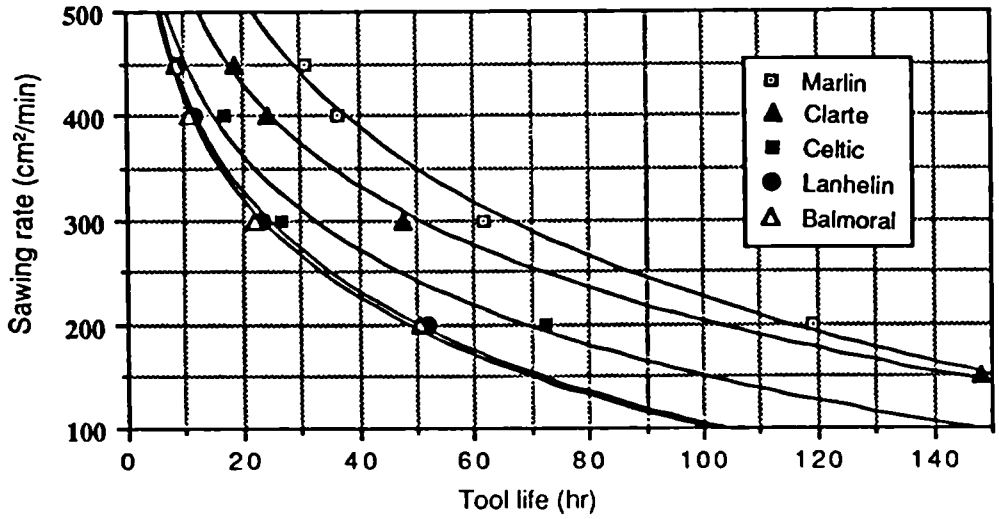


Figure 5.22: The relationships between tool life and sawing rate

Studies in machining operations and tool life behavior have led to introduction of the following relationships:

$$A_s T^x = C_s \qquad (5.10)$$

Where, A_s = sawing rate (cm^2/min)

T = tool life (hr)

x = tool life exponent

C_s = cutting constant

Tool life equations were obtained as follows for five granites:

For Marlin: $A_s T^{0.592} = 3399$ (5.11)

For Rose De La Clarte: $A_s T^{0.529} = 2172$ (5.12)

For Celtic: $A_s T^{0.462} = 1425$ (5.13)

For Lanhelin: $A_s T^{0.454} = 1220$ (5.14)

For Balmoral: $A_s T^{0.448} = 1168$ (5.15)

Equations 5.11- 5.15 were obtained from linear regression after a logarithmic transformation for the tool life and sawing rate. The tool life exponent represents the slope of the linear regression line and the cutting constant represents the intercept of the linear regression after anti-logarithm. The results of the linear regression are shown in Table 5.10.

Table 5.10: Regression analyses of log tool life and log sawing rate

	Eq. 5.11	Eq. 5.12	Eq. 5.13	Eq. 5.14	Eq. 5.15
Slope	- 0.5918	- 0.5293	- 0.4621	- 0.4543	- 0.4477
SE of slope	0.0144	0.0344	0.0659	0.0149	0.0143
t value	41.10	15.37	7.01	30.49	31.31
p value	$p<0.001$	$0.001<p<0.01$	$0.01<p<0.02$	$0.001<p<0.01$	$0.001<p<0.01$
R^2	0.9988	0.9916	0.9801	0.9978	0.9980

Table 5.10 shows that there is strong evidence of the linear relationship between the log tool life and log sawing rate. All the p-values are smaller than the significant level ($\alpha = 0.05$) and these equations can explain the variance of sawing rate at least 98% by the tool life.

Although diamond segmented tools had long been employed as an essential tool for rock cutting and diamond relative wear tests were carried out by many researchers, this is the first time that a tool life equation is develop for rock cutting and this research would form a theoretical basis for diamond cutting.

The developed tool life equation can also be expressed as:

$$T = T_i \left(\frac{A_{sr}}{A_s}\right)^{1/x} \qquad (5.16)$$

Where, T_i is the measured tool life for a given sawing rate A_{sr}.

The variability in the values of tool life equation coefficients has a strong influence on the cost, production rate, and on the selection of optimum machining conditions. A smaller tool life exponent and the cutting constant means that the sawing rate will affect the tool life greatly. For example, the exponent **x** for Marlin is larger than the exponent for Balmoral and the value of cutting constant C_s is much larger. Thus, for all sawing rates, the tool life is greater for sawing Marlin than for sawing Balmoral.

5.4.5 R-C characteristic curve

In hard rock cutting, tool life varies greatly with the sawing rate. Based on the test results, the tool lifes of sawblade DTA used for sawing different rock samples and the corresponding sawing rates are given in Table 5.11. This table shows that there is a big variation in tool life corresponding to different sawing rates. As diamond tool costs are a significant factor in the overall cutting cost, the optimization of the sawing process becomes necessary. It is known that higher sawing rates result in

increased productivity, but this also means an increased tool wear and tool cost. In order to select the sawing rate corresponding with a tool life which minimizes the production costs, by taking account the productivity and tool cost, there arises a need to develop an approach for determining the optimum sawing rate.

Table 5.11: The variable extent of tool life of DTA blade for sawing different rocks

Samples	Sawing rate (cm^2/min)	Tool life (hours)
Black Marlin	200 - 450	119.0 - 31.0
Rose De La Clarte	200 - 450	91.0 - 18.5
Grey Celtic	200 - 450	72.5 - 11.0
Lanhelin	200 - 450	52.0 - 9.0
Balmoral	200 - 450	50.0 - 8.5
Limestone	300 - 800	1113.4 - 104.0

The total cost of an operation can be expressed by the formula:

$$C_T = t_m c_m + (\frac{t_m}{T})c_t + t_o c_m \qquad (5.17)$$

Where, t_m = machine time

c_m = machine and operator (including overheads) cost per unit time

c_t = purchase price of the sawblade

t_o = down time (loading and unloading, transport, inspection)

T = Tool life

If the tool life equation 5.10 is taken to be valid, and further, if the surface area of rock material to be sawn is Δ, the machine time will be:

$$t_m = \frac{\Delta}{A_s} = (\frac{\Delta}{C_s})T^x = K_s T^x \qquad (5.18)$$

From Equations (5.17) and (5.18):

$$C_T = K_s T^x c_m + \frac{K_s T^x}{T} c_t + t_o c_m \qquad (5.19)$$

Then, the optimum tool life T_o can be obtained from the condition $dC_T/dT = 0$,

$$T_o = \frac{1 - x}{x} \frac{c_t}{c_m} \qquad (5.20)$$

As an example, if the price of the sawblade is 430 Pounds, the machine and operator cost per hour is 10 Pounds, the optimum tool life for sawing these rocks can be calculated as:

For Marlin: $T_o = 0.69 \frac{c_t}{c_m} = 29.67$ (hr)

For Rose De La Clarte: $T_o = 0.89 \frac{c_t}{c_m} = 38.27$ (hr)

For Celtic: $T_o = 1.16 \frac{c_t}{c_m} = 49.88$ (hr)

For Lanhelin: $T_o = 1.20 \frac{c_t}{c_m} = 51.60$ (hr)

For Balmoral: $T_o = 1.23 \frac{c_t}{c_m} = 52.89$ (hr)

For a given operation, the optimum production cost can be easily determined by submitting the optimum tool life and corresponding sawing rate to Equation 5.17.

The first part of Equation 5.17 is the machining cost, which is reduced as the sawing rate is increased. The second part is the tool cost, which increases as the sawing rate increases. The final part is the non-productive cost, which is constant for the particular operation. The effect of sawing rate on the cost of production can be shown more clearly in the form of a graph shown in Figure 5.23. The curve clearly indicates the relationship between sawing rate and production cost, which is defined as the R-C characteristic curve by the author.

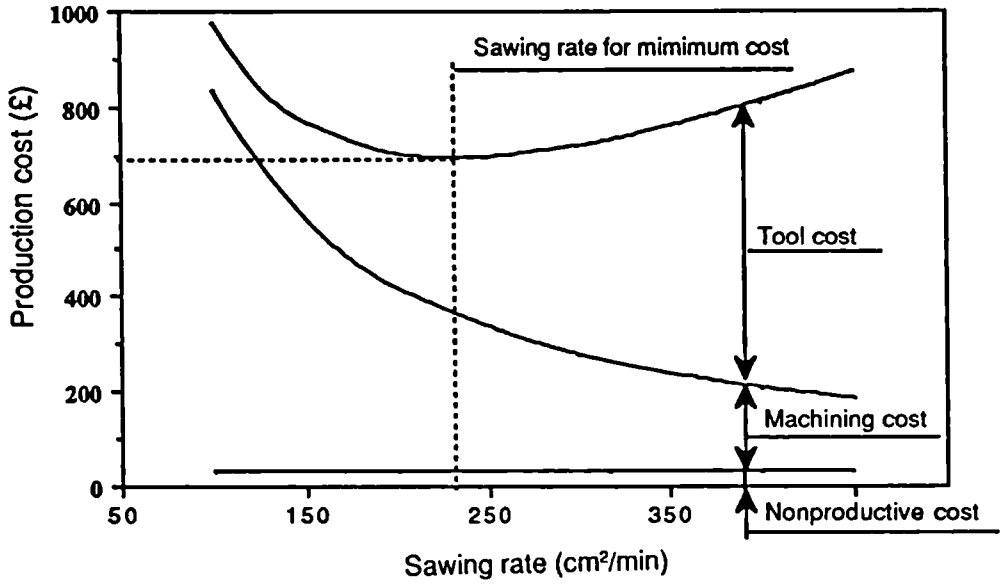


Figure 5.23: R-C characteristic curve for sawing 50 m² of Celtic
Where, c_m=10 (Pounds/hour); c_t=430 (Pounds); t_o=3 (hours)

Using the same cutting conditions including the time and sawblade cost as shown in Figure 5.23 for Celtic, the R-C curves for sawing Marlin, Rose De La Clarte, Lehelin and Balmoral are given in Figures 5.24 - 5.27. These curves contain all possible combinations of machining conditions (for a given combination of rock

material and sawing tool) for which at any given sawing rate the production cost is defined and conversely, for any given production cost, the sawing rate is defined. It has been demonstrated that the most economic conditions (minimum cost, optimum sawing rate, maximum potential profit) can be found along the **R-C** characteristic curve.

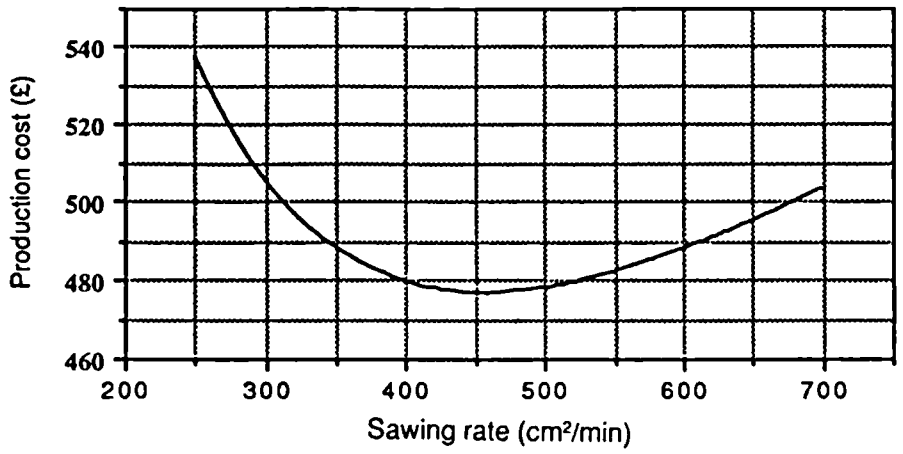


Figure 5.24: R-C curve for sawing Marlin

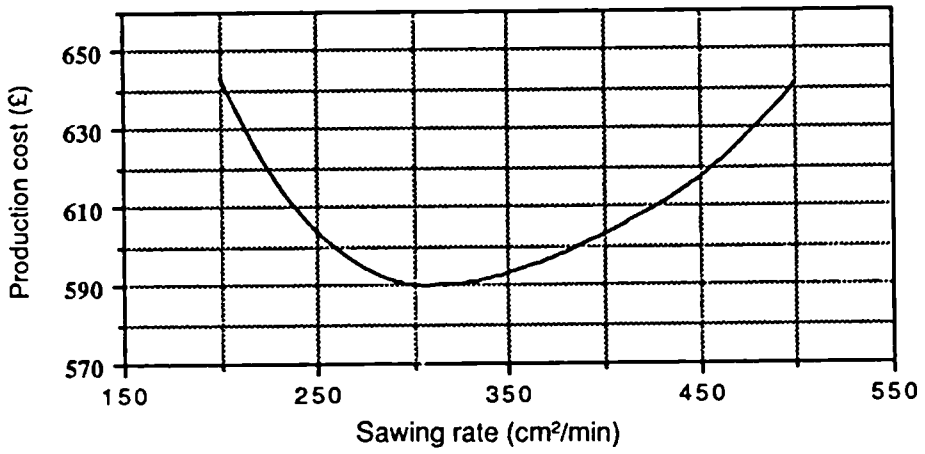


Figure 5.25: R-C curve for sawing Rose De La Clarte

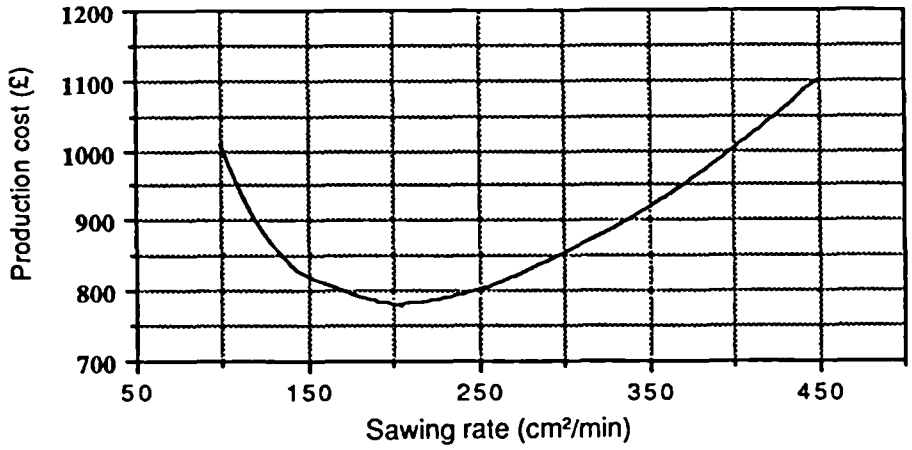


Figure 5.26: R-C curve for sawing Lanhelin

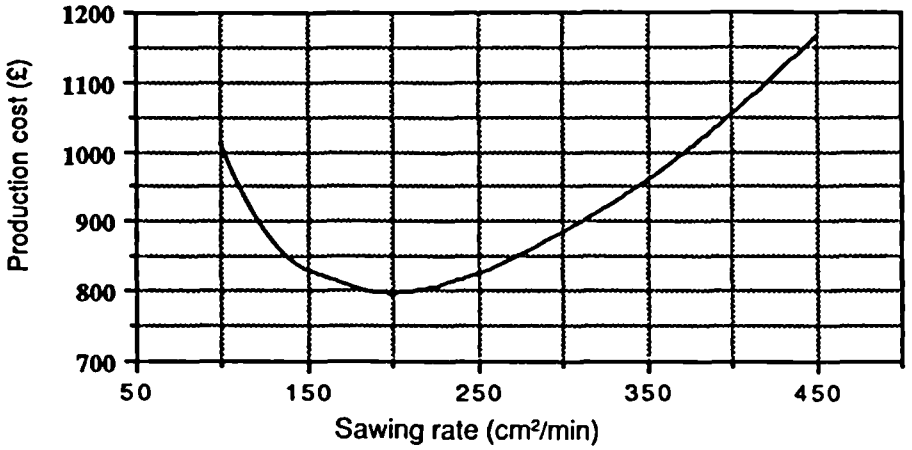


Figure 5.27: R-C curve for sawing Balmoral

It should be noted that in the case when the tool cost is not a significant portion of the total production cost, the expected optimum sawing rate may higher than the actual maximum sawing rate. For example, test results for sawing limestone of Laporte Minerals showed that a maximum sawing rate of 900 cm^2/min can be achieved using the DTA sawblade. The relative wear for sawing this kind of grey limestone is very small (i.e. 1/40 to sawing Balmoral). Because of the small relative wear for sawing soft rock, the machine time cost becomes relatively much more important in the total production cost. Using the same cutting conditions as shown

above for the five hard rocks, the optimum sawing rate calculated for sawing this kind of limestone will be about 980 cm^2/min. The expected optimum rate is already higher than the maximum sawing rate. In this case, the maximum profit would be obtained from the maximum sawing rate from the R-C concept. Certainly, a sawblade used for hard rock cutting may not suitable for soft rock cutting, i.e., the diamond size used for soft rock cutting (US mesh 20/30) should be bigger than the size for hard rock cutting (US mesh 40/50).

5.5 CUTTING MECHANISMS AND SAWING FORCES

5.5.1 Resolution of forces in circular sawing

In circular sawing, two reference systems have been adopted to determine the components of the sawing forces: (I) the reference system connected with the machine, (II) the reference system concerned with each tooth of the sawblade.

The reference system connected with the machine consists of:

(a) The reference line constituting the axis of cutter spindle. The projection of the cutting force on this line is called the axial component the reference F_x.

(b) The reference line perpendicular to the spindle axis and situated in the vertical plane. The projection of the cutting force on this reference line is called the vertical component or supporting component F_y.

(c) The reference line perpendicular to both the preceding lines. The projection of the cutting force on this reference line is called the horizontal component or transverse component F_z.

The reference system connected with the machine does not depend on the kinematics of cutting and is stationary. Therefore, the force measurement is usually carried out according to this reference system.

The reference system concerned with the cutting tooth consists of:

(a) A line constituting the cutter axis; the projection of the cutting force on this direction is called the axial component $\mathbf{F_x}$. This term is justified by the fact that the sawblade being correctly mounted, the blade axis and the spindle axis coincide. This force usually is very small and could be negligible during analysis the sawing processes.

(b) A line perpendicular to the cutter axis and passing through the tip of the tooth. The projection of the cutting force in this direction is called the thrust component or radial component $\mathbf{F_v}$.

(c) A line perpendicular to both preceding lines, tangential to the circle circumscribed on the contour of the cutter. The projection of the cutting force on this line is called the tangential component or peripheral component $\mathbf{F_t}$.

The directions of forces acting the sawblade according to both two reference system are illustrated in Figure 5.28.

5.5.2 Mode of sawing

The two basic methods of circular sawing used, down-cutting and up-cutting as shown in Figure 5.28, generate different influences on the sawing process. In down cutting, feed speed, is in the same direction to that of blade rotation, and the cutting

process starts with maximum chip thickness, and can add an extra load to the rock material. In up cutting, the feed speed, is in a direction opposite to that of blade rotation, the cutting process starts with the minimal chip thickness, and can lead to lifting of the rock material.

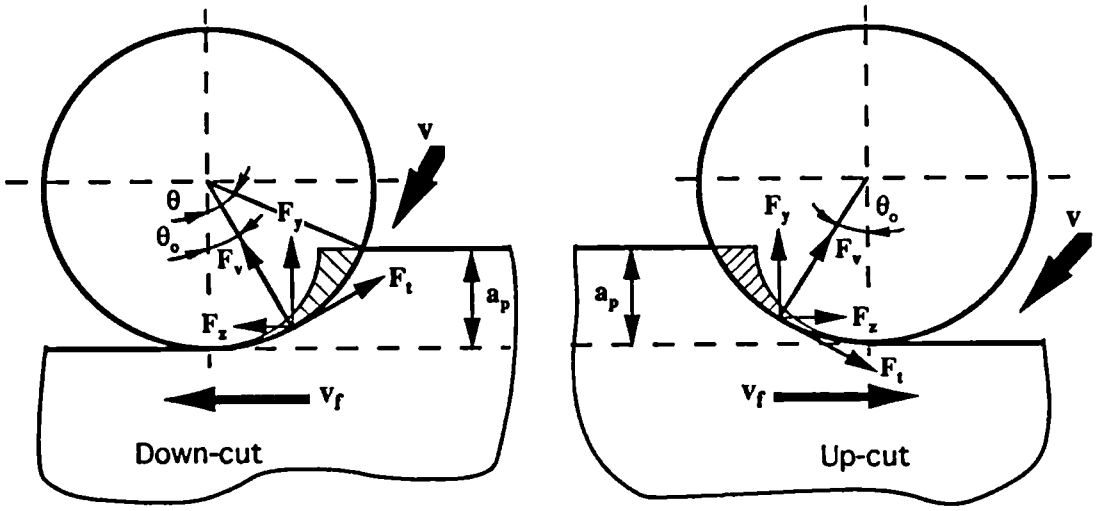


Figure 5.28: Diagram of sawing forces on a sawblade in both down- and up-cutting modes

In practical rock cutting operations, the electric current consumption of the blade motor is often measured as a means of monitoring blade behavior in the cut. The power drawn is mainly determined by the tangential cutting force. In order to characterize the phenomenon of cutting in general, some times it is necessary to investigate the tangential and thrust forces generated at the blade periphery. Actually, the values measured by the dynamometer are the horizontal force F_z and vertical force F_y with the reference system connected with the machine. However, tangential force F_t and thrust force F_v can be calculated from the measured values of horizontal force and vertical force.

Because the blade peripheral speed is far greater than the feed speed, it is assumed that the shape of the cutting surface is approximately the arc of a circle. If the point of application of the mean cutting force is defined by θ_0 in Figure 5.28, the following equations are easily obtained from the geometry which determines the values of F_t and F_v in terms of F_y, F_z and θ_0[86].

Up-cut mode:

$$F_v = F_y \cos\theta_0 + F_z \sin\theta_0$$
$$F_t = F_z \cos\theta_0 - F_y \sin\theta_0 \qquad (5.21)$$

Down-cut mode:

$$F_v = F_y \cos\theta_0 + F_z \sin\theta_0$$
$$F_t = F_y \sin\theta_0 - F_z \cos\theta_0 \qquad (5.22)$$

Down-cutting and up-cutting will generate different influences on the sawing process. Test results showed that down-cutting generates proportionately greater vertical forces and smaller horizontal forces than up-cutting as shown in Figure 5.29.

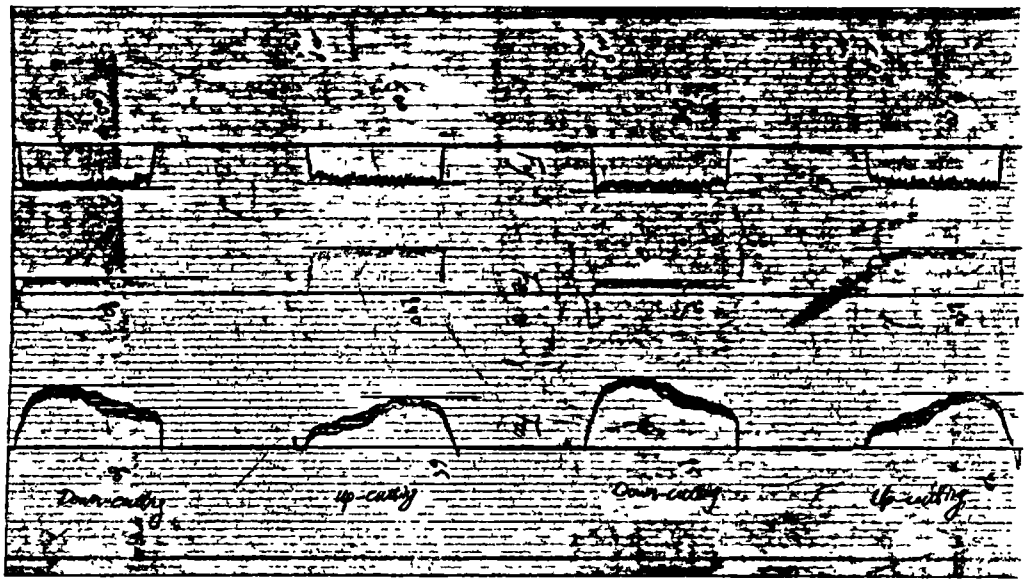


Figure 5.29: Cutting forces verses down- and up- cutting for sawing Rose De La Clarte (v_f = 300 cm/min, a_p = 10 mm)

5.5.3 The hypothesis of diamond abrasive cutting mechanism

As indicated in Section 3.4, some suggestions were given on the diamond abrasive cutting mechanism. However, as the sawing operation is a very complex process involving a combination of many factors, it is difficult to judge which explanation can be accepted as a preferable answer. Based on observations of the actual sawing operation and analysis the specific features of abrasive processes the author believes that the following hypothesis would offer a better explanation to the abrasive cutting mechanism. The process of diamond abrasive cutting with a single particle may consists the following phases (Figure 5.30):

Phase I: elastic friction - In the case when the penetration depth of the diamond particle is less than the minimum penetration depth, a cutting process does not occur. Depending on the penetration depth, there may be: (a) friction within the limits of elastic deformations, (b) friction within the limits of plastic deformations, accompanied by scratching.

Phase II: plastic extruding - In cutting, there also occur friction and extruding processes. The larger the penetration depth, the larger becomes the share of chip plastic deformation energy and the more the percentage share of external friction energy.

Phase III: plastic deformation - The shape of chips are formed by plastic deformation, which are variable and also shapeless.

The number of points which do not cut but only rub against the work surface is considerable, because of the non-uniformity of particle distribution in the segment.

For example, if two successively working particles are situated very close to each other then a case of rubbing may occur instead of cutting. This is one of the causes of higher vertical cutting forces in the abrasive process.

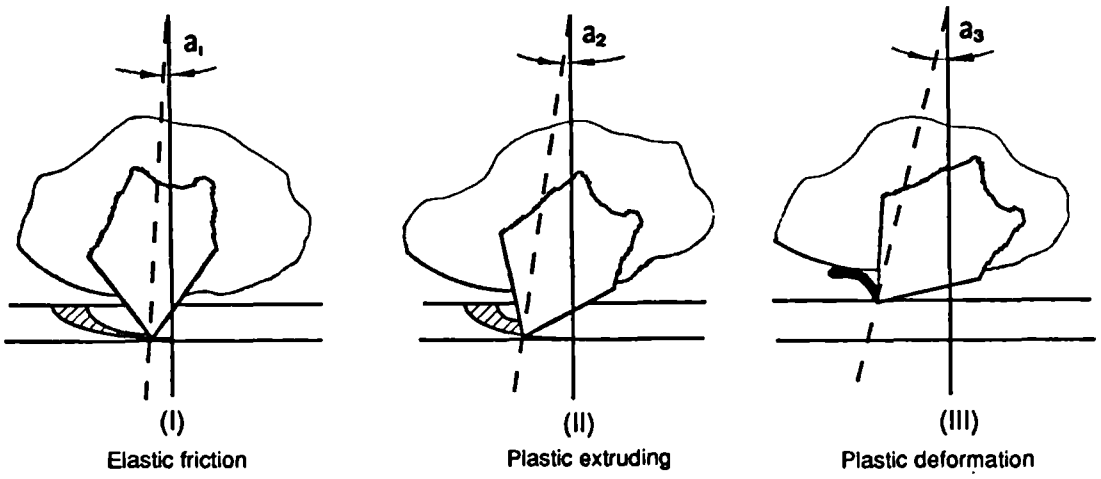


Figure 5.30: Diagram illustrating the abrasive cutting mechanism

5.5.4 Force ratio of diamond abrasive cutting

In the stone cutting process, a characteristic index of the share of penetration and cutting energy is the ratio of the components of cutting force: thrust force F_v and tangent force F_t (Equation 5.23). A small ratio means that it is easier for the tool to penetrate the rock material.

$$W_y = \frac{F_v}{F_t} \qquad (5.23)$$

This ratio is considerably changed depending on the different cutting methods and cutting conditions. For example, when cutting rock using picks, the ratio is about 0.7 - 0.8[87]. Snowdon *et al*[88] investigated rock cutting by disk cutter with an 80^0 edge angle and a tip radius of 2.5 mm and indicates that the ratio of the normal force to rolling force changes from 13.8 to 4.8 as the penetration increases from 2 mm to 10 mm. A further conclusion was that there was little relationship between different rock types and the ratio. Although this ratio described by Snowdon is not the ratio of thrust force to tangent force as defined before, for any rolling cutting, this characteristic index of the share of penetration and cutting energy can be approximately described by the ratio of vertical force to horizontal force.

Figures 5.31 - 5.32 show the authors test results of the force ratio of vertical force to horizontal force for diamond abrasive cutting, from which the specific feature of the characteristic force index can be investigated.

The test results showed that there was a little difference in the force ratio in the overall behaviors of the different rock types as shown in Figure 5.31. The force ratio gives the result that the smaller the ratio, the stronger penetrating ability of the tool. In other words, the tool becomes sharper. It is noted that from Figures 5.31(a) and 5.31(b) both at a sawing rate of 400 cm^2/min applied for the test, that the force ratios changed according to the different combinations of the feed speed and depth of cut. Therefore, it can be said that the force ratio depends on the engineering parameters and the shapes of diamond particles not the rock types. Figure 5.32 shows the effect of operating parameters on the force ratio.

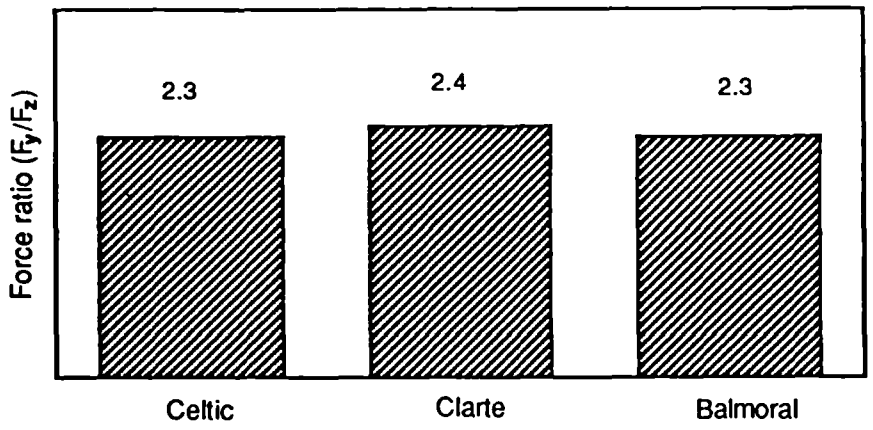


Figure 5.31(a): Effect of rock types on the force ratio
(v_f = 400 cm/min, a_p = 10 mm)

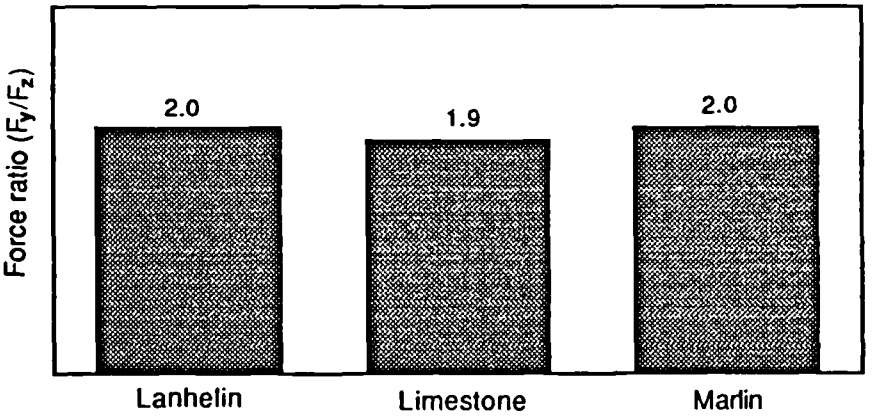


Figure 5.31(b): Effect of rock types on the force ratio
(v_f = 222 cm/min, a_p = 18 mm)

It can be postulated that the force ratio should decrease with cutting temperature increase. From Figure 5.32, at a constant sawing rate of 300 cm^2/min for sawing Rose De La Clarte, the fact that the force ratio decreases with the increasing of depth of cut and decreasing feed speed is due to the cutting temperature increase. As indicated in Section 5.4.3, as the cutting temperature increases, the rock becomes relatively "soft", which leads to the situation that the tool more easily penetrates the rock.

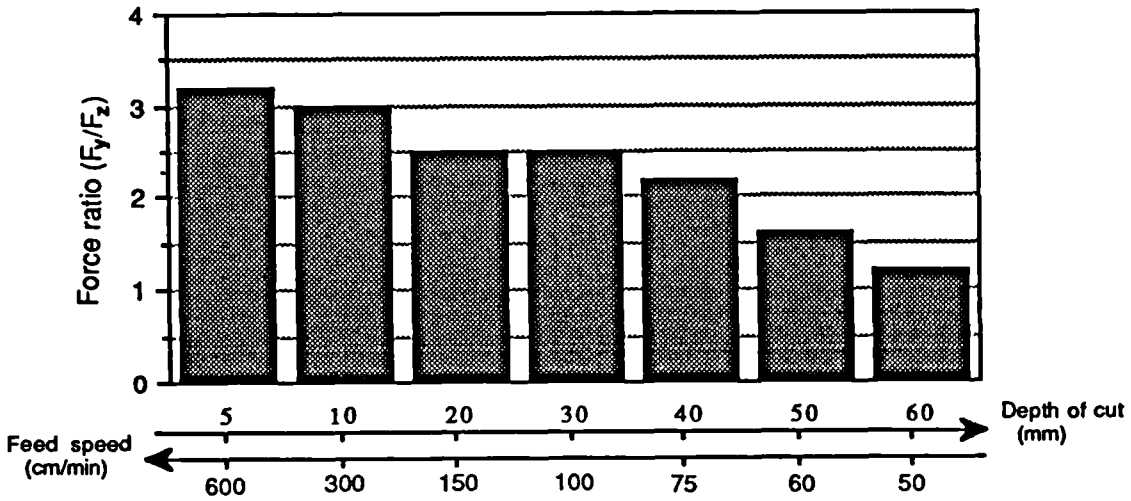


Figure 5.32: Effect of operating parameters on the force ratio

5.5.5 The effects of engineering parameters on cutting forces

To start the cutting process it is necessary to apply a force sufficiently great and suitably situated in space. This force must be able to overcome the resistance of the material to elastic and plastic deformation, the frictional resistance and the resistance to the destruction of cohesion and to the creation of a new surface. Cutting force is greatly affected by the machining tool, the rock material and cutting parameters. Here, the effects of cutting parameters on cutting force will be discused. The relationship between cutting forces and relative wear will be explained. Such a discussion enables one to understand more clearly the process of diamond cutting. For example, one might have expected that an increased sawing force means higher loads acting on the segment, which should result in increasing tool wear. Unfortunately, test results showed that this is not true. But what are the reasons behind this and what are the main factors affecting the sawing forces? Firstly, we discuss how the feed speed affects the sawing forces.

The effect of feed speed

Figures 5.33 - 5.34 show sawing forces against the feed speed. These curves clearly indicate that although the horizontal force was kept stable or with little change, the vertical cutting force did not increase but rather decreased as the feed speed increased at a constant depth of cut. This is due to:

- with lower feed speed, or lower cutting forces, the plowing function is enhanced and the cutting edges of the diamond particles become progressively round (flat wear) and the clearance angle is reduced. These flattened edges require relatively bigger cutting forces in the sawing process.

- higher feed speeds result in more volume of rock material removed and increases the cutting forces. On the other hand, higher forces generate stronger impact action, thereby producing sharp new cutting edges (microfracture) and reducing the depth of penetration of the diamond particles. These sharp edges therefore require relatively smaller cutting forces in the sawing process.

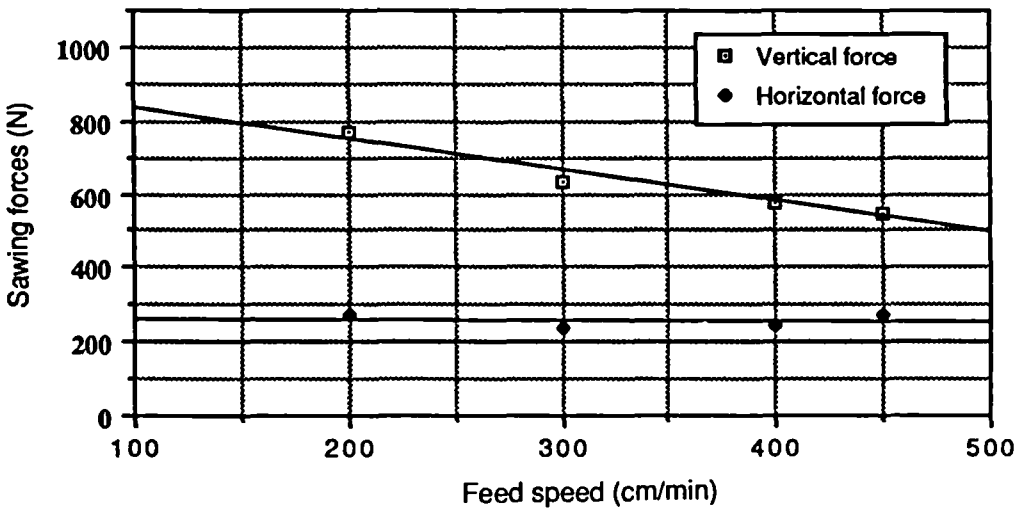


Figure 5.33: Sawing forces relative to feed when sawing Balmoral (a_p=10 mm)

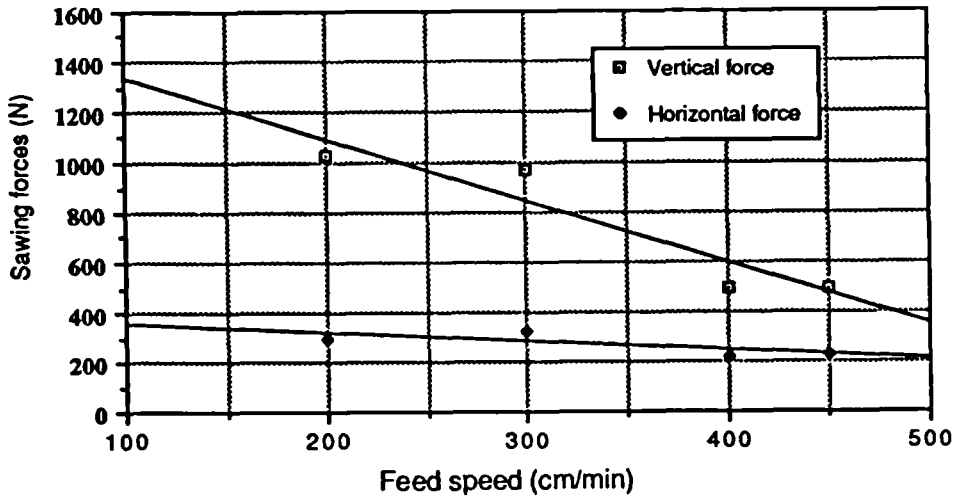


Figure 5.34: Sawing forces relative to feed when sawing Celtic (a_p=10 mm)

The forces actually produced depend on which function prevails, impact or plowing. In other words, the worn diamond types of microfracturing and flat wear will be directly affecting the sawing forces. The fact that cutting forces are decreased with increasing feed at a depth of cut of 10 mm is due to a reduction in load caused by an increase in microfracturing. As shown in Figures 5.35 - 5.36, the microfracturing was increased and the flat wear was decreased as feed rate increases, when Balmoral and Celtic were sawn.

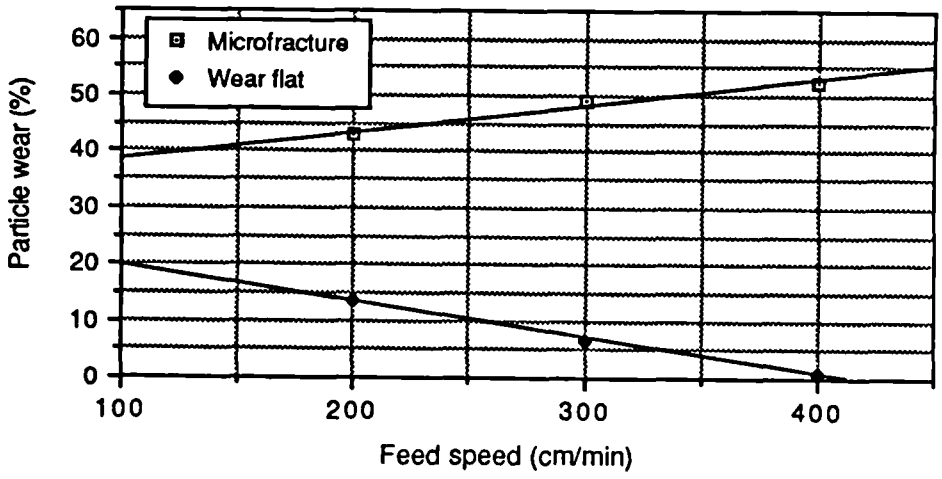


Figure 5.35: Microfracture and flat wear relative to feed speed (for Balmoral)

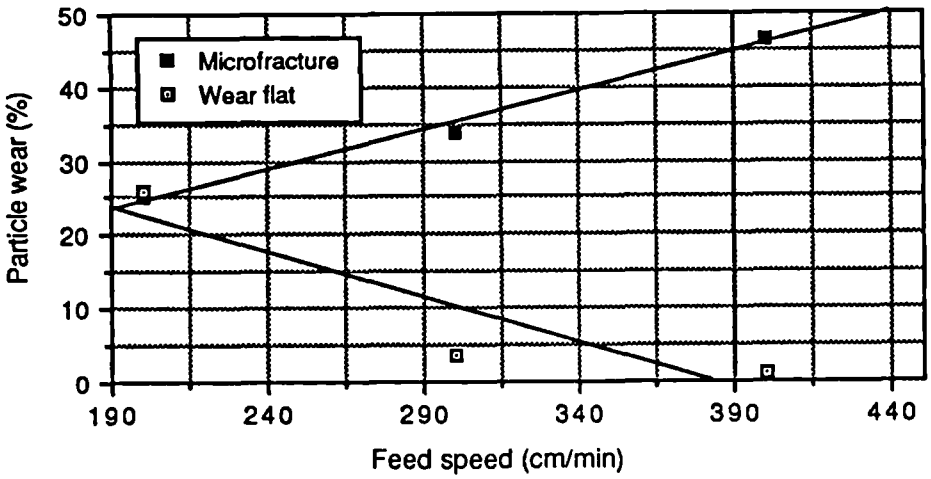


Figure 5.36: Microfracture and flat wear relative to feed speed (for Celtic)

It should be noted that Figures 5.33 and 5.34 relate to the uniform wear region only as the feed speed increases. In the whole wear region including the rapid wear region, it is also shown that there is a good match between the cutting forces with the worn diamond particle form as shown in Figures 5.37 and 5.38.

As indicated above, a smaller cutting force should correspond to a higher degree of microfracture of diamond particles. Figure 5.38 clearly indicates that as the feed speed is increased to a certain level, the approximate balance between the increasing force due to feed and the decreasing force due to the sharp edges is overturned. Then diamond is worn by crushing to shallow penetration and or leaves a deep hole rather than microfracture and the rapid relative segment wear occurs accompanied with a greatly increased sawing forces. Compared with Figure 5.17 of the wear curve and Figure 5.37 of the force curves both in the whole wear region, this match can be clearly seen.

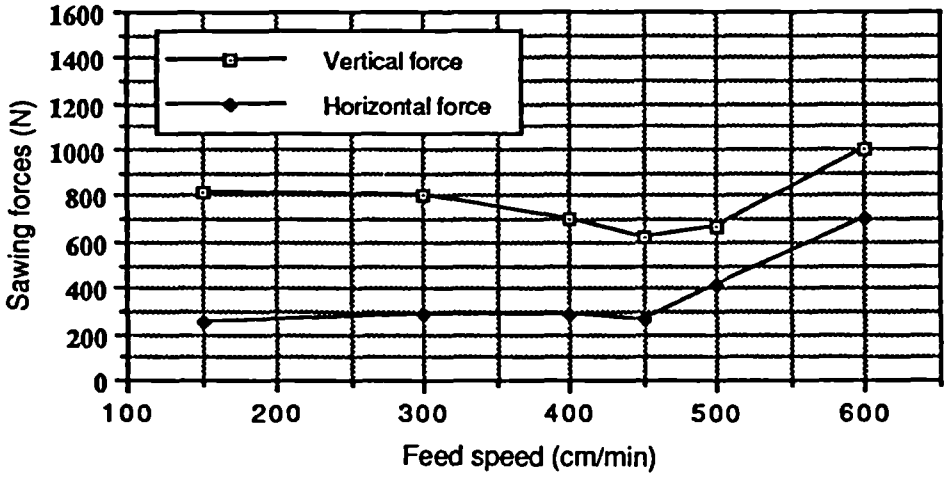


Figure 5.37: Force curves relative to feed in both the uniform and rapid wear region

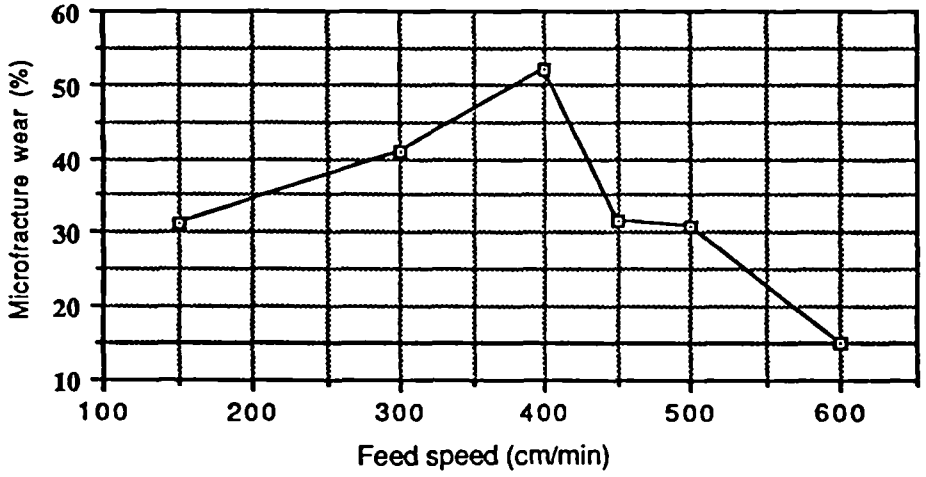


Figure 5.38: Microfracture relative to feed in both the uniform and rapid wear region

The effect of depth of cut

Figure 5.39 shows the effects of changing depth of cut on cutting forces. This figure suggests that the depth of cut has a significant effect on cutting forces. An increase in feed speed together with a decrease in depth of cut leads to a substantial reduction in cutting forces. It may be concluded that the cutting forces acting on a diamond

blade are minimized by employing a shallow depth of cut and a high feed speed to achieve the same sawing rate.

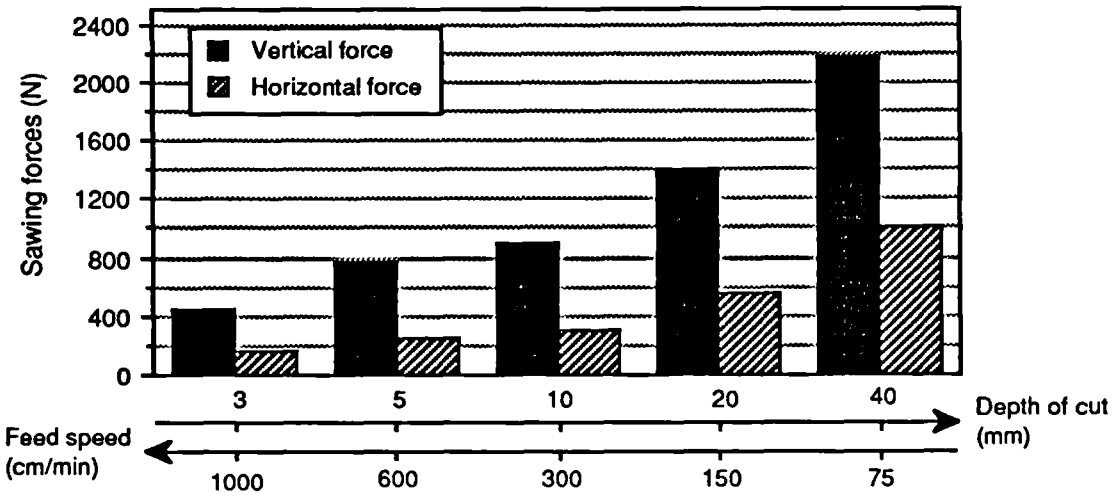


Figure 5.39: Sawing forces relative to depth cut and feed speed at constant sawing rate when sawing Rose De La Clarte

As indicated in Section 5.4.2, the different combinations of feed speed and depth of cut have no significant effect on relative segment wear in the balanced wear region, this will affect the sawing forces as shown in Figure 5.39. Therefore, it can be concluded that the cutting forces which mainly determine the power can not be used to directly predict the diamond relative wear. In fact, the cutting force is directly affected by the worn diamond types of microfracturing and wear flat. The degree of microfracturing will be increased with the increase of feed speed due to the enhanced impact action and the wear flat will be increased with the increase of depth of cut due to the enhanced cutting temperature as shown in Figure 5.40.

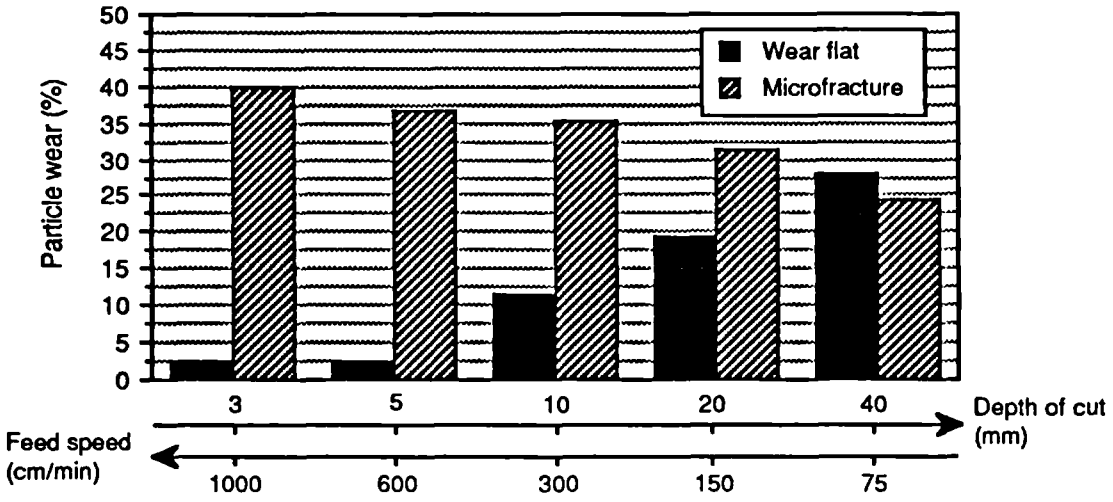


Figure 5.40: Microfracture and flat wear relative to depth of cut when sawing Rose De La Clarte

The effect of sawing speed

Figure 5.41 shows the relationship between the cutting forces and sawing speed for Rose De La Clarte granite. The figure suggests that the sawing forces will increase with increasing sawing speed due to the increasing of flat wear and decreasing of microfracturing caused by a high sawing temperature as shown in Figure 5.42.

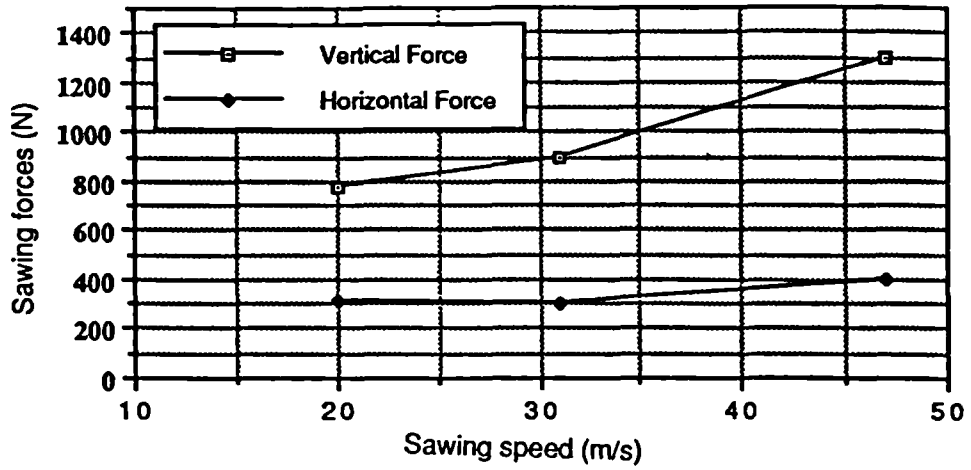


Figure 5.41: Cutting forces relative to sawing speed (v_f=300cm/min, a_p=10mm)

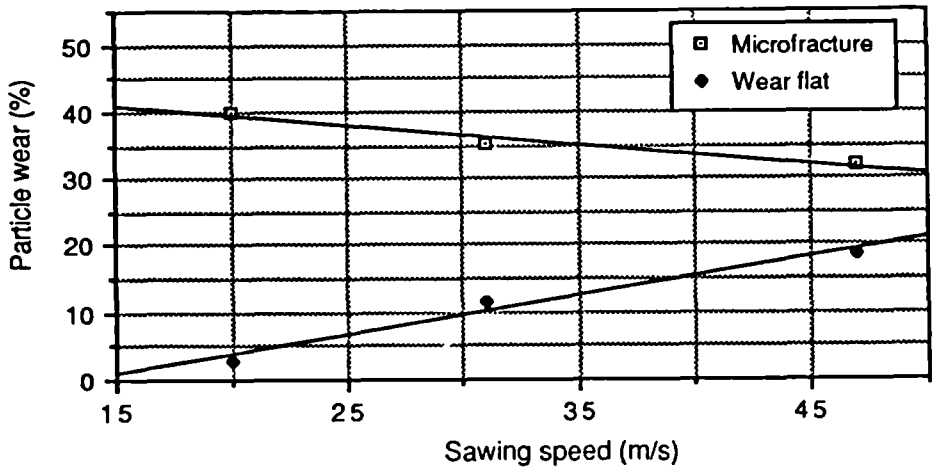


Figure 5.42: Microfracture and flat wear relative to sawing speed for sawing Rose De La Clarte

5.5.6 A possible force pattern for diamond abrasive cutting

It was thought that, as the feed speed increases, the increased load will create more particle microfracture and may reduce the cutting forces, on the other hand, the increased depth of cut will result in an increase in cutting forces due to the enhanced flat wear caused by high cutting temperatures. A compromise result should lead to a quasi-stable force pattern if the sawing parameters are chosen in a reasonable combination.

Test parameters designed for sawing Marlin are described in Table 5.6. The sawing rate was increased by increasing the feed and depth of cut simultaneously. Test results showed that, in this cutting condition, the forces were kept on a quasi-stable pattern just as expected. These are presented in Figure 5.43. Under these conditions, the microfracturing and flat wear should remain almost constant. Although the test

results showed that microfracturing was decreasing a little as the sawing rate increased (Figure 5.44), these results were very much different from the effect observed in Figures 5.35 - 5.36, in which the microfracturing greatly increased as sawing rate increased by increasing feed speed only. It was also found that flat wear did not change during the cutting ("0" was assigned to every cut).

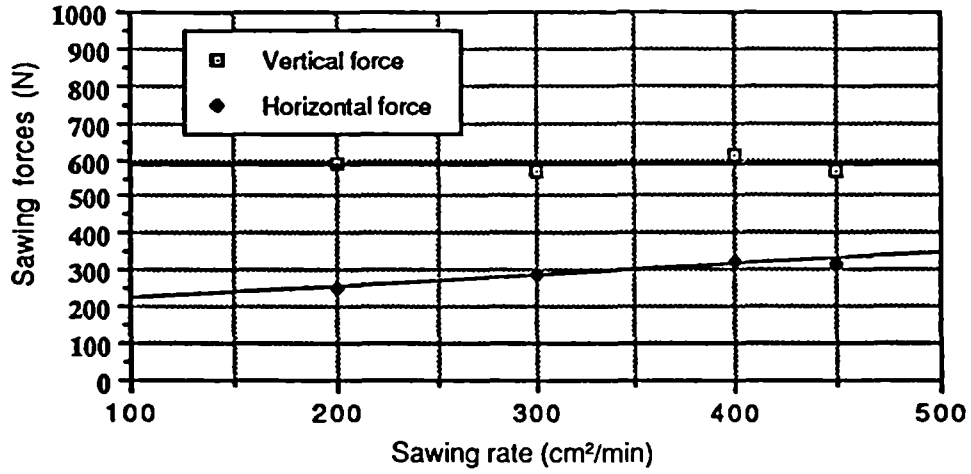


Figure 5.43: Sawing forces versus sawing rate when sawing Marlin
166x12; 200x15; 223x18; 243x18.5 (cm/min x mm)

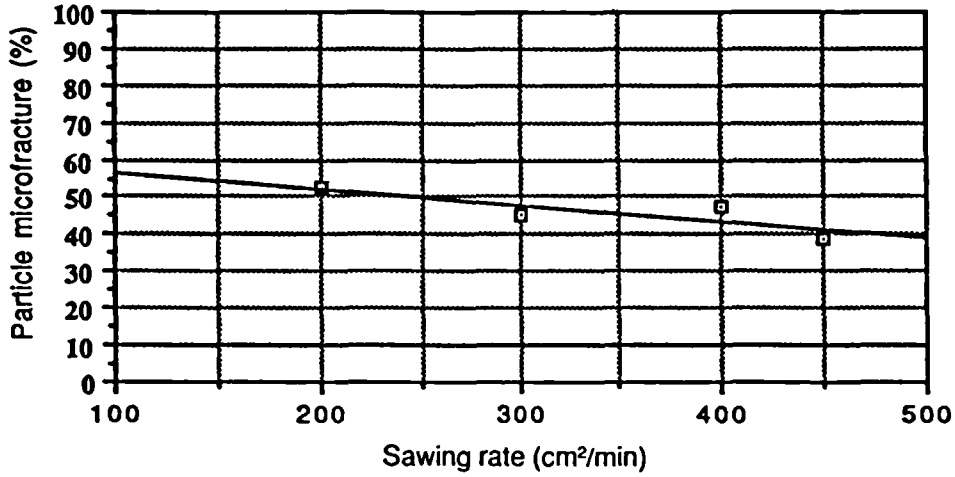


Figure 5.44: Microfracture versus sawing rate when sawing Marlin
166x12; 200x15; 223x18; 243x18.5 (cm/min x mm)

As a summary, sawing forces are directly affected by the worn diamond types of microfracturing and flat wear and are not related to the relative segment wear. An increase in depth of cut or sawing speed will result in an increase of cutting force, but an increase in feed speed, is likely to reduce the cutting force. Therefore, sawing forces can be kept in the quasi-stable state conditionally as sawing rate increases and also can be minimized by employing a shallow depth of cut and a high feed speed at a constant sawing rate.

5.6 THE RELATIONSHIP BETWEEN ε - s

In Section 2.2.3, Detournay's cutting and friction model was described in detail. The model suggested that for a blunt cutter (cutter with a wear flat), a linear relation exists between ε and s, which is presented as follows (Equation 2.11):

$$\varepsilon = \varepsilon_o + \mu_c s$$

In the above equation ε is defined as the specific energy (F_z/A_o) and s is defined as the friction energy (F_y/A_o).

Where, F_z - horizontal cutting force (N)

F_y - vertical cutting force (N)

A_o - cross sectional area of the cut (mm^2)

μ_c - friction coefficient between the cutting tool and the rock

It could be suggested that the nature of diamond abrasive cutting is same with Detournay's assumption that the rock cutting is a combination of "pure" cutting and frictional contact underneath the cutter. The authors test results showed that a linear

relation also exists between ε and s for diamond sawing. The model was computed for eight different depths of cut at a constant sawing speed of 300 cm^2/min and a medium sawing speed as shown in Table 5.12 for sawing Rose De La Clarte. As can be seen from Figure 5.45, the results are a straight line and a linear regression equation ($R^2 = 0.9$) is given as follows:

$$\varepsilon = 2.8 + 0.25\, s \qquad (5.24)$$

Table 5.12: Parameters for studying the relationship ε - s

Depth cut	3	5	10	20	30	40	60	80
A_o (mm^2)	13.5	22.5	45	90	135	180	270	360
F_h (N)	170	245	300	550	900	1000	1520	1635
F_v (N)	450	775	900	1400	2300	2175	1900	2000
ε	12.6	10.9	6.67	6.1	6.67	5.56	5.6	4.5
s	33.3	34.4	20.0	15.56	17.0	12.1	7.0	5.56

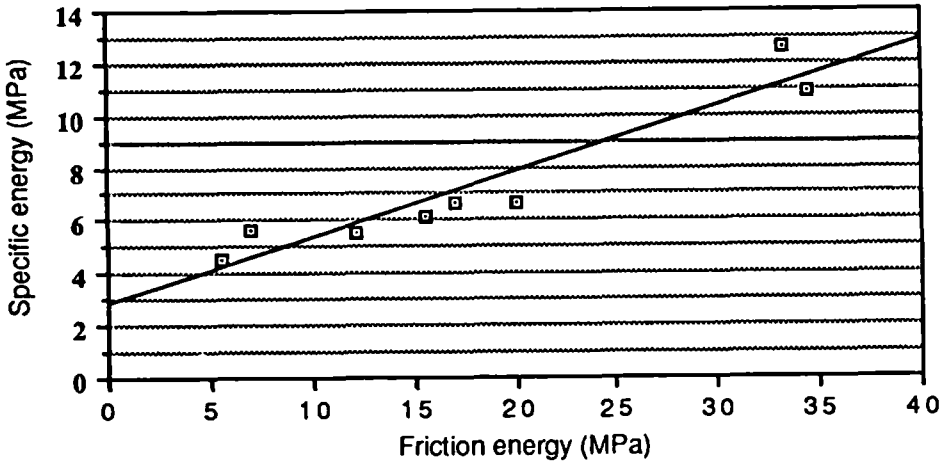


Figure 5.45: ε - s diagram for abrasive diamond cutting with different depths of cut

From the above equation, the friction coefficient between the diamond abrasive cutting tool and rock at a medium sawing speed region is obtained as 0.25 and this parameter will be used in Chapter 6. However, it can not be said that this is a rigorous method for determining the coefficient of friction between the tool and rock material. As calculated by the author from his test results, this coefficient was at least varied with the different sawing speeds. Therefore, this calculated value could only be used as an estimation of the relevant engineering problem.

CHAPTER 6

THEORIES OF DIAMOND WIRE SAWING AND UNDERGROUND TRIALS

6.1 INTRODUCTION

One of the research targets is to prove diamond wire sawing technology in underground mines and to develop mining methods which would allow the mechanization of ore production with the use of diamond wire saws. As indicated in Chapter 4, the main advantages of using diamond wires are safety, reliability and high productivity especially related to the large block extraction. In addition to that various sawing/cutting methods can be employed to suit to the different working sites available. It was decided therefore that a diamond wire saw would be used in underground mining activities.

The site trials of diamond wire sawing underground were carried in the Milldam Mine, Laporte Minerals and the diamond wire was used to cut slots prior to making raises. The rock is a kind of grey limestone, therefore, electroplated diamond wire was used for the site trials rather then the impregnated diamond wire.

It is necessary to point out that the machining characteristics for electroplated diamond tools is different from that for impregnated diamond tools as studied in Chapter 5. The electroplated diamond bead is a surface set diamond tool without the function of self-dressing and therefore can be considered as having multiple cutting

points. Its cutting mechanism can be referred to as the "pure cutting mechanism" as described in Section 2.2.

In this chapter, the theories of diamond wire sawing are also studied, because nowadays the use of diamond wire is mostly based on experience and research is lacking in the aspect of theoretical studies. As indicated in Chapter 4, diamond wire is very flexible to use and there are several possibilities for using it in stone extraction. With regard to wire cutting locus, there are two ways of threading the wire around the cutting surface, namely changeable cutting locus and stable cutting locus. The sawing methods shown in Figures 4.5-4.6, result from a changeable cutting locus and the cutting forces are not steady at an identical feed. The sawing methods shown in Figures 4.7-4.9, result from a stable cutting locus as the wire feeds into the rock. Therefore, for the purpose of using diamond wire as an underground mining tool, it is considered that stable cutting locus will be adopted. The analyses shown below will mainly relate to this cutting technique.

6.2 DEVELOPMENT OF THE THEORIES OF DIAMOND WIRE SAWING

6.2.1 The principle of drives utilizing friction force

Considering the friction drive between the driven pulley connected by a diamond wire rope in Figure 6.1, the wire behaves as a rigid body in tension only. If the force S_t is reversed, or the wire speed was to fall momentarily below $r\varphi$, this rigidity would be lost. Assuming that the pulleys are free to rotate about a fixed axle, complete kinematic closure is obtained when an endless flexible wire is stretched tightly over the rock face and pulley. The effects of elasticity are neglected, so that

the wire behaves as a rigid body on the straight portions and the motion can then be reversed. The fundamental tension relationship is supposed to obey the following Equation 6.1[89]:

$$S_t = S_s e^{\mu\theta} \qquad (6.1)$$

Where,

S_t = Tight side wire tension

S_s = Slack side wire tension

μ = Adhesive factor between the wire and packed groove surface of drive pulley

θ = Angle of wrap or contact (radians)

e = Base of Napierian logarithms (2.718)

The above equation shows the relationship between the values known as S_t, the tight side tension (and generally the tension for which the wire must be designed), and S_s, the slack side tension (the minimum value which must be available for driving the wire successfully). When the system is at rest, the tensions in the two straight portions are equal, and will be referred to as the initial tension. If a torque is applied to the drive pulley, and the initial pressure between the contact surfaces is sufficient, slipping will be prevented by friction, with the result that the tensions in the straight portions will no longer be equal. As shown in Figure 6.1, this means that when the power is transmitted from the pulley to the wire, the approaching portion of the wire will have the larger tension S_t and the departing portion will have the smaller tension S_s. The difference between the two tensions will be determined by the resistance to motion of the drive pulley. With regard to the diamond wire cutting system, it is obvious that the resistance to motion around the pulley is caused by the tangential cutting force, which is:

$$S_t = S_s + F_t \tag{6.2}$$

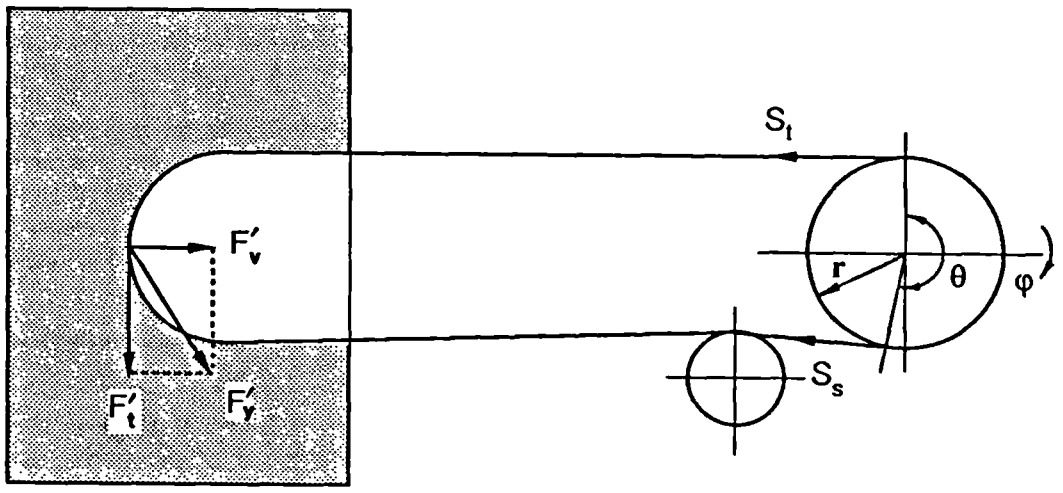


Figure 6.1: Diagram of diamond wire cutting

From Equations 6.1-6.2, the relationship between the tangential sawing force F_t and the wire tension S_s can be obtained:

$$F_t = S_s(e^{\mu\theta} - 1) \tag{6.3}$$

If v_i = the mean wire speed in m/s, the power transmitted by the drive pulley P_w is:

$$P_w = (S_t - S_s)\, v_i \tag{6.4}$$

Alternatively,

$$F_t = \frac{P_w}{v_i} \tag{6.5}$$

An important feature of rope or V-shaped drives is the virtual coefficient of friction (adhesive factor). During cutting, the wire rope rests on the bottom of the groove which is packed with a relatively soft material, such as leather. In addition to diminishing the wear on the diamond wire this gives a greater coefficient of friction. The adhesive factor μ between the wire and pulley mainly depends on the friction coefficient between the wire and the packed grove material of the pulley and the contact condition of the wire with the pulley's groove (Figure 6.2).

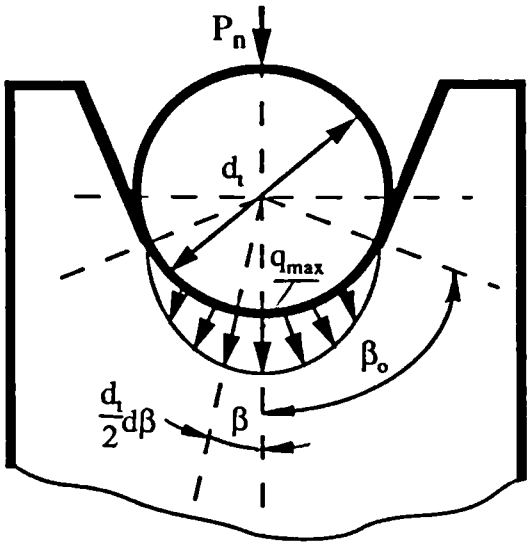


Figure 6.2: Wire rope rests on the V-shaped drive pulley

Suppose that the cross section of the wire is a perfect circle. $\mathbf{P_n}$ is the normal force acting on the pulley's groove and $\sum q_1$ is the total of the counter-forces acting on the wire. Therefore the friction force between the wire and the drive pulley is:

$$P_f = \mu_o \sum q_1 = \mu P_n \qquad (6.6)$$

Where, μ_o = the friction coefficient between diamond wire and the groove material of the drive pulley.

If the sum of the counter-forces in the distributing direction are larger than the normal force, then the adhesive factor is larger than the friction coefficient. That is:

$$\sum q_l > P_n \; ; \quad \mu > \mu_o$$

As shown in Figure 6.2, the counter-forces distribution might be described as:

$$q_l = q_{max} \cos\beta \tag{6.7}$$

$$\sum q_l = 2 \int_0^{\beta_o} q_l \frac{d_t}{2} d\beta = 2 \int_0^{\beta_o} q_{max} \frac{d_t}{2} d\beta \cos\beta = q_{max} d_t \sin\beta_o \tag{6.8}$$

Where, β_o = contact angle between the wire and the groove surface of the pulley

d_t = diameter of the diamond wire

The normal force acting on the pulley surface is:

$$P_n = 2 \int_0^{\beta_o} q_l \frac{d_t}{2} d\beta \cos\beta = \frac{1}{2} d_t q_{max} (\beta_o + 0.5\sin 2\beta_o) \tag{6.9}$$

Submitting Equations 6.8 and 6.9 to Equation 6.6, then:

$$\mu = \frac{\mu_o \sum q_l}{P_n} = \frac{2 \mu_o \sin\beta_o}{\beta_o + 0.5\sin 2\beta_o} \tag{6.10}$$

As indicated in Equation 6.10, when the friction coefficient μ_o is a constant, the closer the contact angle β_o is to 90°, the greater the adhesive factor μ will be and driving efficiency can be enhanced.

6.2.2 The proposed wire tension equation

As shown in Figure 6.1, the feeding of a diamond wire into the rockmass is achieved by the action of the tangential force and the thrust force on each diamond point that exceeds the failure strength of the rock plus the friction. Figure 6.3 illustrates the forces on a diamond wire and the tension distributions. Rock resistance to sawing can, therefore, be resolved into the reaction against thrust, and the frictional (plowing) resistance that opposes the rotation of the wire.

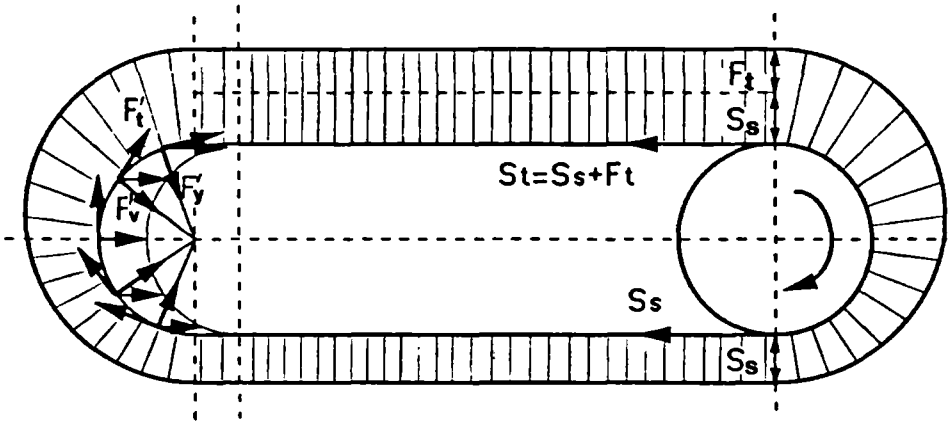


Figure 6.3: Forces and tensions on a diamond wire

Clark[90] who studied the abrasive drilling of rock, stated that the mechanism of friction by the diamonds is somewhat similar to the mechanism of friction developed between metal surfaces. He supposed that the coefficient of friction μ_c between diamond abrasives and rock could be calculated according to Equation 6.11, which is

actually quoted from the consideration of friction behavior in metal cutting between the chip and tool surface[91].

$$\mu_c = \frac{\tau}{\sigma_c} \tag{6.11}$$

$$\mu_c = \frac{\tau}{\sigma_c} = \frac{\tau}{dP/dA} = \frac{\tau\, dA}{dP} = \frac{n_d\, \tau\, dA}{F_V} \tag{6.12}$$

Where, τ is the shear strength and σ_c is the yield strength. **dP** is the average of the applied force for each diamond and **dA** is the mean cross-sectional area of each crater formed in the rock and F_V is the total thrust force. n_d is equal to the number of diamonds contacting the rock. Since the number of diamonds performing abrasion and **dA** cannot be evaluated, the coefficient of friction likewise cannot be calculated directly from Equation 6.12. Its value also varies with the frictional behavior of the diamond surface, the properties of the rock, and so forth. However, an average value of $\mu_c = 0.4$ was assumed by Clark. There is a way that this friction coefficient could be directly calculated according to the relationship between ε - S as described in Section 2.2.3. The calculated result of this coefficient using that method comes to about 0.25 (see Section 5.6) and is far smaller than Clark's assumed value.

The resistance to wire rotation due to friction F_f with normal thrust F_V is

$$F_f = \mu_c F_V = \mu_c \sum_{i=1}^{n} F'_V \tag{6.13}$$

The friction resistance F_f then can be calculated using the following equation referring to Figure 6.4.

$$\frac{1}{2}F'_V = (S_s + \frac{i}{n}F_t)\sin\frac{d\phi}{2} = (S_s + \frac{i}{n}F_t)\frac{\Delta l}{2R}$$

$$F_f = \mu_c \sum_{i=1}^{n}(S_s + \frac{i}{n}F_t)\frac{\Delta l}{R} = \frac{\mu_c \Delta l}{R}[nS_s + \frac{n+1}{2}F_t] \qquad (6.14)$$

Where, Δl is the length of cutting bead, n is the number of diamond beads in cutting surface simultaneously, R is the mean radius of the cutting locus.

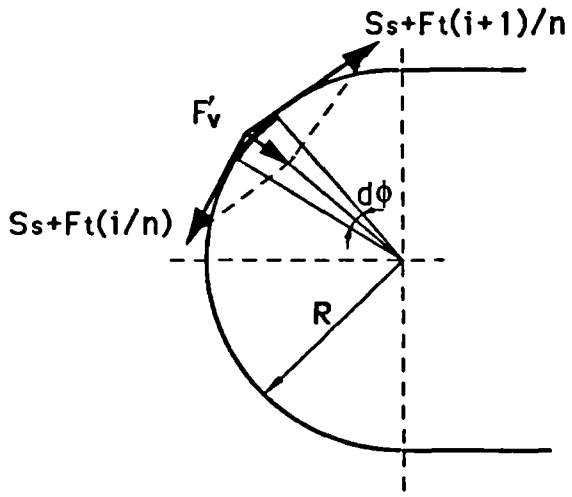


Figure 6.4: Diagram of the friction force of the diamond wire cutting

It is realized that the useful work done by the feed motor due to the wire feed into the rock in the direction of machine advance is very small and can be calculated using following equation, which is determined by the wire tension S_s, cutting force F_t, dead weight of diamond wire F_w, resistance of machine advance M_R due to the moving distance of the machine f_r.

$$W_f = (2S_s + F_t + F_w + M_R)\, f_r \qquad (6.15)$$

The main work consumed on the cutting force is discussed as follows. When a tangential force F_t is applied to the cutting beads, the force required to abrade the rock - that is, overcome the sawing strength - is the difference of F_t and F_f. Therefore, the useful work transmitted by the drive pulley per cutting locus of the wire along the rock surface W_t is:

$$W_t = \pi R (F_t - F_f) = \pi R F_t - \pi \mu_1 \Delta l \, n \, S_S - \pi \mu_1 \Delta l \, F_t \frac{(n+1)}{2} \qquad (6.16)$$

When electroplated diamond beads are used for the rock cutting and assuming the effective sawing strength of the rock is σ_s, then the work to cut certain volume of rock per cutting locus can be assumed as W_a:

$$W_a = \sigma_s (2 R d_t \Delta f) \qquad (6.17)$$

Let $W_t = W_a$ and submitting Equation 6.3 to Equation 6.16, therefore the wire tension equation was proposed as:

$$S_s = \frac{4 R \sigma_s d_t \Delta f}{\pi A [2R - \mu_c \Delta l (n+1)] - 2\pi \mu_c \Delta l \, n} \qquad (6.18)$$

Where,

$A = e^{\mu\theta} - 1$

S_s = Diamond wire slack side tension (N)

R = The mean radius of the cutting locus (mm)

σ_s = The sawing strength of the rock (MPa)

d_t = Diameter of the diamond wire beads (mm)

Δf = Advance per round of cutting locus of the wire in the feed direction (mm)

μ_c = Friction coefficient between the diamond beads and rock

Δl = Length of the diamond beads (mm)

n = Number of diamond beads in cutting locus simultaneously

In the proposed wire tension Equation 6.18, wire tension is expressed as a function of the cutting volume, sawing strength of rock, sizes of the cutting beads, friction coefficient between wire and rock and driving conditions. The equation will help to analyze how these parameters affect the wire tension, which shows that the wire tension will be increased with an increase of the cutting volume, sawing strength of the rock, length of beads, number of beads cutting and the friction coefficient between wire and rock. On the other hand, the wire tension can be reduced by increasing the adhesive factor or the angle of wrap between the pulley and the wire. Qualitatively, this equation shows a very promising result.

In the above equations, the sawing strength of rock σ_s, is an unknown term which may be linked with a rock strength parameter and needs to be determined by test.

6.3 UNDERGROUND DIAMOND WIRE SAWING TRIALS

6.3.1 Test site and test procedures

The first site trials of diamond wire sawing underground were carried out in Milldam Mine, Laporte Minerals, in England (Figures 6.5 - 6.8). During the test, a diamond wire was used to make rise 12, as shown in Figure 6.9. The dimensions of the rise were rectangular, therefore diamond wire was used to cut slots on the side walls of the rise. The TDV55 diamond wire saw machine was set up in drive C for making the rise from drive C to drive B. The sawing layout for two slots parallel to the drive (from hole 1 to 2, 3 to 4) is shown in Figure 6.10. For these two cuts, only

the movement of the drive pulley from one side of the machine to the other was necessary (no need to move the machine rails). For back slot cutting (between hole 2 and hole 3), the arrangements of the pulleys are shown in Figure 6.11.

The rock is a kind of grey abrasive limestone. The general specifications of diamond wire used for this test are as follows:

- electroplated diamond beads: ϕ10mm x 8.5mm long, on ϕ5mm steel cable,
- synthetic diamond grit size: 40/50 US mesh,
- pitch: 31.5mm (32 beads/meter),
- spring spacers and copper joints.

Tests were arranged as follows:

(1) The feed speed was increased manually from 4.1 cm/min (sawing rate 4.9 m^2/h) to a maximum of 8.4 cm/min (sawing rate 10.1 m^2/h) at a constant wire speed of 35.6 m/s (800 r.p.m.). For each defined feed, the cut was continually performed in half hours and the voltages and consumed amperes for each defined feed were recorded by use of the recording meters.

(2) The effect of wire speed (cutting speed) on the sawing process was also investigated during this test. The consumed power was kept at a constant of 5.5 kW. Each defined wire speed was increased after each half hour cut and the feed speed was measured. The speed increased range is from 31 m/s (700 r.p.m.) to 40 m/s (900 r.p.m.).



Figure 6.5: Site preparation for kerf cutting (drilling)

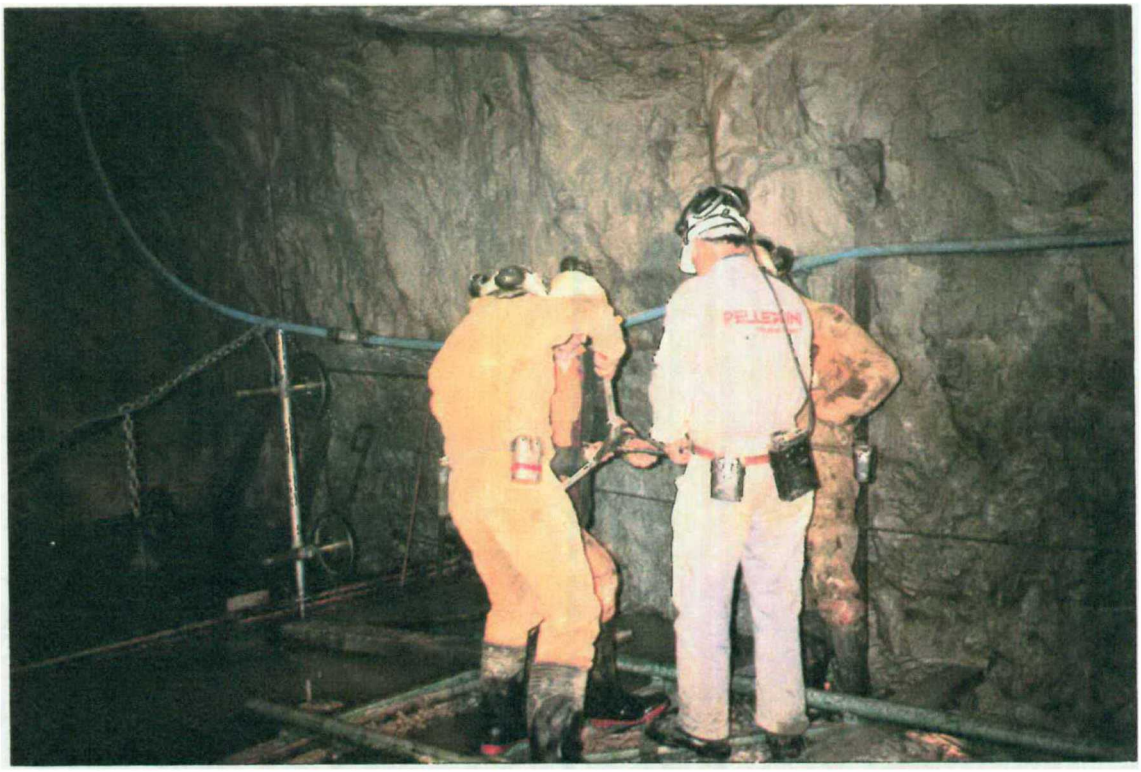


Figure 6.6: Copper joints used for wire connection

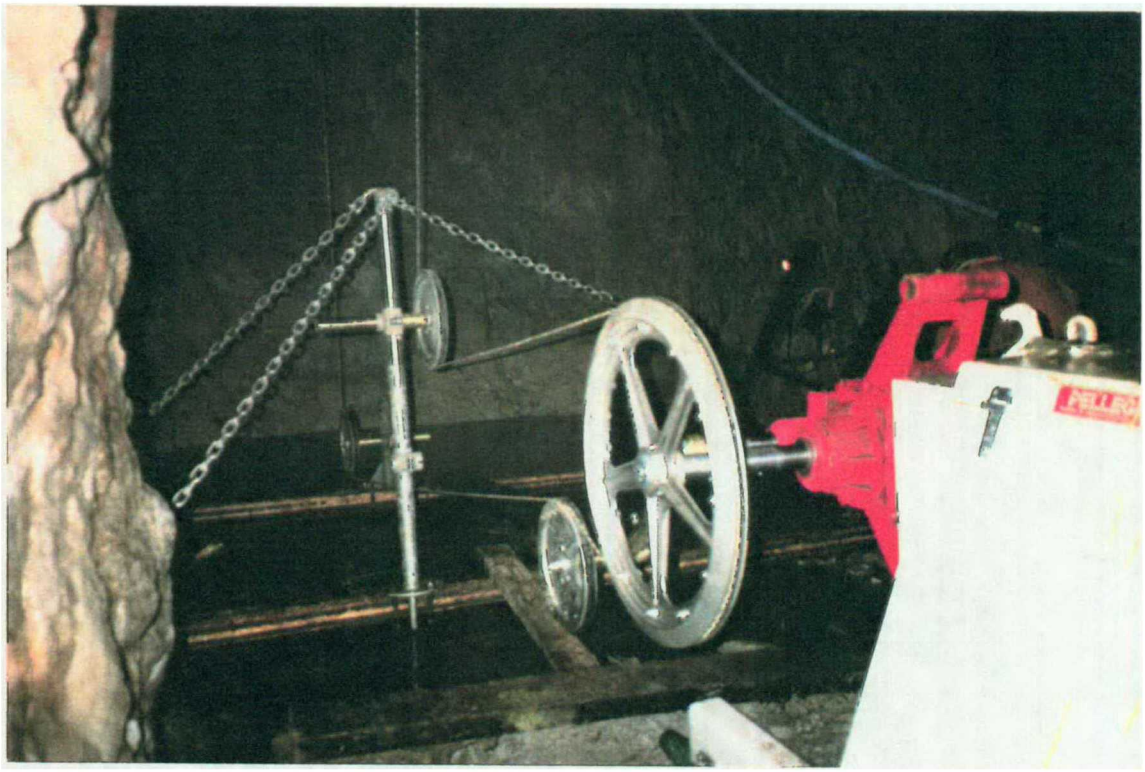


Figure 6.7: The arrangement of the guide pulleys and the drive pulley



Figure 6.8: Underground test of diamond wire sawing at Milldam Mine

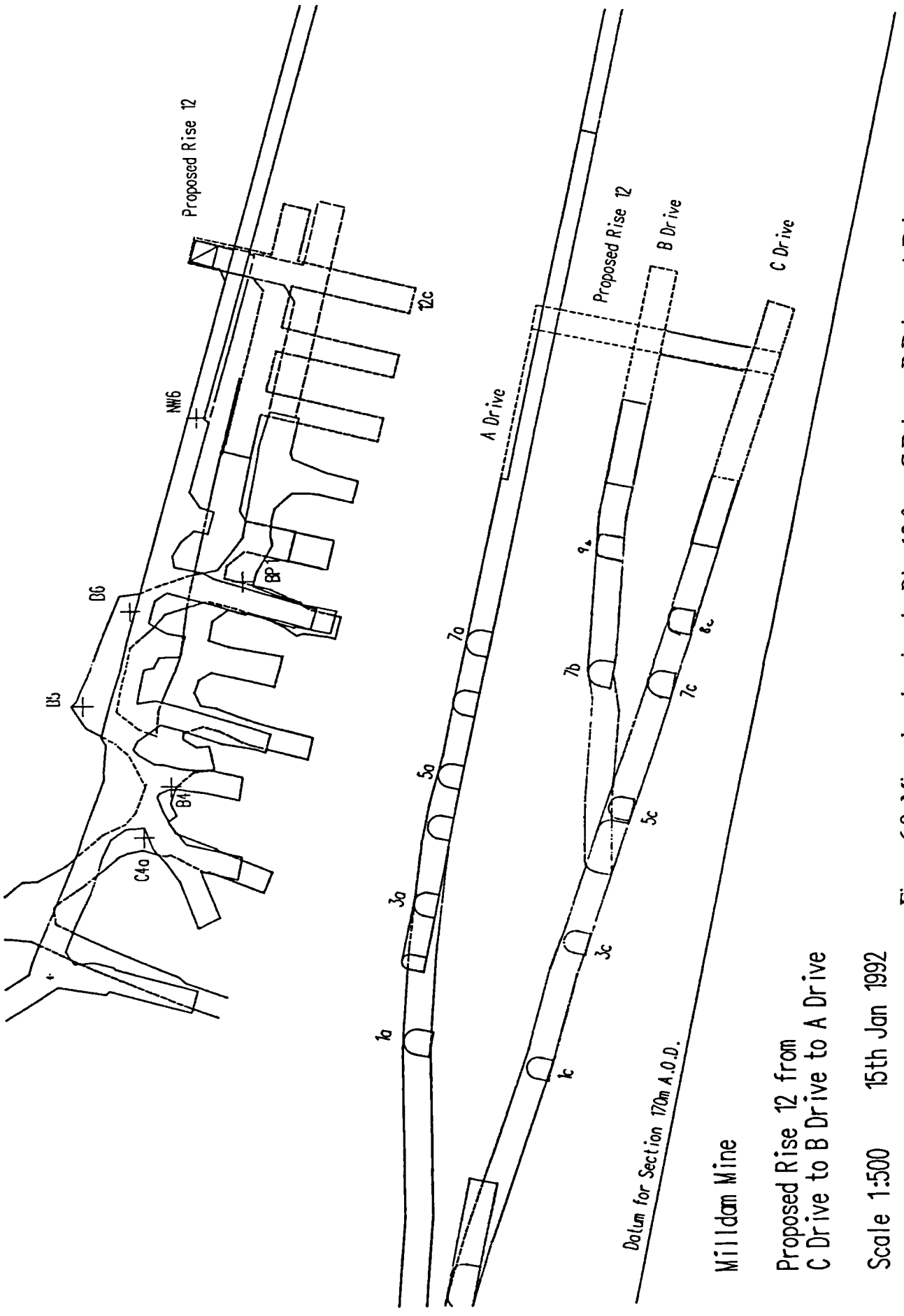


Figure 6.9: Mine plan showing the Rise 12 from C Drive to B Drive to A Drive

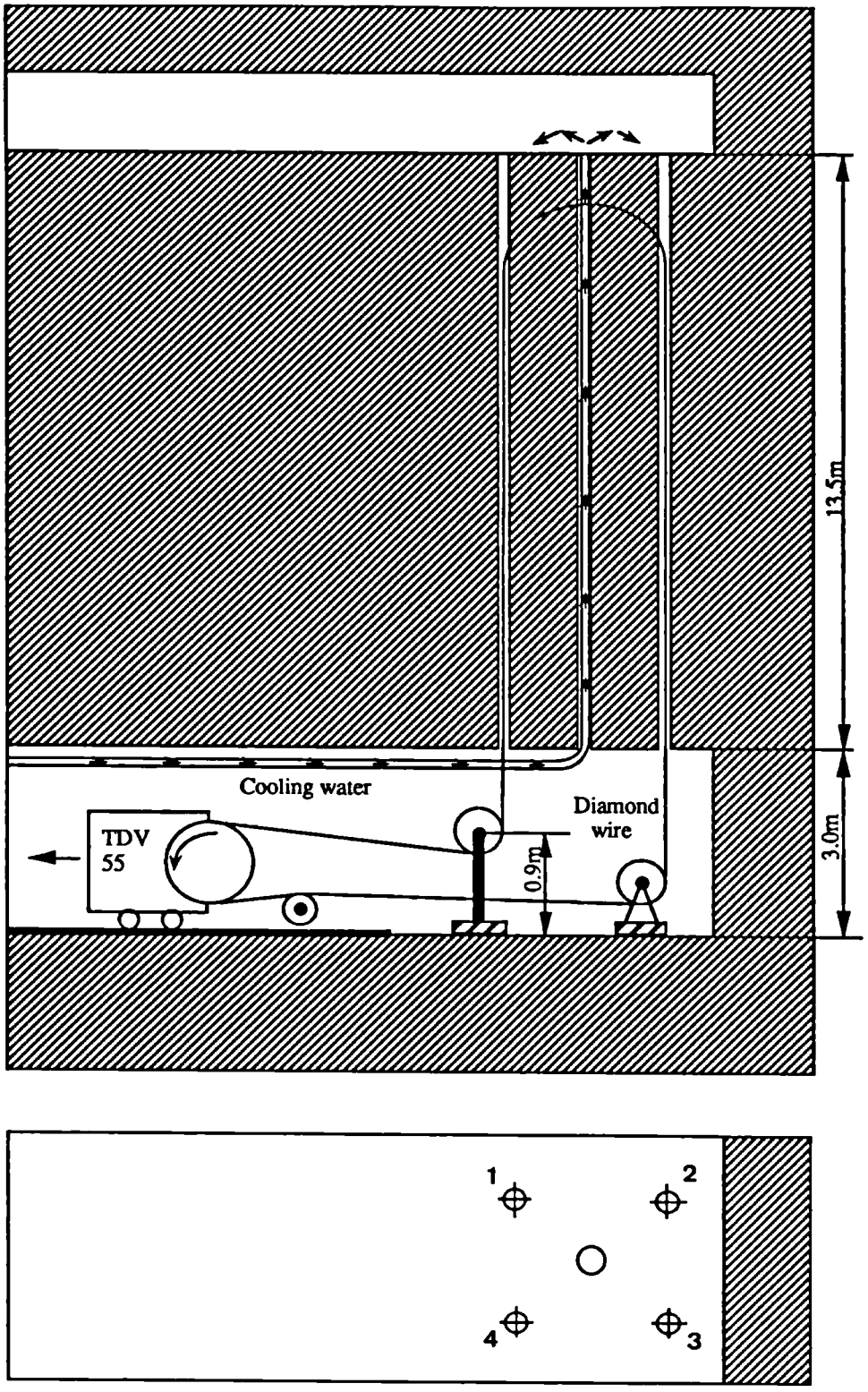


Figure 6.10: Diamond wire sawing layout for parallel cuts

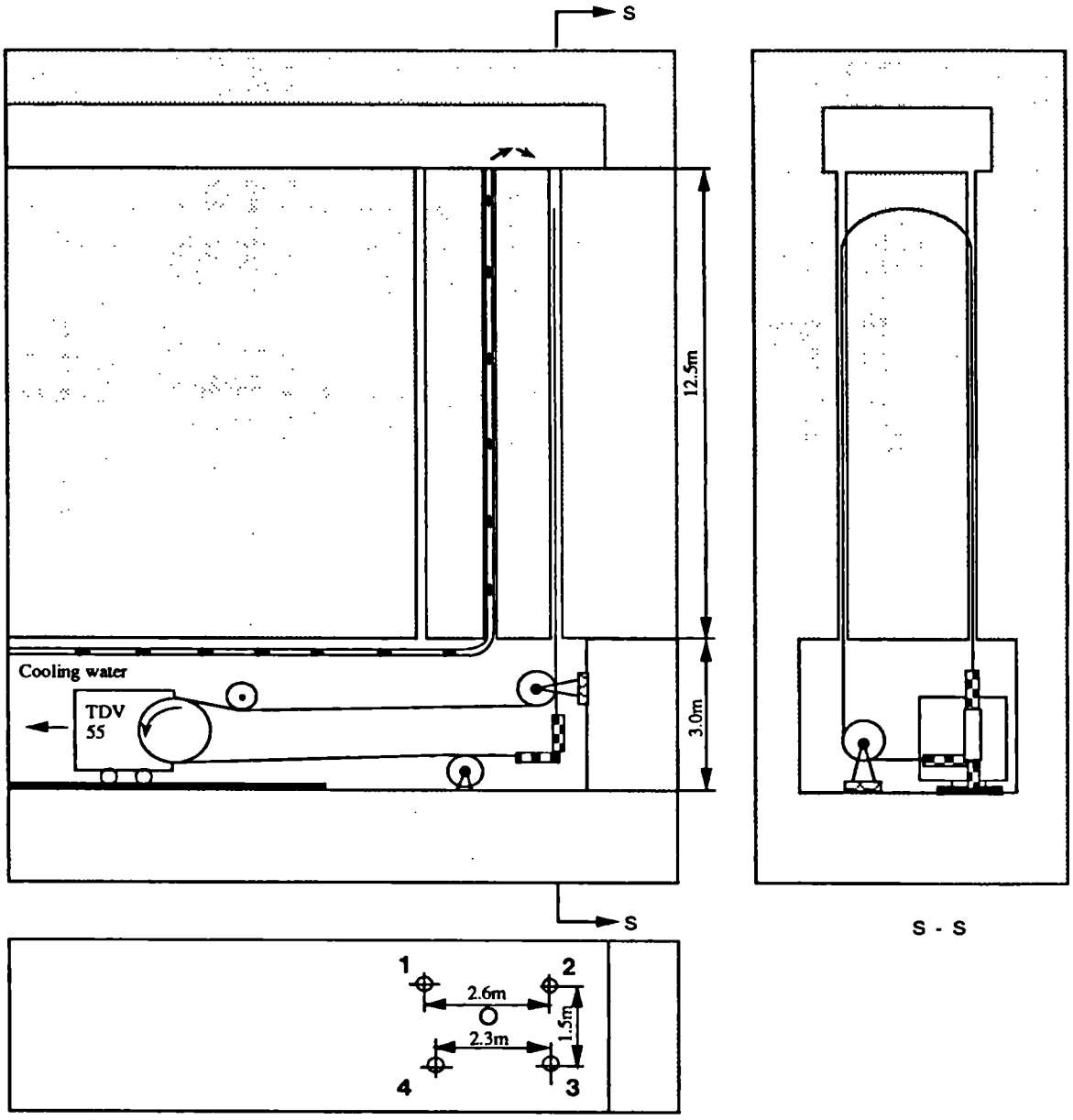


Figure 6.11: Diamond wire sawing layout for back slot cutting

6.3.2 Discussions of the test results

Sawing performance evaluation

Due to the fact that this was the first time that diamond wire was used underground, the cutting was carried out in a small rate at the beginning and increased to a maximum sawing rate of 10.1 m^2/hour gradually. If cooling water is abundantly applied and the guide pulleys were installed properly, the performance of the wire underground is almost the same as it is on surface. The cutting layout as illustrated in Figure 6.10 is a well organized means for using diamond wire underground. An average cutting rate of 8.5 m^2/hr can be achieved for sawing this kind of grey limestone and the maximum cutting rate achieved was 10 m^2/hr without any difficulties. With regard to diamond wire life, the test result showed that the electroplated diamond wire was very suitable for the limestone cutting. After a total area of 125 m^2 have been cut, the wire itself was still in good working condition, as shown in Figure 6.12.

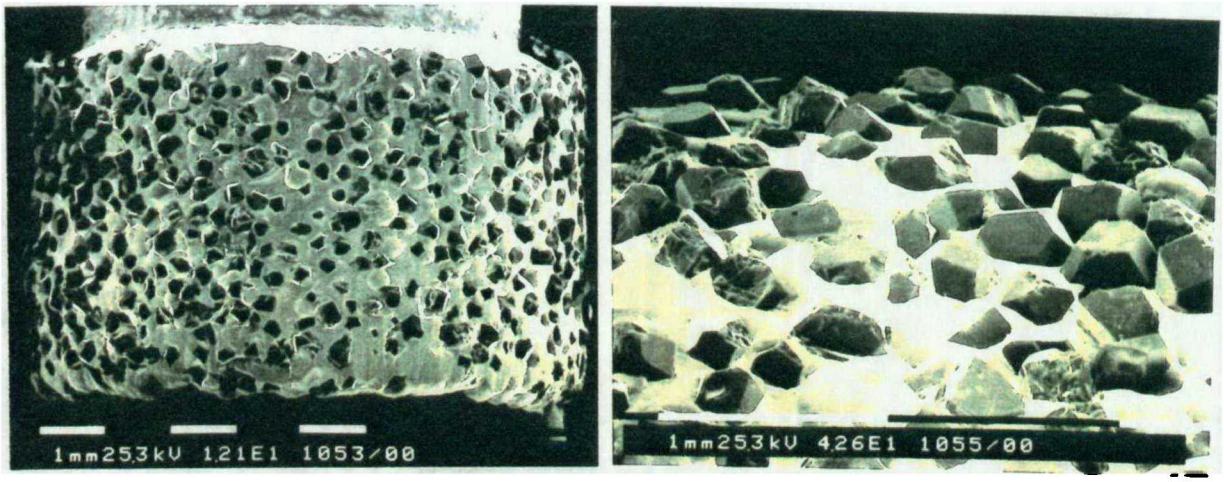


Figure 6.12: The electroplated diamond bead after 125m^2 of cut of limestone

In conclusion, a diamond wire saw was successfully used in underground for mining purpose and the well finished raise is shown in Figure 6.13.

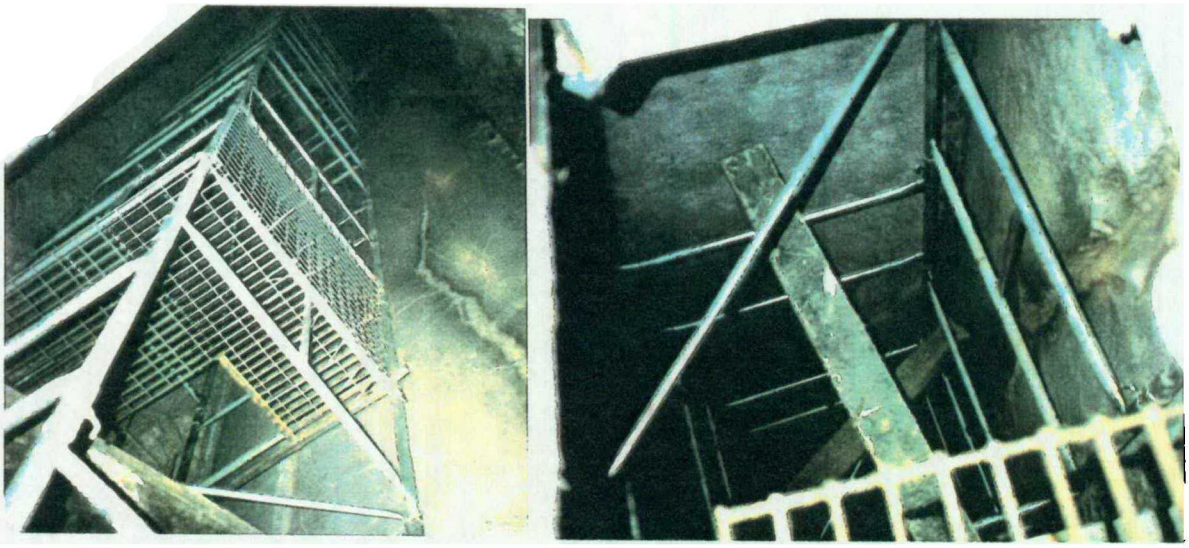


Figure 6.13: Finished raise made by using diamond wire saw

During the test, it was found that the diamond wire was not properly used for back slot cutting (between hole 2 and hole 3), as the pulleys were arranged as shown in Figure 6.11. Due to the fact that the rotation direction of the drive pulley was perpendicular to the slot cut, this kind of pulley arrangement leads to one side of the wire needing to change direction through 90° twice in order to cut in the back slot position. It can be said that if the guide pulleys are not strong enough to support the direction changes, the performance of the sawing will be affected. Test result show that for this kind of cutting, a sawing rate of only 4.1 m^2/hr can be achieved. A better sawing layout can be achieved by changing the position of the drive pulley to 180^0 paralleled to the machine using the crank A as shown in Figure 6.14. This will improve the wire support conditions as shown in Figure 6.11.

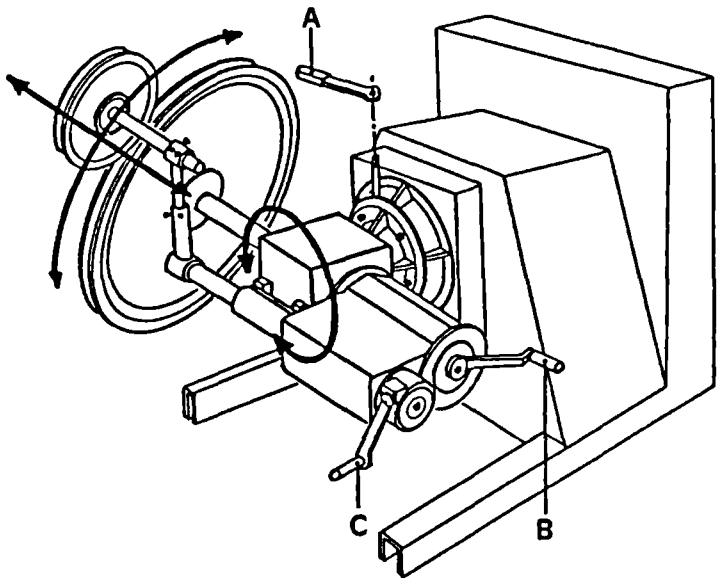


Figure 6.14: The change of direction of the drive pulley

It can be seen that from Figures 6.10 - 6.11, The kerf sawing is carried out from the top of the raise to the bottom. Alternatively, it is also no problem that the diamond wire can be used to cut the kerf from the bottom to top depending on site convenience for setting up the machine.

From the point of view of using the diamond wire machine for mining, it was realized that the rails on which the machine was mounted were not strong enough for underground use due to uneven working surface. It was also found that the machine was not easily transportable underground. Therefore, a special supporting structure incorporating a towing device and axle mountings was manufactured to improve the using condition of the diamond wire machine for underground mining applications.

Tension equation evaluation

According to test procedure described in test arrangement (1), the voltages and consumed amperes were recorded as shown in the Table 6.1.

Table 6.1: Underground wire sawing test results obtained in Laporte Minerals

Feed	Sawing rate		Volt and Ampere		Power	C. force	Wire tensions	
cm/min	cm^2/m	m^2/h	(V)	(I)	(kW)	F_t (N)	S_s (N)	S_t (N)
4.1	820	4.92	380	55	4.35	122	99	221
5.6	1120	6.72	380	60	6.34	178	145	323
7.0	1400	8.4	380	65	8.32	234	190	424
8.4	1680	10.1	380	70	10.3	289	235	524

The power consumed, sawing force and wire tensions shown in Table 6.1 were calculated according to the recorded voltages and amperes. The power consumed by the drive motor is calculated by using Equation 6.19.

$$P_w = \sqrt{3}\, I\, V \cos\xi\, \eta \qquad (6.19)$$

Where,

P_w = Machine power for drive pulley (kW)

I = Electrical current (Amp)

V = Voltage (Volts)

$\cos\xi$ = Power factor (0.86)

η = Efficiency (0.70)

The sawing force F_t, wire tensions S_s and S_t are calculated by using Equations 6.5, 6.3 and 6.2 alternatively. As an example, the calculation procedure for the feed speed of 4.1 cm/min is given and these results are shown in Table 6.1.

From Equation 6.19, the power transmitted due to the sawing force:

$P_m = \sqrt{3}\, I\, V \cos\xi\, \eta = 1.73 \times (55\text{-}44) \times 380 \times 0.86 \times 0.70 = 4.35$ (kW)

Where, the current = 44 (Amp), when the machine is idle.

From Equation 6.5,

The sawing force: $F_t = \frac{P_w}{v_i} = \frac{4350}{35.6} = 122$ (N)

Where, wire speed is 35.6 m/s (800 r.p.m, Radius of drive pulley =425 mm).

From Equation 6.3,

The slack side tension: $S_s = \frac{F_t}{e^{\mu\theta} - 1} = \frac{122}{e^{0.23 \times 3.49} - 1} = 99$ (N)

Where, the wrap angle between the wire and the drive pulley $\theta = 200^0 = 3.49$. The adhesive factor is calculated using Equation 6.10:

$$\mu = \frac{2 \times 0.2 \times \sin 60}{(\pi/3) + 0.5 \sin(2 \times 60)} = 0.23$$

Where, the contact angle β_0 is 60^0, the friction coefficient between wire rope and pulley is taken as 0.2 with reference to the winding engine calculations[92,93].

From Equation 6.2,

The tight side tension: $S_t = S_S + F_t = 99 + 122 = 221$ (N)

The proposed wire tension equation 6.18, therefore, can be examined by comparing the results of this test program as listed in Table 6.1 with the calculated results using the proposed tension equation. It was noted that the sawing strength σ_s is an unknown term. However, the results from this test showed that Unconfined Compressive Strength (UCS) of the rock times 1.50 gave the best fit for σ_s. These results are presented as follows:

When: A=1.23 (μ=0.23, θ=3.49); R=1000(mm); $\sigma_s = 1.5\sigma_b = 1.5 \times 166 = 249$(MPa);

$d_t = 10(mm)$; $\mu_c = 0.25$; $\Delta l = 6.5(mm)$; $n = 100$

Then,

feed speed = 4.1 cm/min ($\Delta f = 0.0603$ mm), Ss = 99 (N)

feed speed = 5.6 cm/min ($\Delta f = 0.0823$ mm), Ss = 135 (N)

feed speed = 7.0 cm/min ($\Delta f = 0.1029$ mm), Ss = 169 (N)

feed speed = 8.4 cm/min ($\Delta f = 0.1235$ mm), Ss = 203 (N)

It can be see that he calculation of the wire tension for the grey limestone based on 1.5 times the compressive strength of the rock and the friction coefficient between diamond tool and rock of 0.25 is in good agreement with the experimental data (listed in Table 6.1) for the proposed Equation 6.18. Therefore, this equation could be used for estimating the wire tensions and analysis of the diamond wire sawing process.

The effect of wire speed

The effect of wire speed on the sawing process was also investigated during the site trials of the diamond wire saw. Test results are shown in Figure 6.15.

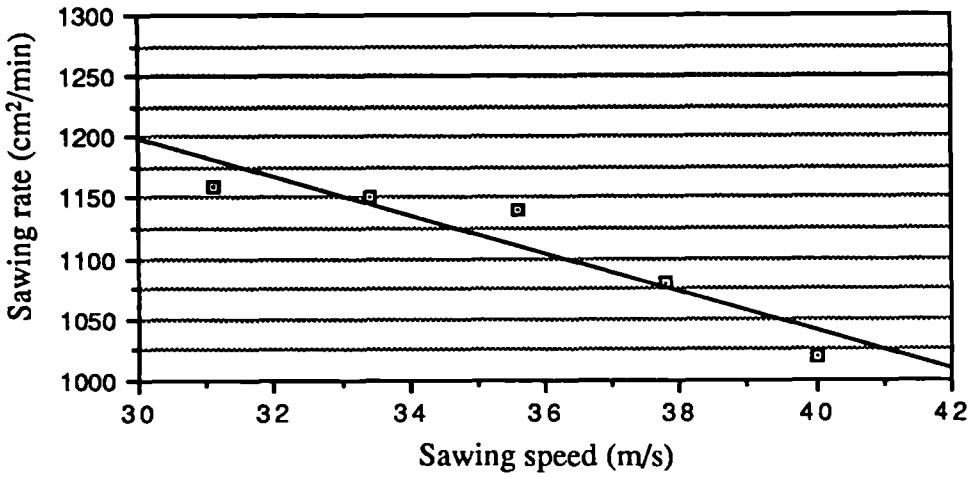


Figure 6.15: Relationship between sawing rate and wire speed at a constant power

Figure 6.15 suggests that, the sawing rate will decrease with increasing wire speed at a constant power. In other words, the sawing force or the wire tensions decreases as wire speed increases. In actual operation, the higher wire speed should be accompanied with the higher feed speed, otherwise the diamond wire will vibrate. As indicated above, this is due to the reduction in wire tensions as wire speed increases at constant feed speed.

CHAPTER 7

DETERMINING, COMPARING AND ASSESSING THE SAWABILITY OF STONE

7.1 INTRODUCTION

There have been many tests and discussions on rock cutting on the specific topics of machinability including so called sawability, drillability, cuttability as described in literature. However, these tests only consider the properties of rock which affect their machining performance. In the authors opinion, these tests can not be defined as general machinability tests. Since fundamental understanding of machinability is lacking, it is not possible to suggest a correct way to measure and determine the machinability of stone.

The increasing demand for stone products has inevitably led to the opening of numerous new stone quarries all over the world. As a result of this expansion, the variety of stone type has increased and stones hither to regard as uneconomical to cut are now being more frequently exploited. This however, can present major problems when attempting to predict the cost, process planning and the correct specifications for the diamond impregnated tools used to cut these materials. Therefore, research is still needed into the development of the methods for predicting the machining performance based on rock properties.

The main objective of this research has to develop a comprehensive theory for sawability and the testing methodology. This chapter also describes the research

work which attempted to correlate various rock properties with the sawing performance obtained during actual sawing trials. The rock tests included a number of physical property tests together with thin section analysis of the rocks used.

7.2 DEFINITION OF SAWABILITY

Sawability is a commonly used but often misunderstood term that refers to the machining response of a rock material in terms of the rate of rock removal, the ease of the sawing process, the duration of tool life, and if necessary the state of the machined surface.

The sawability response of a given rock material depends on many rock properties and on the sawing operation being performed including the specific sawing machine, diamond sawing tool, sawing fluid and operating parameters of sawing speed, feed speed and depth of cut. Since the sawability response is known to be different for different operating conditions, sawability should be viewed as an interaction rather than a property.

The author believes that there is a need to define this interaction quantitatively whenever we wish to test, compare and use this information for production decisions. Attempts to arrive at a quantitative definition of sawability must tend to focus especially on the characteristics of the sawing process such as the tool wear rate, the energy required for a standard rate of rock removal, or the quality of the machined surface that can be produced. Therefore, it is hard to agree with the custom of regarding sawability solely as a property of the rock material - a custom that has led to a variety of descriptive sawability definitions.

From a practical viewpoint, it is always possible to identify and use the most appropriate characteristic term for determining the machinability. Although in the area of rock cutting, cutting rate[94], the specific energy[95], penetration rate[96], and tool wear[32,46,47,48] have been chosen as these characteristic terms, it is hard to say these terms can most appropriately characterize the machinability. In fact, the cutting forces and the energy required for machining were, from actual machining process, considered to be relatively unimportant for either operational or economic reasons in practice of machining rock. It will be further noted that the cutting rate can not be looked at in isolation except in the emergency situation when the highest production rate is required without considering the economic aspects. Furthermore, in many practical operations of rock cutting, surface quality is not of interest to the engineers.

From above analysis, the author suggested that considerations of cutting energy, production rate and surface quality should not figure in the terms for determining the sawability. Since in modern high-production hard stone processing, diamond tool costs are a significant factor in the total cost picture, perhaps the economic benefit for sawing could be considered to be a most appropriate measure of sawability. The economic advantage of making the right choice of sawing conditions has been well documented in Chapter 5. Production costs and times can be significantly reduced by making the appropriate choice of production rate, especially in rock sawing where the tool cost is a significant portion of the total production cost. For the purpose of deriving this economic benefit, it is necessary to use specific relationships between the sawing response and the relevant sawing conditions. Therefore, one major impetus to the study of sawability testing is the development of a methodology for the generation of statistically valid relationships between the sawing response and the sawing conditions, namely the absolute sawability.

Another important concept is the relative sawability, the comparison of the characteristic terms at one set of machining conditions with another one. This can be used for the assessment of new tools and rock materials.

The most active research area in rock cutting at present is the study of how the rock parameters affect the machining performance which is one aspect of machinability studies. This only assesses the machinability at a specified machining condition. In this research, rock properties were studied for the purpose of assessing defined sawability.

7.3 PROPOSED METHODOLOGY FOR SAWABILITY TEST

7.3.1 Objectives

The first step in absolute sawability testing is to clearly define the objective. As indicated earlier, in rock cutting, we simply wish to achieve a "satisfactory production process" at the lowest possible cost. In other words, the economic benefit for stone cutting is considered to be the most appropriate measure of sawability. Therefore, in the analysis, absolute sawability is introduced by means of empirical relationships between sawing rate and production cost, where absolute sawability is expressed in terms of R-C characteristic curves in which the sawability can be determined.

Having restricted the meaning of absolute sawability in this way, it is necessary to specify tool life in terms of relative sawability, because estimates of sawability are of importance to industry for material selection, cost estimation, and process planning. Therefore, there is much interest in comparing the relative sawability.

7.3.2 R-C curves for determining sawability

In this research, a rigorous methodology for the application of sawing economics was developed as described in Section 5.4.5, the relationships between sawing rate and production cost can be expressed in the form of graphs. These relationships are called the R-C characteristic curves.

The theories developed on the absolute sawability enabled the development a computer program (see Appendix), which will help to correctly determine the sawability. Figures 7.1 and 7.2 show the computer screens from the program developed for determining the absolute sawability of rock.

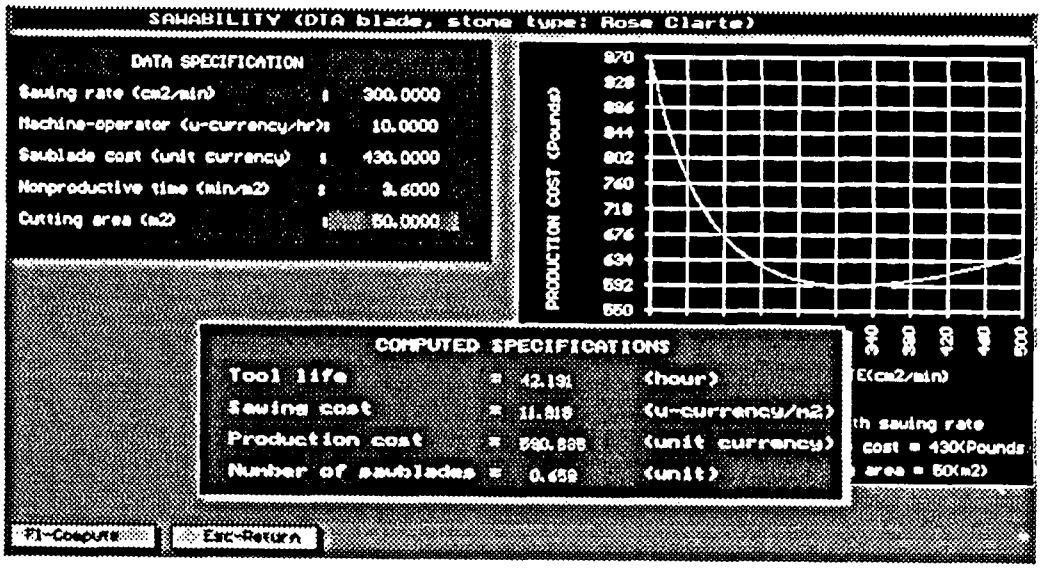


Figure 7.1: Computer screen from the program used for determining sawability of rock utilizing the R-C curve concept

The minimum cost, optimum sawing rate and the potential profit can be found along this curve. The curve also provides an approach to the generation of tool life data useful to the optimization of sawing operations. The optimum tool life which minimized the production cost then can be calculated.

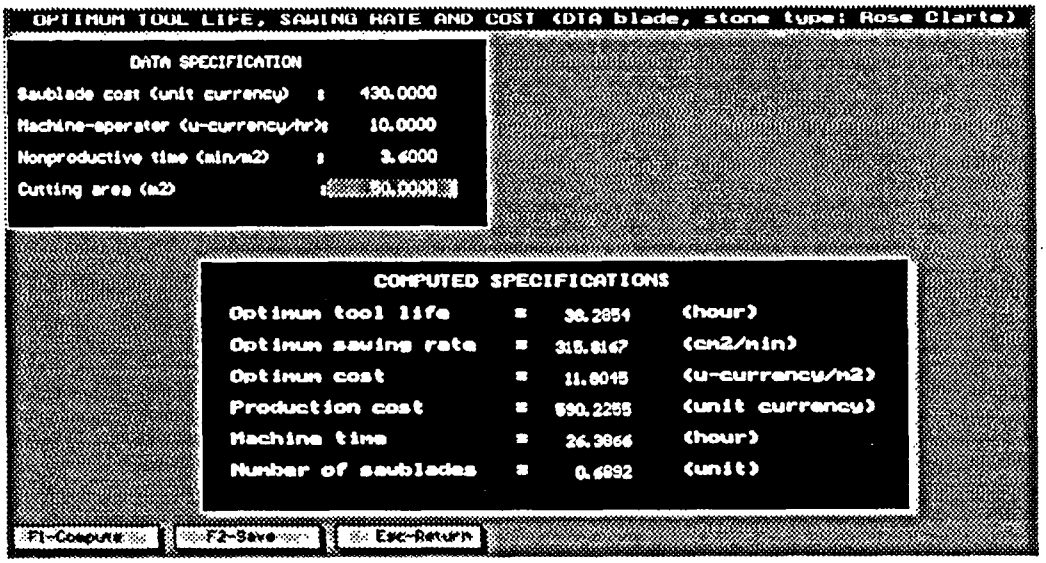


Figure 7.2: Optimum sawing conditions for sawing Rose De La Clarte

7.3.3 Sawability index for comparing the relative sawability

To evaluate the effect of relative sawability it is necessary to be able to compare the machining character at a specified sawing condition. Therefore the sawability index or rating is introduced for comparing the relative sawability. It can be used for the comparison of a new tool and rock materials. If, for example, a new rock material is being exploited it is important to establish the machining characteristics of the rock for a wide range of cutting conditions, tool materials and specifications and, perhaps more importantly, determine the economical aspects of the machining.

Tool life can be used to determine the production cost when the sawing rate is fixed. Therefore, the sawability index for a rock material is defined as the ratio of the tool life produced by a specified sawing rate to the tool life at the same sawing rate while sawing a reference rock material. An expression for sawability index, **SI**, is:

$$SI = \frac{(T_i)_r}{(T_i)_R} \qquad (7.1)$$

Where, $(T_i)_r$ is the tool life produced at a specified sawing rate **i** for material **r** and $(T_i)_R$ is the tool life produced at the same sawing rate **i** while sawing the reference material **R**. The value of the **SI** can be expressed as a percentage.

During the tests carried out in this research, Rose De La Clarte was chosen as the reference rock. According to Equation 7.1, the sawability index at the sawing rate of 300 cm^2/min for sawing another five kinds of rocks are listed in Table 7.1.

Table 7.1: Comparison of the sawability index

Rock types	Limestone	Marlin	*Rose De La Clarte*	Celtic	Lanhelin	Balmoral
Sawability index	233%	129%	*100%*	54%	48%	45%

On plot of log sawing rate versus log tool life, such as shown in Figure 7.3, the two conditions indicated by point **1** and **2** are used to establish **SI**. The sawing rate - tool life relationship for both materials is defined by a straight line drawn through points **1, 3** and points **2, 4**. However, these lines do not have the same slope, where the slope is the exponent in the Tool Life Equation. The different sawing rate response to different tool lifes of points **1,2** and **3,4** for different materials can be clearly seen

from Figure 7.3. Therefore it is a fact that this computation of the sawability index is restricted to that particular sawing rate only. To evaluate the effect of sawability on cost and productivity reliably and sufficiently, it is necessary to be able to compare the sawability in the whole range of machining conditions. The answers could be found in the following section.

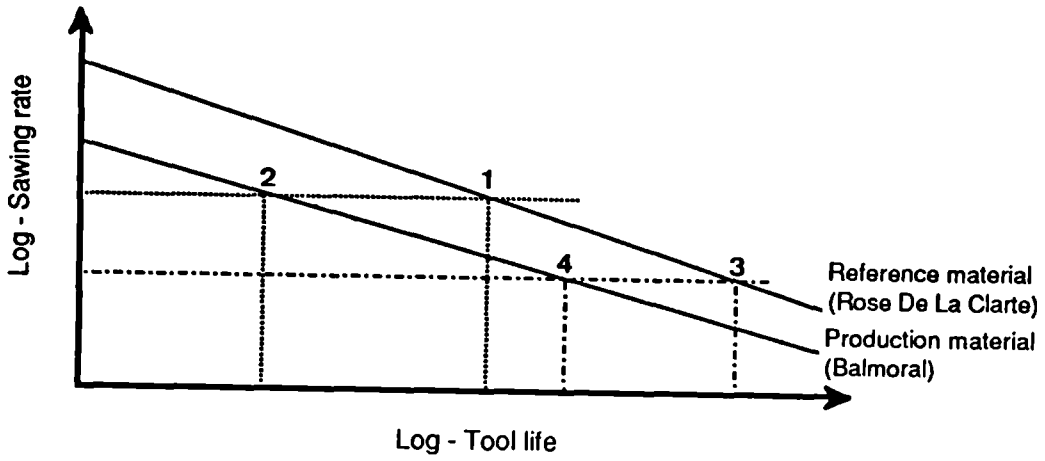


Figure 7.3: Slopes expressing the relationship between tool life and sawing rate

7.3.4 R-C curves for comparing the relative sawability

It is realized that sawability index is limited by the compression of the machining characteristic at a specified sawing condition only. People may also doubt the universal mean of the standard material because the rock is a natural material. However, another important consequence for the R-C concept is that it provides a more rigorous basis for the comparison of sawability. The R-C characteristic curves show that the production cost of two rock materials, or different sawing rates can be compared. Figure 7.4 illustrates how this comparison can be made for two kinds of granites, Celtic and Lanhelin, in a systematic fashion.

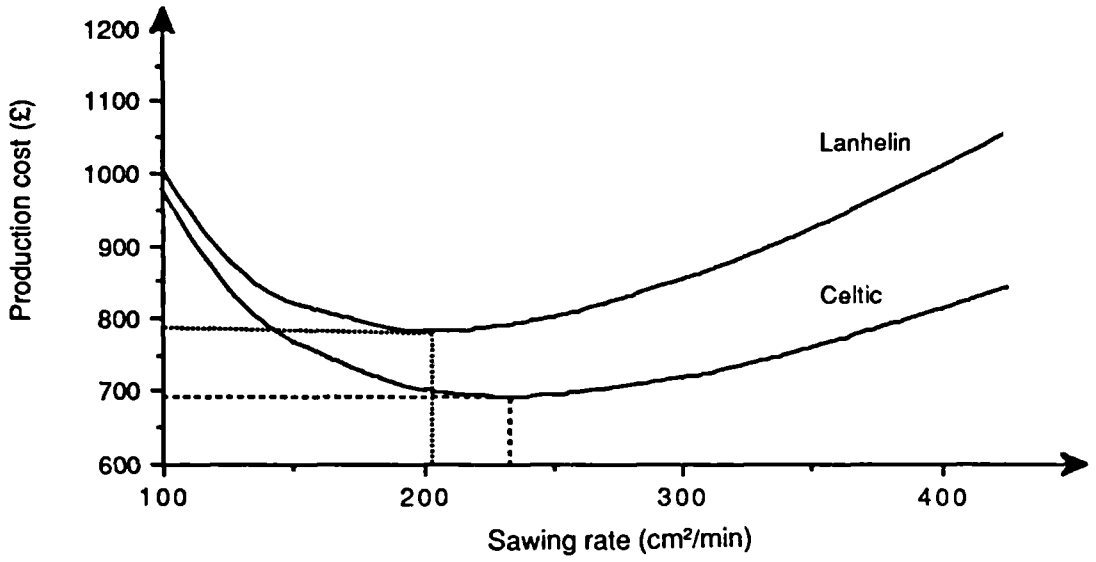


Figure 7.4: R-C curves used for in comparing the relative sawability

The production cost of sawing these two rocks can be compared at their respective sawing rates where the cost is optimal. Figure 7.4 shows that on the basis of sawability response, Celtic is superior to Lanhelin, because of the low production cost and high sawing rate.

An overall comparison of sawing six samples are given in Table 7.2, in which the relative sawability of these rocks can be compared.

Table 7.2: Comparison of the relative sawability using the R-C concept

Rock type	Optimum production cost Pounds/m²	Optimum sawing rate cm²/min
Marlin	9.5	457
Clarte	11.8	316
Celtic	13.9	234
Lanhelin	15.6	203
Balmoral	15.9	197
Limestone	3.5	979

In Table 7.2, it is assumed that the cost of DTA sawblade is 430 Pounds and the machine and operator cost per hour is 10 Pounds. It is noted that the calculated optimum sawing rate for sawing Limestone under this condition is already higher than the maximum sawing rate 900 cm^2/min when the DTA sawblade is used. In this case, it is indicated that the machine time cost is the significant portion of the total production cost and therefore, the highest sawing rate that can be maintained by the operation should be selected.

The potential profit also can be compared according to the **R-C** concept as shown in Table 7.3.

Table 7.3: The potential profit when sawing five granites

Rock type	Cost (Pounds/m^2) (rate 150 cm^2/min)	Cost (Pounds/m^2) (rate 500 cm^2/min)	Optimum cost (Pounds/m^2)	Potential saving (%)
Marlin	14.2	9.6	9.5	33
Clarte	14.8	12.9	11.8	20
Celtic	15.4	18.8	13.9	26
Lanhelin	16.4	24.0	15.6	35
Balmoral	16.6	25.5	15.9	38

From Table 7.3, the potential profit that is the profit from the use of **R-C** concept instead of the use of diamond tools by experiences, can be obtained either from the saving of machining time cost such as for sawing Marlin and Rose De La Clarte or from the saving of tool cost such as for sawing Celtic, Lanhelin and Balmoral.

In such a way the **R-C** concept provides a rigorous basis for sawability testing. Therefore, a standard sawability test is recommended by the author and it is hoped that it would be accepted by the stone sawing industry in the future.

7.3.5 The recommended standard sawability test

In metal cutting, a specification for a standard machinability test has been available since 1977 (ISO 3685 -1977). The aim of the standard is to ensure, as far as possible, that future machinability testing of the type described should be carried out using standard conditions for the various variables so that the information obtained may be used to generate compatible comprehensive machinability data arising from many sources. Clearly, much thought has gone into the choice of recommended conditions for testing in an attempt to adequately cover a wide range of practical cutting conditions. The main body of the ISO 3685-1977 report in metal cutting is contained in several sections which deal with reference materials, reference tool materials and tool geometries, reference cutting fluids, reference cutting conditions, tool life criteria and tool wear measurement, equipment, test procedure, and the recording and reporting of the results.

In diamond rock cutting, there is no doubt that a standard sawability test is also desirable. The following listing is primarily according to ISO for metal cutting and mainly is drawn from the testing experiences of the author and engineers in Diamant Boart's pilot station.

Reference rock

In all tests where the rock itself is not the test variable a reference granite should be used depending on the Shore hardness and quartz content. As the standard, Shore hardness should be in the range of 91-92 and quartz content in the range of 25-26%. The size and shape of rock should be satisfactory for proper mounting on the working table. For example, 1000mm x 600mm x 200mm with machined surfaces.

Reference sawblade and specifications

If the tool itself is not the test variable then it should meet the following specifications:

- ϕ600mm impregnated diamond sawblade with 36 segments;
- the diamond particle: De Beers SDA100 with the size of 40/60 US mesh;
- the concentration: 25

Tool should be correctly set on the machine, i.e. the blade should be perpendicular to the table where the rock material is clamped. The tolerance limit should not exceed 0.05 mm/m. For the sawing advance, the movement of table (of the blade) should be done strictly in the plane of the blade (of the table). The tolerance limit for the parallelism between the point of cut in and the point of cut out of the sawblade should not exceed 0.2 mm.

Reference sawing fluids

If the sawing fluid is not the test variable then sawing should be carried out either dry or using plain water. If a cutting fluid is considered to be necessary, the fluid flow should not be less than 25 litre/min and the fluid should flood the active part of the cutting zone.

Sawing conditions

Sawing rates are governed by feed speed, and depth of cut - these are intended to cover conditions from light to heavy operations. When more than one of the above are the test variables it is recommended that only one be changed at a time and that, the maximum depth of cut should be no more than 40 mm and feed no more than 600 cm/min. At least four different sawing rates should be chosen for each test and

ideally the sawing rate should be such that the resulting relative tool wear is changed from a big value to the possibly smallest one.

If the sawing speed is not the test variable then sawing rate is recommended as 35m/s. The sawblade must withstand failure of the tool due to direct forces or vibration for given combinations of feed speed, depth of cut and sawing speed.

Tool life and tool wear measurement

Tool life of diamond sawblade should be used to determine the useful life of the cutting tool which is measured in terms of actual cutting time. The type of diamond particle wear should be reported and all relevant wear measurements should be taken for the purpose of checking the useful tool life. Other wear phenomena, such as different zone, protruding tool middle or tool corner should be recorded but all of these will eventually result in the useful tool life. In the unusual case of premature failure of the sawblade which is invariably caused by a "hard spot" in the rock material, a machine malfunction or unduly severe cutting conditions, tool failure are unpredictable and values obtained should never be used as a measure of tool life. It is recommended that the relative volumetric wear should be accurately measured irrespective of the methods used.

Equipment

The test sawing machine should be in good condition and have an infinitely variable feed speed drive which covers the range of cutting rates to be used. Other equipment should include:

(1) Equipment for measuring tool set on the machine accurately to ensure that it conforms to the tolerances specified for the test;

(2) A suitable dial indicator for measuring the radial loss of the segment or, preferably, measuring equipment to measure the segment profile;

(3) A suitable stereo-microscope for measuring the diamond particle wear;

(4) A stop-watch to measure sawing time and to check that feed speed is correct;

(5) Equipments for Shore hardness measuring and quartz content;

(6) A tachometer or other suitable method of measuring sawing speed;

(7) Equipment for measuring the flow rate of the cutting fluid where necessary.

Evaluation of tool life data

Tool wear measurements should be made at suitable intervals. The interval should be taken depending on the rate of wear. For each measurement, it is recommended that at lest 2 m^2 of rock material should be cut for hard rock and 10 m^2 for soft rock. In any case each tool wear - sawing rate curve should contain at least four points from within the uniform wear region. For each sawing rate, the tool life can be expressed in hours. The cutting conditions, tool specifications and rock material, etc. should be fully specified. In the more general case the tool life equation $A_s T^x = C_s$ can be obtained from the sawing rate versus tool life graph either by fitting the best straight line to the graph or by using a regression analysis.

7.4 ASSESSING THE DEFINED SAWABILITY

7.4.1 Introduction

Although the sawability tests indicated earlier give a complete picture of the machining characteristics, the effort, under many circumstances, is still needed with a view to the development of a way of assessing the sawability from the rock properties without doing the actual sawability test. One relationship which must be

established by anyone about to conduct sawability tests is that between the cost of the test and the potential benefit of carrying out the test. For example, one of the main tasks for an engineer is to assess in-coming materials to a machine station to ensure that the saws to be used under specified conditions will not fail prematurely. However, before a test is considered to be suitable, it is important that the user establishes the likely incidence of premature tool failure by understanding the properties of the rock. Only on this basis can more economic testing results and more effective sawability determination and assessment be achieved.

In the area of rock cutting, there has been a considerable interest in the assessing techniques, which employed many tests devised to find out the fundamental parameters of rock affecting the machining performances. Although there appears to be little or no correlation between the different tests being exploited, there may, at least, exist some general guidelines for the assessment of sawability.

The objective of this research is attempt to find a worthwhile answer on this aspect, and at the same time, a more complete and clear picture of the previous test results can be re-drawn, so that the defined sawability of a given rock without carrying out extensive machining trials can be assessed.

7.4.2 Test procedure for assessing the defined sawability

Selection of the measure of defined sawability

The first step in the test is to clearly define the purpose which should be stated in terms of why, where and how the information obtained from the test is to be used. The concept of sawability has clearly shown the need for consideration of the characteristic term to quantitatively define the sawability. In the past, relative tool

wear was chosen as a characteristic term to define the sawability by most previous researchers. Actually it already followed this concept intentionally or unintentionally, because at a defined sawing rate and sawing condition the tool wear is the characteristic term for indicating the production cost.

The basic problem is that there are different ways to express the tool wear as described in Section 3.3. For example, previous tests used the relative linear wear (mm/m^2) or its reverse form (m^2/mm) as the measure. These quantitative definitions lack comparability and accuracy. Therefore it is suggested that, T_l, which is the tool life produced to require a specified sawing rate and determined by the volumetric wear, is taken as the characteristic term for the defined sawability.

Selection of stone parameters for testing

Stone is a natural material and its characteristics differ in many ways. Considering the technical aspects of the rocks to be tested, the parameters of the rock must be specified by easily measurable and widely acceptable terms in order to give a universal meaning to the assessment technique. For practical purposes, it may be useful to develop special equipments for sawability assessment, however, the entire mechanism of sawing can not be truly represented by a single equipment. Therefore, the author believes that actual sawability tests are essential for the realistic evaluation of sawability.

In our test, in addition to analysis of thin sections of the rock samples tested to determine the quartz content and to examine the rock abrasiveness by use of Cerchar equipment, a number of conventional tests were conducted and the following parameters are determined: Shore scleroscope hardness, Schmidt hardness, Uniaxial

compressive strength, Fracture toughness, Sound velocity, Tensile strength, Cohesion and Internal friction angle.

Analysis of the data base

In order to facilitate the analysis and interpret the results, the observed specified tool life T_1 was referred to as a dependent variable and the properties of the rock were referred to as independent variables. The data collected then can be analyzed in order to develop tentative relationships between observed specified tool life and individual properties of rock. If it is necessary, a predictive equation could be developed by means of regression analysis.

7.4.3 Rock tests for determining the properties

The Shore scleroscope hardness test was carried out at Diamant Boart's pilot station and the Cerchar abrasiveness test was carried out at Nottingham University. Other tests were carried out at the Rock Mechanics Laboratories of Imperial College. It is not the intention of the author to dwell on the testing techniques further, except to emphasise the importance of these parameters in the final analysis.

Shore scleroscope hardness test

Hardness can be defined in many different ways. Rock hardness could simply be another name for resistance against cutters penetrating the rock. If so, hardness should be a very good measure to affect the sawability. Nowadays the Shore Scleroscope instrument has been adapted by many geotechnical engineers for the determination of rock hardness, since it was invented by A.F. Shore in 1907 and was the first commercially built metallurgical hardness tester. The instrument consists of a vertically disposed steel tube containing a diamond tipped hammer. The hammer is

dropped from a predetermined fixed height onto the surface of a specially prepared rock specimen which strikes the specimen a blow and then rebounds. the rebound height however, falls short of its original height since some of the energy in the falling hammer is dissipated in the production of a minute indentation. The height of rebound is proportional to the hardness of the face specimen and is recorded on an integral dial gauge mounted on the top of the tube.

Because natural rock is seldom similar in nature to the consistent homogeneous man made materials such as metals, the standard hardness tests are usually performed on a very small surface and this gives inconsistent results. One way to overcome this is to make a large number of tests over a comparatively large area in order to obtain a representative value of rock hardness rather than the mineral hardness. Surface finish of the prepared face of the rock specimen can also affect the integrity of the test results. However, a standard specimen specification and the minimum number of tests to achieve an acceptable degree of confidence with the results has been proposed by the International Society for Rock Mechanics[97]. Although the ISRM recommend that at least 20 determinations should be made on each specimen with no two readings made on the same spot, in many cases, this is insufficient. Nowadays the general rule adapted may be that a minimum volume of 40 cm^3 is suggested to obtain consistent values. The mean of at least 50 readings made on 5 specimens can then be taken as the Shore hardness of a rock[98]. However, 30 determinations were used in our tests based on Diamant Boart's experience.

Schmidt hardness test

A similar hardness measurement, but on a larger scale, is the Schmidt hammer test. The plunger of the hammer is placed against the specimen and is depressed into the hammer by pushing the hammer against the specimen. The main difference between

this and the Shore hardness, is that the Schmidt hammer does not penetrate into the rock. Subsequently the Schmidt hammer has been used in a similar manner to estimate the uniaxial compressive strength[99]. The test is "non-destructive" and does not cause any failure or fracturing in the specimen. It should therefore be classified as a dynamic elastic property rather than a hardness. This may be the reason that this method is of limited use on very soft or very hard rocks.

Our test procedure followed the suggested method by ISRM[97]. 20 individual tests were conducted on one rock sample and the lower 50% of the values were discarded. The average obtained of the upper 50% values was accepted as the Schmidt rebound hardness.

Uniaxial compressive strength test

The unconfined compression test is the most frequently used strength test for rocks. Its purpose is to measure the uniaxial compressive strength of a rock sample in the form of specimens of regular geometry, and is mainly intended for strength classification and characterization of intact rock. During the test, a load is applied on a cylindrical specimen in the direction of the axis, in which the strength is expressed as the ratio of the peak load to the initial cross-sectional area. The test procedure followed the ISRM recommendations[100].

Fracture toughness test

Fracture toughness is a material property of the intact rock and a measure of the stress intensity required to initiate crack propagation, or the fracture energy consumption rate required to create new surfaces.

Two different methods are recommended by the ISRM[101]. They are the short rod and the chevron bend test. The force applied to the short rod specimen is a direct tensile force. In the chevron bend test, the tensile force is applied indirectly by bending a beam. Two levels of testing are offered in each method. Level **1** requires only the registration of maximum load to be made during the test. Level **2** requires continuous load and displacements. Level **1** is a simple test that will give an index value. Level **2** testing is more complicated but gives values which are independent of core size and correlate well with results. For level **1** testing which was used in this project, the fracture toughness of the Chevron Bend specimen is calculated by the following equations:

$$K_{cb} = A_{min} \frac{F_{max}}{D^{1.5}} \qquad (7.2)$$

With the failure load, F_{max}, in KN and the specimen diameter, **D**, in cm the fracture toughness will be in $MN/m^{1.5}$. The factor A_{min} is dimensionless.

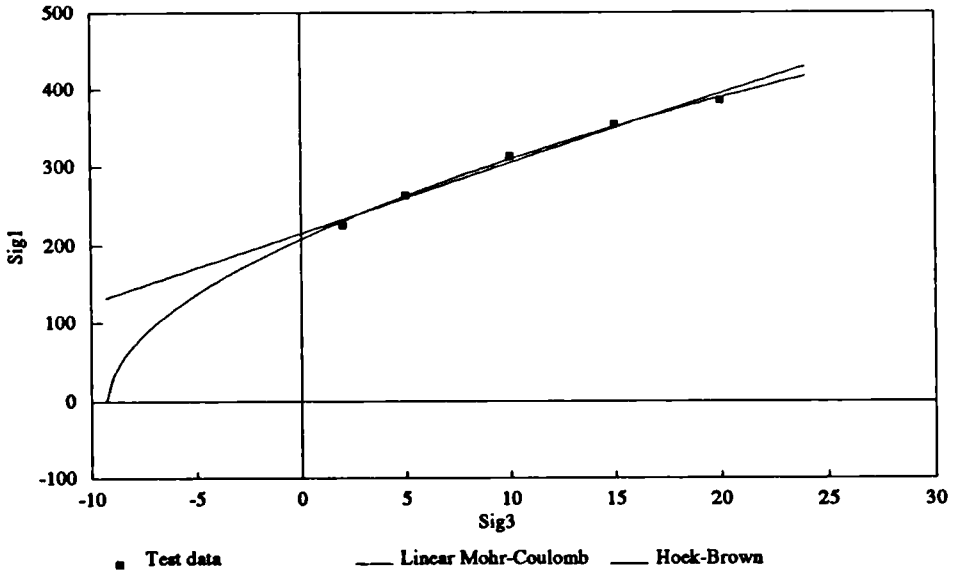
Sound velocity test

This test is intended as a method to determine the velocity of propagation of elastic waves in laboratory rock testing. Three different variations of the method are recommended by the ISRM[102]. These are: the high frequency ultrasonic pulse technique, the low frequency ultrasonic pulse technique and the resonant method. In our test, the first method high frequency ultrasonic pulse technique was used.

Multiple failure state strength test

Multiple failure state test was carried out and the test procedure follows the suggested method by ISRM[103]. The test induces more than one consolidation and

shearing on the same rock specimen loaded inside a triaxial cell. During the shearing stage the specimen is strained to produce a significant amount of shear stress. Then the specimen is released from the deviatoric stress and subjected to a higher confining pressure before the following shearing stage commences. The major principle stress (σ_1) was applied along the axis of the cylindrical test specimen by the loading actuator and the minor principle stress (σ_3) was applied in stages to the curved surface of the specimen by a constant pressure system. From the test data, the axial stress - confining pressure curves, digitized and converted from a computer, were obtained. Figure 7.5 shows the results of a typical multistage triaxial compression test at increasing confining pressures for isotopically confined Balmoral granite. The confining stresses applied were 1.99, 5.0, 10.0, 15.0 and 19.99 MPa respectively.



Mohr-Coulomb linear strength criterion :

Cohesion c	=	35.987	MPa
Friction angle	=	53.041	degs
Correlation r	=	0.992	

Hoek-Brown empirical strength criterion :

UCS	=	207.928	MPa
Parameter m	=	22.323	
Parameter s	=	1.000	(intact rock)
Tensile strength	=	-9.296	MPa
Correlation r	=	0.997	

Figure 7.5: Test data and strength envelopes for Balmoral granite

From the above test, the cohesion and internal friction angle can be calculated by using the Mohr-Coulomb linear strength criterion[104]. The tensile strength can be determined by using the Hoek-Brown empirical strength criterion[105].

Cerchar abrasiveness index test

According to the test description made by Wright and Cassapi[46], the Cerchar abrasiveness test is extensively used in the French coal mining industry and has been described by Des Lauriers and Broennimann. The apparatus basically consists of a sharp conical steel stylus mounted in a swinging arm. The stylus is scratched over the rock surface for a distance of 10 mm under a normal load of 7 kg. Abrasiveness is determined by the resultant wear flat at the point of the stylus, measured on a travelling microscope. A wear flat of 0.01 mm is assigned an Abrasiveness Index of 1. Current classifications would suggest that a wear flat diameter of 0.4 mm equals an Abrasiveness Index of 4 and would be regarded as highly abrasive.

Quartz content determination

The quartz content, provides a convenient measure of rock abrasiveness for a wide range of rock types, because it has been found that a good relationship exists between the abrasiveness of the rocks and their quartz content[106]. Therefore, it could be practical to use quartz content in evaluating the abrasiveness of rock.

During this research, the percentage values on quartz content for the micro-medium grained rocks were examined by thin section analysis using a polarizing microscope, and, for coarse-grained rocks (average grain size > 5mm), direct measurements by using of a scaled transparency on the polished rock surface (measured area = 100 mm^2) were used.

7.4.4 Test results in assessing the defined sawability

Table 7.4 illustrates the test results obtained from above conventional rock tests and the specified tool life T_1 obtained from the sawing trails on these samples.

The abbreviations used in Table 7.4 are explained as follows: T_{300} - Specified tool life at the sawing rate of 300 cm^2/min (hours); **SSH** - Shore scleroscope hardness; **SH** - Schmidt hardness; **UCS** - Uniaxial compressive strength (MPa); **FT** - Fracture toughness (K_{cb}: $MN/m^{1.5}$); **CAI** - Cerchar abrasiveness index; **QC** - Quartz content (%); **SV** - Sound velocity (V_p: m/sec); **TS** - Tensile strength (MPa); **Coh** - Cohesion (MPa); **IFA** - Internal friction angle (degrees).

Table 7.4: Test results in assessing the defined sawability

	Marlin	Rose clarte	Celtic	Lanhelin	Balmoral	Limestone
T_{300}	61.7	47.8	25.8	23.2	21.8	1113.4
SSH	82	92	90	90	98	56
SH	54.7	51.6	50.4	51.5	49.9	43.9
UCS	427.6	167.7	148.7	198.5	200.7	165.9
FT	2.50	1.71	1.88	2.33	1.52	1.01
CAI	3.43	3.95	4.48	5.03	4.49	1.75
QC	10	26	27	30	31.5	0
SV	4419	4001	5035	5154	4708	5043
TS		3.9	7.5	9.3	9.3	
Coh		25.3	29.8	33.3	36	
IFA		57.4	52.3	50.2	53	

As a preliminary step in the test result analysis, the data was analyzed to calculate if individual rock parameters could be linearly correlated to the specified tool life.

Table 7.5 shows correlation coefficients and p-values between independent and dependent variables based on the test results.

Table 7.5:Correlation coefficients between T_{300} and various parameters

Dependent variable	Independent variables	R^2	p-value
T_{300}	SSH	89.8%	0.004
	SH	75.4%	0.025
	UCS	4.8%	0.677
	FT	52.0%	0.106
	CAI	81.0%	0.015
	QC	66.6%	0.048
	SV	10.3%	0.535
	TS	95.4%	0.023
	Coh	81.4%	0.098
	IFA	82.3%	0.093

Having examined the above results from statistical analysis, it can be seen that significant linear correlations between specified tool life and Shore hardness and tensile strength exist (R^2=0.9, p=0.004 and R^2=0.95, p=0.023 respectively). But the results very clearly show that the ranking of the samples according to their quartz content and cohesion follows exactly the tool life ranking. Perfunctorily, according to these analyses predictive equations for sawability might be given in relation to Shore hardness and tensile strength, or simply state that the quartz content and cohesion are the predictors due to tool life ranking.

However, the following considerations led the author to recognize that it is not a rigorous method to simply suggest a predictive equation or direct statement for assessing the sawability:

- Based on the fact that it was always possible to find some rock parameters that gave a reasonable correlation to the defined machinability in the past although there appeared to be little or no common points between different tests being exploited by different researchers with their own test standards. Therefore the reliability of the direct predictive techniques were always questioned.

- Due to the testing difficulties, the statistical data is always very limited for every researcher to drive a definite conclusion.

- Because natural rock is seldom similar in properties to the consistent homogeneous man made materials such as metals, the number of rock properties measured will greatly affect the correctness of the direct prediction.

- Even if a predicative equation is available, it is strictly restricted to the defined machining condition. One particular case can not represent a comprehensive concept, particularly for the machining process which has various working conditions.

7.4.5 Discussions

Quartz content and Shore hardness

The theoretical and practical analyses of the test results suggest that quartz content and Shore hardness can be linked together as an indicator in assessing the defined sawability.

Theoretically, this suggestion fits with the proposed theory of wear mechanisms of diamond abrasive tools. As indicated in Section 5.4.1, abrasive wear and fracture

wear are the two typical wear types caused by plowing and impact of sawing thrust. Therefore, it may be reasonable to say that rock parameters related to abrasiveness and hardness can be used to assess the sawability, as these parameters reflect the principle process of diamond wear. Keeping this in mind, Shore scleroscope hardness provides a suitable term for describing the fracture wear caused by the impact of sawing, because the hardness test is basically a rebound test which measures resistance to penetration. The quartz content, provides a convenient measure for describing the abrasive wear, because it has been found that a good relationship exists between the abrasiveness of the rocks and their quartz content.

In practice, abrasive wear and fracture wear of diamond tools occur at different rates depending on the actual sawing conditions. From this point, it is not surprising that different results were achieved by different researchers. As each researcher had his/her own test conditions and changes in the diamond wear modes and different wear figures were obtained. Seeking common ground while reserving differences, one fact found by different tests is that when the rocks show the same Shore hardness, the higher the percentage content of quartz, the greater rates of tool wear will be created and it is the same the other way round. The rock with the highest quartz content and highest Shore hardness is the most difficult material to saw. Tables 7.6 - 7.7 show the results when re-analyzing the data of the previous researchers which support this view. The authors test results also showed a good agreement in this aspect as shown in Table 7.8.

Table 7.6: Re-analyzing the data of D.N.Wright's results

Rock type	Shore hardness	Quartz %	Linear wear (mm/m^2)
Pink granite	91.77	20	0.064
Diorite	81.08	20	0.030
Red granite	98.8	30	0.204*

Table 7.7: Re-analyzing the data of D.Birle's results

Rock type	Shore hardness	Quartz %	Linear wear (mm/m^2)
Bright red granite	102	20	0.555
Black granite	99	20	0.217
White granite	90	24.9	0.107
Quartz diorite	90	9.6	0.081

Table 7.8: Analyzing the data of authors results

Rock type	Shore hardness	Quartz %	Linear wear (mm/m^2)
Lanhelin granite	90	30	0.240
Celtic granite	90	27	0.215
Balmoral granite	98	31.5	0.255**

* - According to Wright's result, the red granite which has the highest quartz content and highest Shore hardness within his eight samples, therefore it is the most difficult material to saw.

** - Similarly, Balmoral granite is most difficult to saw within the authors six samples due to its highest Shore hardness and quartz content.

Sawing force

The use of sawing force as an accurate factor to assess the sawability may be not reasonable because sawing force can not be approved as the characteristic measure of sawability. Actually, as it was proved in Section 5.5, sawing forces are directly affected by the worn diamond forms of microfracturing and wear flat and are not related to relative wear. Although previous tests[32,46,47] claimed that vertical cutting force follows that produced by relative wear in figure, it is hard to say that a

relationship exists between sawing force and the diamond relative wear in nature. Figures 7.6(a) and 7.6(b) show the results at a sawing rate of 400 cm^2/min in different combinations of feed and depth of cut. These results support the view that sawing forces do not follow the relative wear in diamond cutting as fully indicated in Section 5.5.5.

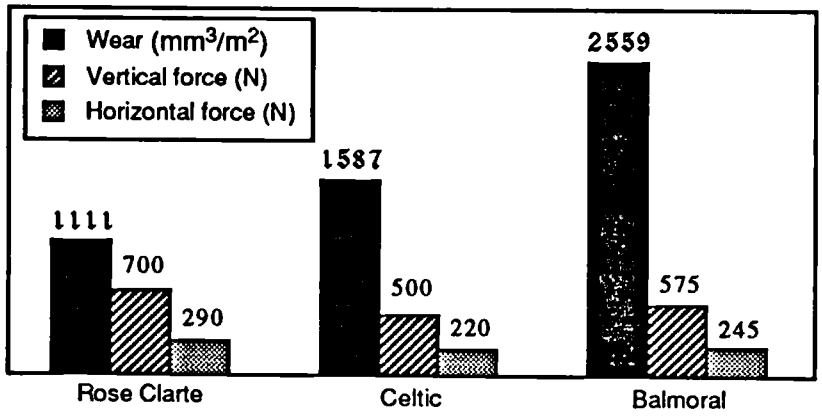


Figure 7.6(a): Diamond relative wear and sawing forces for different rocks (v_f = 400 cm/min, a_p = 10 mm)

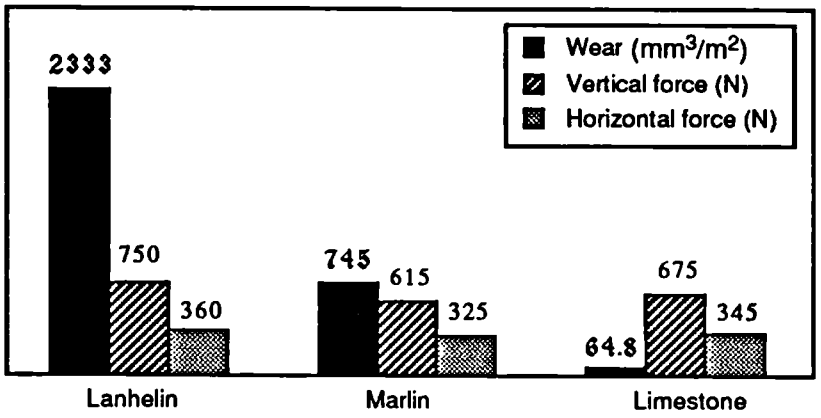


Figure 7.6(b): Diamond relative wear and sawing forces for different rocks (v_f = 222 cm/min, a_p = 18 mm)

Suggestion

It is suggested that research on the prediction of sawing performance with the use of rock parameters should be suspended at this stage. The only objective that can be achieved by this kind of research is to obtain a general idea of how easy or difficult the rock is to saw according to the rock properties. It is already proved that higher percentage content of hard rock-forming minerals (such as quartz) and higher Shore hardness will lead to greater rates of diamond wear. Therefore, further attempts to look for a single rock parameter with the sufficient data for statistical analysis or to develop a special equipment to assess the defined sawability could not be cost effective. For the purpose of making precise judgements on sawability for any given stone type, the most effective and rigorous method is the R-C characteristic curves gained from the absolute sawability trial as suggested by the author.

CHAPTER 8

CONCLUSIONS AND RECOMMENDATIONS FOR FURTHER RESEARCH

8.1 GENERAL CONCLUSIONS

Despite the research performed on rock cutting during the past 40 years or so, a comprehensive theory for machinability has not yet evolved. Researchers have tried to correlate the rock properties with the performance of cutting, which may only assess a very specific case only.

Research into rock cutting with diamond impregnated sawblades by the author developed new concepts on sawability:

- Sawability was viewed as an interaction rather than a property. the tests were clearly subdivided into three basic categories: determining the absolute sawability, comparing the relative sawability and assessing the defined sawability. Quantitative definition of absolute sawability was given in terms of economic benefit. For the defined sawability, this characteristic term is tool life. Other terms such as cutting rate, and the specific energy are not the most appropriate characteristics for use in determining sawability. For example, the cutting forces which particularly interested many researchers in rock cutting are considered to be relatively unimportant for either operational or economic reasons.

- The new concept of **R-C** curve provides a rigorous approach for determining the absolute sawability and also in comparing the relative sawability. The **R-C** curves contain all possible combinations of machining conditions for a given combination of rock material and cutting tool. The most economic conditions (optimum sawing rate, minimum production cost, maximum potential profit) can be found along the **R-C** characteristic curve. It also provides an approach to the generation of tool life data useful in the optimization of sawing operations. For example, when sawing Balmoral granite, a sawing rate of 200 cm^2/min - 450 cm^2/min is usually selected by the operating engineers according to their experience. Alternatively, if the **R-C** curve is used to determine the sawability, more than 30% potential profit can be achieved.

- To compare the relative sawability of rock with respect to a reference material at a specified cutting condition, the sawability index was introduced. Although this comparison does not attempt to determine the optimum machining conditions, it can be used for the comparison of sawability for new tools and rock materials.

- For the purpose of assessing the defined sawability according to the properties of the rock material without carrying out actual sawability tests, relationships between the rock properties and the sawing trials have been established. The investigation has served to show which of the various parameters obtained from the rock test results affect the defined sawability predominantly. It is recognized that it is not a rigorous way to simply suggest a predictive equation or direct statement for assessing sawability. However, it is confirmed that Shore hardness and quartz content can be linked together as

the indicator in assessing sawability. This view is in agreement with the theory developed on diamond wear mechanism.

In conclusion, actual machining tests are indispensable for determining machinability. The basis of this work has been to provide an approach to the optimization of cutting operations. The concept of **R-C** curve appears to be a very promising concept for rock cutting. The idea is so simple and clear, however, it is a gross over-simplification of the true nature of machining performance in relation to the cutting mechanism, wear mechanism, the interactions of operating parameters, machining tool and the rock material. Chapter 5 of this thesis describes how the **R-C** curves can be established and the development of the relative theories on diamond cutting. All the sawing trials were conducted at Diamant Boart's Pilot Station in Brussels. Six rock samples were cut by using a diamond circular sawblade.

The main contributions made by the author can be listed as follows:

- The wear mechanism of diamond cutting was investigated and theories developed through the analysis of diamond particle wear from the laboratory tests. The wear on a diamond segment is caused by: (a) the plowing (cutting) action of the diamond particles on the rock which induces a higher cutting temperature and (b) the impact of sawing thrust which induces a higher shock wave. Then two typical wear processes can be distinguished. The first type of wear which is caused by friction as a result of plowing and is called abrasive wear. The second type of wear consists in exceeding the local ultimate or fatigue strength as a result of impact and is called fracture wear.

- A cutting mechanism was suggested according to the analysis of specific features of abrasive processes. Test results have shown that cutting forces are directly affected by the worn diamond forms of microfracturing and flat wear and it is not related to the relative wear or tool life. Cutting forces can be kept in the quasi-stable state conditionally, as sawing rate increases.

- The effect of operating parameters such as sawing speed, feed speed and depth of cut on the diamond relative wear are of importance in rock cutting. The previous equation derived from the load on a diamond particle is not helpful to correctly analyze this effect. In this research, a new concept is defined as the balanced wear region. Within this region different combinations of feed and depth of cut for a constant sawing rate has no significant effect on the diamond relative wear. The widely accepted view suggesting that different rock materials respond best to a specific sawing speed has been misunderstood due to the limited test configurations used in the past. The fact is that this is only one case if all the selected operating parameters ensure that the relative diamond wear is within the balanced wear region. The validity of the balanced wear region concept has been fully illustrated in Chapter 5.

- As a natural extension of the diamond cutting research, the Tool Life Equation was successfully developed, therefore a sound theoretical basis has been established for diamond cutting. From this, the concept of R-C curves was developed.

- The theories developed on diamond cutting enabled the development of a computer program which will help to determine and assess the sawability of rocks.

- As a result of the theoretical basis already formed by this research, it is believed that absolute machinability test recommended by the author in Chapter 7 for rock cutting should become an important activity.

This research also aimed at proving the diamond wire sawing technique in underground mines. The art of diamond wire sawing has been stated historically and technologically in Chapter 4. The feasibility studies indicated that this technique can be transferred from the surface to underground. The site trials of diamond wire sawing in underground were carried out in Milldam Mine of Laporte Minerals as discussed in Chapter 6.

- Diamond wire saw was successfully used in underground for mining purpose.
. An average cutting rate of 8.5 m^2/hr was achieved for sawing grey limestone. The maximum cutting rate achieved was 10 m^2/hr.

- The site trials confirmed that the theoretical tension equation developed by the author is very promising and this equation can be used for electroplated diamond wire for the estimation of the wire tensions.

8.2 RECOMMENDATIONS FOR FURTHER RESEARCH

The important area of further study for the continuation of the work described in this thesis, must be concerned with the large scale absolute sawability test in order to

build up a expert system for the stone cutting industries universally. It can be imaged that if the sawblades can be linked with a user friendly computer program for quarries and plants, the present situation of using diamond tools by experiences will be greatly improved.

Another important aspect is that research should be conducted on all aspects of cutting tools. Definitely, the specifications of the diamond tool will greatly affect the cutting process, such as: how to ensure that the diamond particles are released from the bond at the right moment? which is the optimum combination of diamond type, size and concentration? In Chapter 5, the author suggested that an optimum self-dressing process may be related to the "optimum temperature", but further research is needed to validate this suggestion.

Further research on diamond wire technology for use in underground could follow the directions of improving the cutting efficiency and modifying the machine structure:

- The research on the reasonable layout of wire arrangements for underground mining and the optimum dimensions of the free faces should be extended.

- The research on methods of assisting diamond wire sawing, such as the use of high pressure water jet and abrasive slurry should be initiated.

- The development of a device which enables the diamond wire rotation automatically during cutting is necessary. The biggest problem when using diamond wire for hard rock cutting is that the diamond beads can not be worn evenly as the twisting force is not always sufficient self released. This mechanism should be investigated further.

REFERENCES

[1] Shaw, C.T., Durucan, S., Wilke, F.L. and Kelly, J.: *Cut and fill mining in hard rock without the use of explosives*, EC Raw materials research programme, Final Report on Grant number MA1M-0076-C(H), April, 1991

[2] Evans, I.: *Theory of the basic mechanics of coal ploughing,* Proc. Int. Symp. Min. Res., Vol.2, p761-798, Univ. of Missouri, Pergamon Press, 1962

[3] Evans, I.: *The force required to cut coal with blunt wedges,* Int. J. Rock Mech. Mining Sci., Vol.2, p1-12, 1965

[4] Nishimatsu, Y.: *The mechanics of rock cutting,* Int. J. Rock Mech. Min. Sci., Vol.9, p261-270, 1972

[5] Roxborough, F.F. and Phillips, H.R.: *Rock excavation by disc cutter,* Int. J. Rock Mech. Min. Sci. & Geomech. Abstr., Vol.12, p361 - 366, 1975

[6] Wang, J. K. and Lehnhoff, T. F.: *Bit penetration into rock - a finite element study,* Int. J. Rock Mech. Min. Sci. & Geomech. Abstr., Vol.13, p11-16, 1976

[7] Ingraffea, A. R.: *Theory of crack initiation and propagation in rock,* Fracture Mechanics of Rock, p71-110, Academic Press, 1987

[8] Detournay, E. and Defourny, P.: *A phenomenological model for the drilling action of drag bits,* Int. J. Rock Mech. Min. Sci. & Geomech. Abstr., Vol.29, p13-23, 1992

[9] McFeat-Smith, I., and Fowell, R.J.: *Correlation of rock properties and the cutting performance of tunnelling machines,* Proc. Conf. Rock Engng., p581-602, University of Newcastle upon Tyne, 1977

[10] Misra, B.: *Correlation of rock properties with machine performance,* Ph.D Thesis, Dept. of Mining and Mineral Science, University of Leeds, 1972

[11] Nelson, P.P. and Ingraffea, A.R. and O'Rourke, T.D.: *TBM performance prediction using rock fracture parameters,* Int. J. Rock Mech. Min. Sci. & Geomech. Abstr., Vol.22, No.3, p189 -192, 1985

[12] McFeat-Smith, I. and Tarkoy, P.J.: *Assessment of tunnel boring machines performance,* Tunnels Tunnelling, 9 (2), p29-33, 1977

[13] Jenni, J.P. and Ballisat, M.: *Rock testing methods performed to predicate the utilization possibilities of a tunnel boring machine,* Proc. 4th Congress I.S.R.M., Vol.2, p267-274, Montreux, Switzerland, 1979

[14] Ingraffea, A.R. and Gunsallus, K.L. and Beech, J.F.: *Fracture toughness testing system for the prediction of tunnel boring machine performance,* Proc. 23rd U.S. Symp. Rock Mech., p463-470, Berkeley, California, 1982 (AIME)

[15] Almenara, J.R.: *Rock characterization for cuttability assessment,* M.Sc. Thesis, Imperial College, London, 1988

[16] Taylor, F.W.: *On the art of cutting metal,* Trans. of ASME, Vol.28, 1906 (after [91])

[17] Ernst, H. and Merchant, M.E.: *Chip formation, friction and high quality machined surfaces,* Surface Treatment of Metals, Vol.29, American Society of Metals, 1941 (after [91])

[18] Merchant, M.E.: *Mechanics of the metal cutting process,* J. Appl. Phys., Vol.16, No.5, and No.6, 1945 (after [91])

[19] Wu, S.M.: *Tool-life testing by response surface methodology,* Transactions of ASME, p105-116, May, 1964

[20] Barrow, G.: *Tool life equations and machining economics,* 12th Int. M.T.D.R. Conf., p481-493, Manchester, September, 1971

[21] Tarasov, L.P.: *An investigation to abrasive machining,* American Machinist, p125-136, April, 1962

[22] Shaw, M.C. and Farmer, D.A.: *An analysis of the abrasive machining of plane surface,* J. of Engineering for Industry, p349-358, August, 1965 (ASME)

[23] Morrel, R.J. and Bruce, W.E. and Larson, D.A.: *Tunnel boring technology: disk cutter experiments in sedimentary and metamorphic rocks,* Report of Investigation 7410, U.S.Bureau of Mines, 1970

[24] Rad, P.F. and Olson, R.C.: *Interaction between disk cutter grooves in rocks,* Report of Investigation 7881, U.S.Bureau of Mines, 1974

[25] Tarkoy, P.J. and Hendron, A.J.: *Rock hardness index properties and geotechnical parameters for predicting tunnel boring machine performance,* Urbana-Champaign, p325, Dept. of Civil Engineering, University of Illinois, 1975

[26] Ranman, K.E.: *Rock fragmentation by cutting, ripping and impacts,* Doctoral thesis (49D), Lulea University, Sweden, 1986

[27] Buttner, A.: *Diamond tools and stone,* Industrial Diamond Review, p89-93, March, 1974

[28] Macro Division of Kennametal: *Metallurgy of diamond tools,* Industrial Diamond Review, p248-250, May, 1985

[29] Herbert, S.: *Laser-welded blade is key to trenching update,* Industrial Diamond Review, p293-296, January, 1983

[30] Thakur, B.N.: *Examination of technical parameters involved in metal bond development for diamond impregnated products (a primer for end - users),* Industrial Diamond Review, p91-93, March, 1977

[31] Zsolnay, L.M.: *Selection of diamonds for segmental saws,* Industrial Diamond Review, p382-384, November, 1977

[32] Jennings, M. and Wright, D.: *Guidelines for sawing stone,* Industrial Diamond Review, p70-75, February, 1989

[33] Walker, R.D. and Wood, M.G.: *Granite sawing techniques,* Industrial Diamond Review, p4-7, January, 1971

[34] Konstanty, J.: *The materials science of stone sawing,* Industrial Diamond Review, p27-31, January, 1991

[35] Bridwell, H.C. and Appl, F.C: *A study of 'free cutting' with diamond saws,* Industrial Diamond Review, p51-53, February, 1974

[36] Wright, D.N.: *The prediction of diamond wear in the sawing of stone,*Ultrahard Materials Application Technology, p47-60, Vol.4, 1988

[37] Jennings, M.: *Sawing stone with diamond tools - performance factors,* Stone Industries, p30-34, May, 1988

[38] Atkinson, T. and Cassapi, V.B.: *Abrasive wear in the mineral industry,* Mining Department Magazine, Vol.1, No.XLI, p105-121, University of Nottingham, 1989

[39] Busch, D.M. and Warker, R.D.: *The sawing of concrete and reinforced concrete with diamond saw blades,* Industrial Diamond Review, p170-178, May, 1973

[40] Miller, D. and Ball, A.: *Rock drilling with impregnated diamond microbits - an experimental study,* Int. J. Rock Mech. Min. Sci. & Geomech. Abstr., Vol.27, No.5, p363-371, 1990

[41] Nakajima, T.: *Cutting mechanism of partially stabilised zirconia with a single point diamond,* Journal of the Japan Society of Precision Engineering, Vol.54(8), p1544-1549, 1988 (In Japanese with English abstract)

[42] Bienert, P.: *Kreissagen von beton mit diamant werkzeugen,* Doctoral thesis, Hanover University, 1977 (in German, after [44])

[43] Lutz, G.: *Einfluss von schnittgeschwindigkeit beim sagen von hartgestein,* Advances in stone cutting, Stone colloquium, Hanover University, 1978 (in German, after[44])

[44] Eingshausen, W.: *Wear processes in sawing hard stone,* Industrial Diamond Review, p254-258, May, 1985

[45] Bailey, M.W. and Bullen, G.J.: *Sawing in the stone and civil engineering industries,* Industrial Diamond Review, p56-60, February, 1979

[46] Wright, D.N. and Cassapi, V.B.: *Factors influencing stone sawability,* Industrial Diamond Review, p84-87, February, 1985

[47] Cassapi, V.B.: *Application of rock hardness and abrasive indexing to rock excavating equipment selection,* Ph.D Thesis, Dept. of Mining Eng., Nottingham University, 1987

[48] Birle, J.D. and Ratterman, E.: *The sawability of stone,* Stone Industries, p24-29, July/August, 1988

[49] Hausberger, P.: *Stone machinability,* Industrial Diamond Review, p259-261, May, 1990

[50] Buttner, A.: *The use of large circular saw blades on hard stone,* Industrial Diamond Review, p474-476, November, 1972,

[51] Mamalis, A.G. and Schilze, R. and Tonshoff, H.K.: *Experimental investigations into hard-rock removal processes using a segmental diamond wheel,* Proc. 20th Int. M.T.D.R. Conf., p361-371, Birmingham, 1979

[52] Hughes, H.: *The early history of diamond tools,* Industrial Diamond Review, p405-407, November, 1980

[53] Bracken, N.: *Methods employed for the non-explosive breaking of hard rock and their potential for use in stopes,* Internal Report, Imperial College, London, 1988

[54] Trancu, T.C.: *Diamond wire machine cuts marble quarrying costs*, Industrial Diamond Review, p329-331, September, 1980

[55] Hallez, C.P.: *Sawing marble with diamond wire*, Industrial Diamond Review, p8-11, January, 1971

[56] Thoreau, B.: *Diamond impregnated wire for sawing hard abrasive stones*, Industrial Diamond Review, p94-95, February, 1984

[57] Herbert, S.: *Diamond wire saw - the in-depth solution*, Industrial Diamond Review, p11-12, January, 1989

[58] Daniel, P.: *More granites succumb to diamond wire*, Industrial Diamond Review, p189-194, May, 1986

[59] Cai, O. and Mancini, R.: *Diamond wire for cutting hard rock*, Industrial Diamond Review, p212-214, May, 1988

[60] Pinzari, M.: *Quarrying stone by diamond wire in Italy*, Industrial Diamond Review, p231-236, May, 1983

[61] Decroly, J.C.: *Stone extraction from the quarry using diamond wire*, Industrial Diamond Review, p80-83, February, 1981

[62] Herbert, S.: *Labour costs halved with one-man diamond wire*, Industrial Diamond Review, p251-253, May, 1985

[63] Daniel, P.: *Granite quarrying-cut waste & costs*, Industrial Diamond Review, p1-4, January, 1986

[64] Tonshoff, H.K. and Panhorst, H.J.: *Development and testing of a diamond wire for the sawing of hard stone*, Industrial Diamond Review, p246-251, July, 1974

[65] Hruska, F.H.: *Calculation of stresses in wire rope*, Wire and Wire Products, September, p766-767, 1951

[66] Hansel, J. and Oleksy, W.: *Life of wire ropes based on stresses in wires*, Wire Industry, p391-394, May, 1986

[67] Scanff, A.I.: *New wire saw machine*, Industrial Diamond Review, p168, April, 1988

[68] Hayes, D.: *Japanese granite trade embraces diamond wire*, Industrial Diamond Review, p67-69, February, 1989

[69] Marles, T.: *Norse Saga*, Industrial Diamond Review, p6-7, January, 1990

[70] Herbert, S.: *Diamond wire cuts at an Irish stone quarry*, Mine & Quarry, p23-26, March, 1986

[71] Trancu, T.: *Concrete cut by diamond wire*, Industrial Diamond Review, p11, January, 1986

[72] Daniel, P.: *Syndrill cuts costs in stone extraction*, Industrial Diamond Review, p46-48, February, 1986

[73] Daniel, P.: *Chain saw cuts costs in stone extraction*, Dimensional Stone, Vol.3(1), p52-54, 1987

[74] Meier, J.M.: *A new concept for sawing stone and concrete*, Industrial Diamond Review, p246-247, May, 1983

[75] Gerhauser, W.: *The diamond bandsaw for cutting stone*, Industrial Diamond Review, p321-328, September, 1980

[76] Buttner, A. and Picker, M.: *A new bandsaw for slabbing natural stone*, Industrial Diamond Review, p90-93, February, 1984

[77] Schulze, R.: *Grinding forces in the diamond frame sawing of natural stone*, Industrial Diamond Review, p258-259, July, 1980

[78] Butler, M.O.: *The successful application of EDC in frame sawing*, Industrial Diamond Review, p124-126, April, 1980

[79] Buttner, A.: *Geganken zum wirtschaftlichen einsatz von kreissageblattern auf hartgestein*, Industrie diamanten rundschau, 5, 1971 (in German after[39])

[80] Lindenbeck, D.A.: *Schleifen von eisenwerkstoffen mit diamantschleifscheiben*, Dr.-ing. Diss., T.U.Hannover, Voroffentlichtin: Fortschrittberichte der Vdi-Zeitschriften, Reihe2, Nr.22, 1970 (in German after[39])

[81] Tonshoff, H.K. and Schulze, R.: *The effect of the coolant in the sawing of hard stone*, Industrial Diamond Review, p252-257, July, 1980

[82] Buttner, A.: *Coolant additives in the sawing of granite*, Industrial Diamond Review, p332-335, September, 1980

[83] Dyer, H.B. and Conradi, V.R.: *Properties of natural Debdust and its use in diamond saw blades*, Industrial Diamond Review, p335-343, August, 1972.

[84] Xu, X.H. and Yu, J.: *Rock fragmentation*, Coal Industry Publishing Company, China, 1977 (in Chinese)

[85] Taljas, P.: *Fundamentals of the thermomechanical destroying of rocks*, Naukova Publishing Company, Kiev, Dumka, 1972 (in Chinese translated from Russian)

[86] Takubo, T. and Ohshita, H. and Kawakita, T.: *A new dressing device for stone cutting saw blades*, Industrial Diamond Review, p284-290, May, 1982

[87] Barker, J.S.: *A laboratory investigation of rock cutting using large picks*, Int. J. Rock Mech. Mining Sci, Vol.1, p519-534, 1964

[88] Snowdon, R.A. and Ryley, M.D. and Temporal, J.: *A study of disk cutting in selected British rocks*, Int. J. Rock.Mech. Min. Sci.&Geomech. Abstr., Vol.19, p107-121, 1982

[89] Stolarski, T.A.: *Tribology in machine design*, Neinemann Newnes Publishing Ltd, p127-136, Oxford, 1990

[90] Clark, G.B.: *Principles of rock fragmentation*, John Wiley & Sons Inc., p218-241, 1987

[91] Boothroyd, G.: *Fundamentals of metal machining and machine tools*, Scripta Book Company, p83-88, McGraw-Hill Kogakusha, 1975

[92] Chatterjee, P.K. and Wetherall, P.J.: *Winding engine calculations for the mining engineer*, University of Queensland Press, St Lucia, 1981

[93] Walker, S.C.: *Mine winding and transport*, Elsevier Science Publishing Company, New York, 1988

[94] Fowell, R.J. and Johnson, S.T.: *Rock classification and assessment for rapid excavation*, Proc. Symp. Strata Mech., Ed. I.W.Farmer, Elsevier, p241-244, New York, 1982

[95] Rabia, H.: *Specific energy as a criterion for drill performance prediction*, Int. J. Rock Mech. Min. Sci. & Geomech. Abstr., Vol.19, p39-42, 1982

[96] Jenni, J.P. and Balissat, M.: *Rock testing methods performed to predict the utilization possibilities of a tunnel boring machine*, Proc. 4th Congr. Int. Soc.Rock Mechanics 2, p267-274, 1979

[97] International Society for Rock Mechanics: *Suggested methods for determining hardness and abrasiveness of rocks*, Int. J. Rock Mech. Min. Sci. & Geomech. Abstr., Vol.15, p89-97, 1978

[98] Rabia, H. and Brook, N.: *The Shore hardness of rock*, Int. J. Rock Mech. Min. Sci. & Geomech. Abstr., Vol.16, p335-336, 1979

[99] Deere, D.U. and Miller, R.P.: *Classification and index properties for intact rock*, Report AFWL-TR-65-116, AF Special Weapons Center, Kirtland AFB, New Mexico, 1965

[100] International Society for Rock Mechanics: *Suggested methods for determining the uniaxial compressive strength and deformabitity of rock materials*, Int. J. Rock Mech. Min. Sci. & Geomech. Abstr., Vol.16, p135-140, 1979

[101] International Society for Rock Mechanics: *Suggested method for determining the fracture toughness of rock*, Int. J. Rock Mech. Min. Sci. & Geomech. Abstr., Vol.25, p72-96, 1988

[102] International Society for Rock Mechanics: *Suggested method for determining sound velocity*, Int. J. Rock Mech. Min. Sci. & Geomech. Abstr., Vol.15, p53-58, 1978

[103] International Society for Rock Mechanics: *Suggested methods for determining the strength of rock materials in triaxial compression - revised version*, Int. J. Rock Mech. Min. Sci. & Geomech. Abstr. Vol.20, p283-290, 1983

[104] Hoek, E. and Bray, J.W.: *Rock Slope Engineering*, Published by the Institution of Mining and Metallurgy, Third edition, p333-334, London, 1981

[105] Hoek, E. and Brown, E.T.: *Underground excavations in rock*, Published by the Institution of Mining and Metallurgy, p513, London, 1980

[106] West, G.: *A relation between abrasiveness and quartz content for some coal measures sediments*, Int. J. Min. Geol. Engng 4, p73-78, 1986

APPENDIX

COMPUTER PROGRAM FOR THE ASSESSMENT OF ROCK SAWING USING DIAMOND CIRCULAR SAWBLADE

The theories developed on diamond cutting enabled the development of a computer program which helps selecting the most suitable cutting conditions. Due to the limitations arising from the number of samples tested, this program is suitable for the assessment of sawing condition for six types of rock (Marlin granite, Rose De La Clarte granite, Celtic granite, Lanhelin granite, Balmoral granite and Grey limestone) using a DTA sawblade (a standard production of Diamant Boart). With further tests the program can be generalized for use with other rocks.

For sawing each kind of rock, four options are included in the program:

(1) Sawing *conditions*: Based on the data provided, the ideal sawing speed with the maximum feed, depth of cut and sawing rate are recommended. The preferred mode of sawing, coolant and the combination of feed and depth of cut are given.

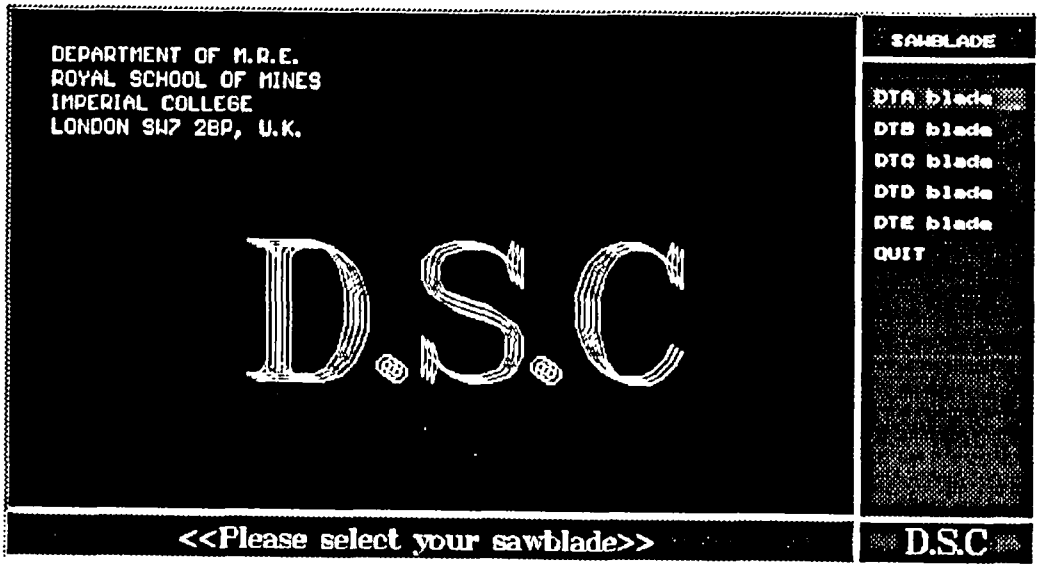
(2) *Sawability*: Sawability is determined using the R-C characteristic curve concept. When the required data sawing rate (cm^2/min), machine and operator (including overheads) cost per unit time (unit currency/hr), purchase price of the sawblade (unit currency), nonproductive time (loading and unloading, transport and inspection) per unit area of cut (min/m^2) and total cutting area (m^2) are typed in, tool life (hr), sawing cost (unit currency/m^2) production cost and number of required sawblades are calculated and listed on the screen. Also, the R-C characteristic curve, which

indicates the relationship between sawing rate and production cost, is presented on the screen.

(3) *Optimum* engineering parameters: The most significant function of this program is that the optimum engineering parameters can be selected according to the calculated results. The optimum parameters that can be calculated and shown on the screen are: tool life, sawing rate, production cost, machine time and the number of required sawblades.

(4) Sawing *forces:*Sawing force patterns and the average vertical and horizontal forces can be listed on the screen.

Some computer output screens representing the results obtained in analyzing the sawability of Balmoral granite are presented in the following pages. The screens are self descriptive.



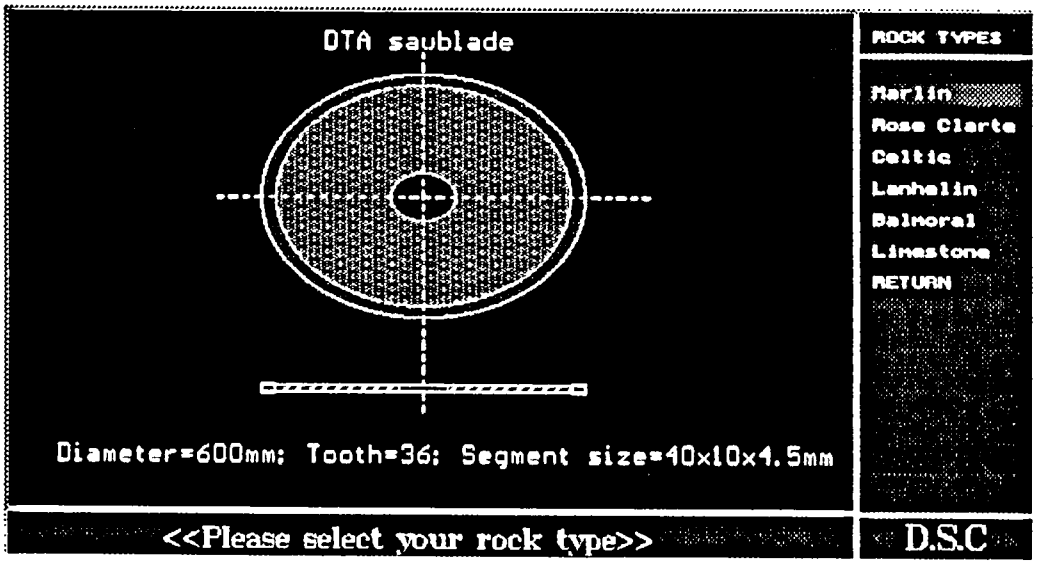


Figure A1

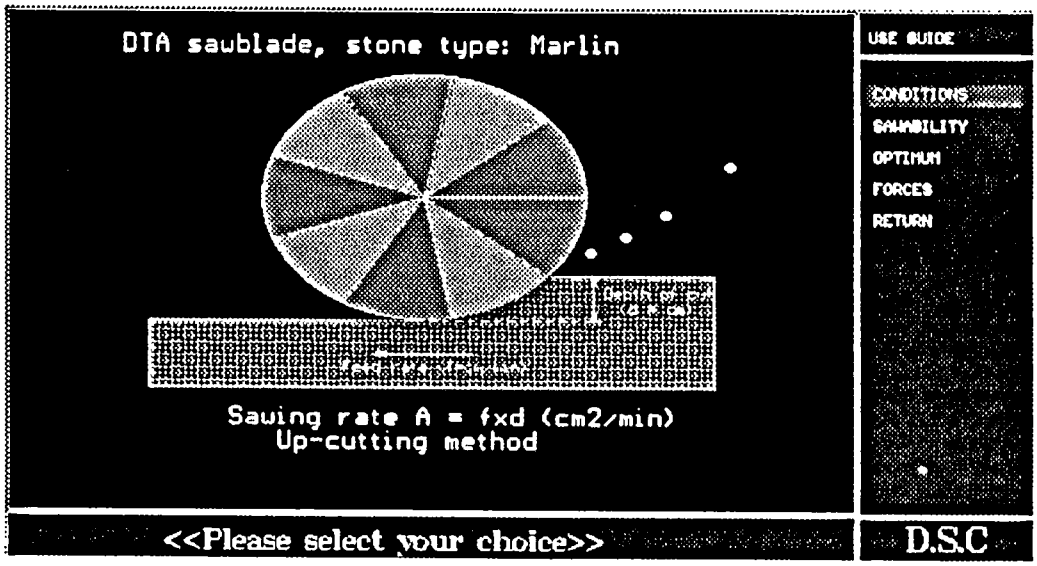


Figure A2

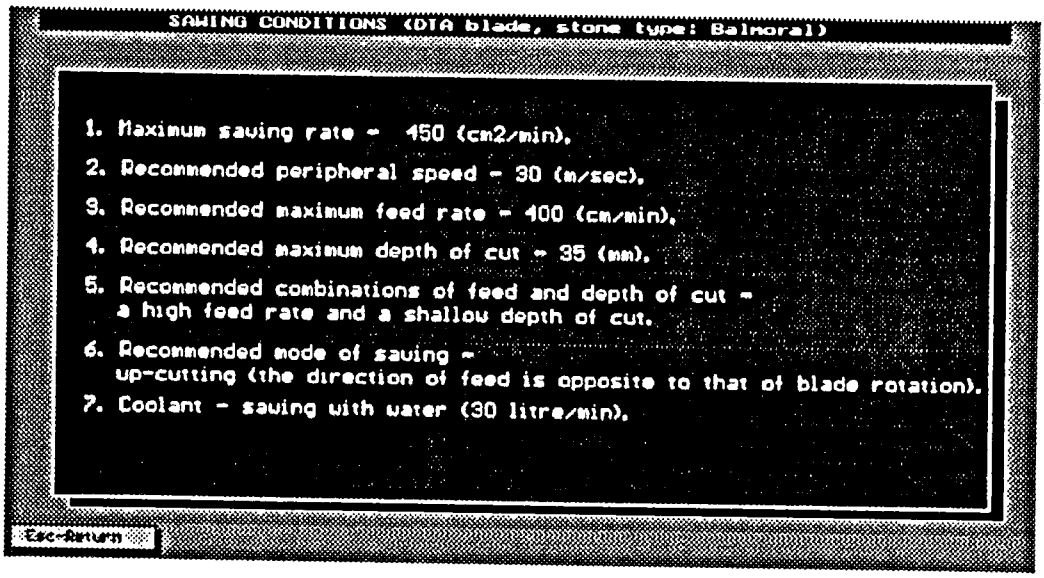


Figure A3

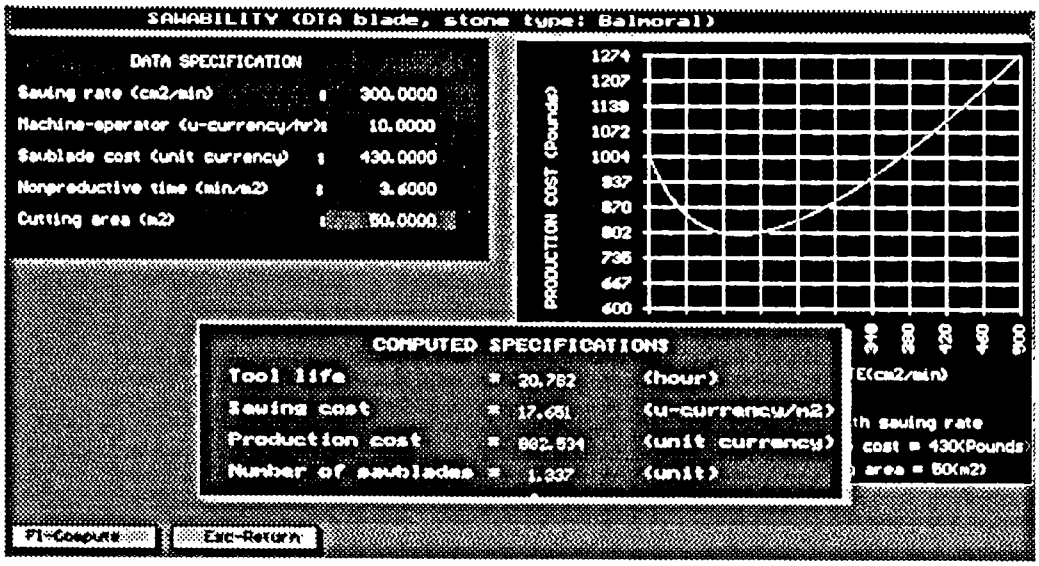


Figure A4

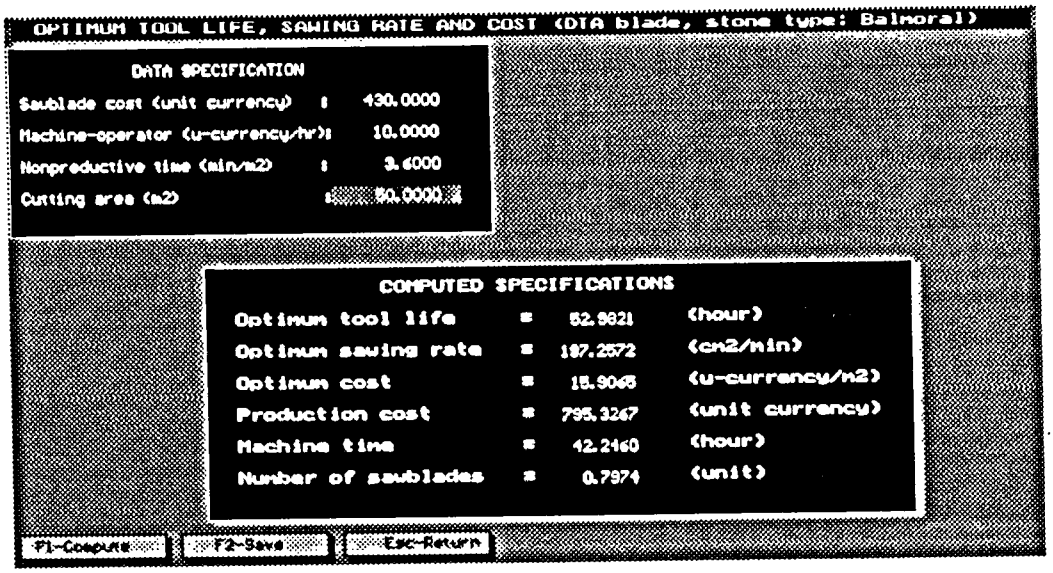


Figure A5

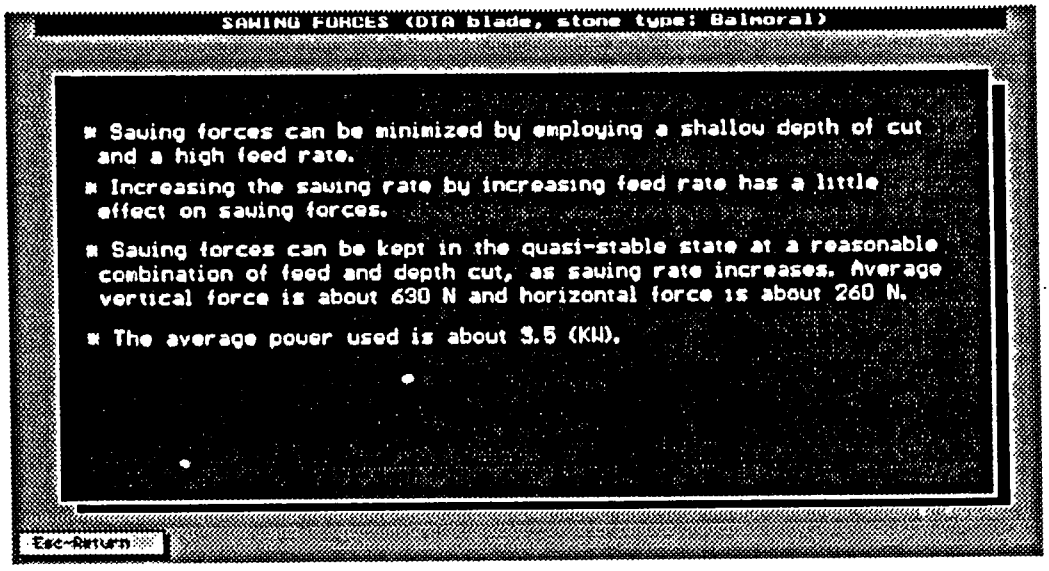


Figure A6